Eur. Phys. J. B **2**, 413–449 (1998)

THE EUROPEAN PHYSICAL JOURNAL B

Effects of a finite screening length on the absorption of electromagnetic waves

R. Balian[1,a] and J.-J. Niez[2]

[1] Service de Physique Théorique, CEA-Saclay, 91191 Gif-sur-Yvette Cedex, France
[2] Service de Physique Nucléaire, CEA, BP 12, 91680 Bruyères-le-Châtel, France

Received: 29 July 1997 / Revised: 24 November 1997 / Accepted: 20 February 1998

Abstract. When an electromagnetic wave impinges on a semiconductor or ionic conductor having a sizeable screening length, it induces diffusion currents in addition to the ohmic currents, which affects the propagation in heterostructures or composite media involving such materials. In the simple geometries and in the low frequency regime studied here, the absorption may be either enhanced or reduced, depending on the parameters, and effects precluded for metals are predicted: extinction of the reflection by a plane wall, complete absorption of an electric multipolar wave by a sphere, disappearance of the scattering by a small sphere, vanishing of both reflection and transmission coefficients for a slab. If the screening length is larger than the skin depth, a slab with intermediate thickness may have a large transparency, and a thick piece of material is expected to be cooled down by the wave near the interface and overheated deeper inside.

PACS. 41.20.Jb Electromagnetic wave propagation; radiowave propagation – 72.20.-i Conductivity phenomena in semiconductors and insulators

1 Introduction

The propagation of electromagnetic waves in composite media or in heterostructures is currently described by characterizing each medium by a single wavenumber k which depends on the angular frequency ω. In an insulator, k is the square root of $\omega^2\mu_0\varepsilon$, where ε is the dielectric constant. In a metal, k is complex with $k^2 = \omega^2\mu_0\varepsilon + \mathrm{i}\omega\mu_0\sigma$, where σ is the conductivity. The field as well as the current $\mathbf{J}$ of the free charge carriers penetrate the conductor over ranges of the order of the skin depth $(\mathrm{Im}\ k)^{-1}$. However, in permanent regimes, the bulk charge density ρ of these carriers vanishes as a consequence of Ohm's law $\mathbf{J} = \sigma\mathbf{E}$, of the charge conservation law

$$\frac{\partial\rho}{\partial t} + \mathrm{div}\mathbf{J} = 0, \tag{1.1}$$

and of the Gauss equation

$$\mathrm{div}\ \varepsilon\mathbf{E} = \rho, \tag{1.2}$$

which altogether provide within the material $(\varepsilon\partial/\partial t + \sigma)\,\rho = 0$. An oscillating surface charge density is concentrated at the interface.

This behaviour originates from the fact that, for metals, the screening length has an atomic order of magnitude. In semiconductors as well as in ionic conductors, colloids or electrolytes, the screening length λ is sizeable, and the charge carriers must spread over ranges of order λ. In a static electric field, the charge density satisfies $\lambda^2\nabla\rho = \varepsilon\mathbf{E}$, hence $\left(\lambda^2\nabla^2 - 1\right)\rho = 0$; it thus decreases exponentially as $\mathrm{e}^{-z/\lambda}$ with the distance z from the interface. Our purpose is to explore the consequences of such a spreading on the distribution of fields and hence on the propagation of e.m. waves, in composite media containing conductors with a finite screening length. We shall consider below only geometries where a plane e.m. wave issued from a dielectric material interacts with a piece of semiconductor or of ionic conductor having a simple shape. The Debye length is also sizeable in plasmas, but the phenomena that we shall study would then refer to reflection and refraction of an e.m. wave on an interface between a motionless collisional plasma and a dielectric medium, a situation which seems experimentally out of reach. The semiconductor or ionic conductor will be described by the simplest model that accounts both for conduction and for screening over a finite range λ.

More precisely, we replace Ohm's law $\mathbf{J} = \sigma\mathbf{E}$, which represents the response of a metal for which $\lambda \simeq 0$, by the equation

$$\mathbf{J} = \sigma\left(\mathbf{E} - \frac{\lambda^2}{\varepsilon}\nabla\rho\right) = \sigma\mathbf{E} - D\nabla\rho, \tag{1.3}$$

expected to hold approximately for the materials that we consider, provided that the frequencies are not too high ($\omega\tau \ll 1$, where τ is the delay between collisions). Equation (1.3) has the required limits, for $\lambda = 0$ (metal), for

[a] e-mail: zaf@spht.saclay.cea.fr

$\rho = 0$ (conduction in a neutral bulk piece of matter), and for $\mathbf{J} = 0$ (electrostatic screening). Its two contributions to the current describe on the one hand the drift of the carriers induced by the electric force applied to them, and on the other hand the diffusion which tends to restore uniformity of the charge density. Since the carriers, with charge q, behave in semiconductors and in ionic conductors as a classical gas, the diffusion coefficient $D \equiv \sigma\lambda^2/\varepsilon$ satisfies Einstein's relation $D = \sigma k_{\mathrm{B}}T/q\rho$; equivalently λ satisfies the Debye–Hückel equation $\lambda^2 = \varepsilon k_{\mathrm{B}}T/q\rho$. We shall assume the temperature to remain uniform.

The constitutive equation (1.3) can be justified through two different means [1]. On the one hand, the semi-phenomenologic macroscopic approach of *non-equilibrium thermodynamics* relies on the proportionality, in isothermal regimes, of the current $\mathbf{J}$ to the electromotive force, that is, to the gradient of the electrochemical potential μ, provided the material is in the vicinity of equilibrium. The two terms of (1.3) then arise from the two contributions to $\nabla\mu$, issued respectively from the external forces and from the non-homogeneity of the density of carriers. The relation between the diffusion coefficient D and the screening length λ expresses simply the Poisson equation at electrostatic equilibrium, with $\mathbf{J} = 0$ in (1.3). On the other hand, the microscopic approach of *kinetic theory* shows that (1.3) results from the solution of the Boltzmann equation in the local equilibrium regime; moreover it yields microscopic expressions for the parameters σ and λ. This approach also exhibits the validity domain of (1.3): the mean free path should be smaller than the wavelengths involved, and the delay between collisions should satisfy $\omega\tau \ll 1$. This makes more precise the condition of "vicinity of equilibrium" required in the thermodynamic approach.

In the language of effective permittivity, the usual conductivity equation $\mathbf{J} = \sigma\mathbf{E}$ gives rise to a frequency dependence of $\varepsilon_{\mathrm{eff}} = \varepsilon + \mathrm{i}\sigma\omega^{-1}$ through the contribution of free carriers. More precisely, if $\mathbf{E}(\mathbf{r})$ and

$$\mathbf{D}(\mathbf{r}) \equiv \varepsilon\mathbf{E}(\mathbf{r}) + \mathrm{i}\omega^{-1}\mathbf{J}(\mathbf{r}) \tag{1.4}$$

denote the ω-components of the electric and displacement fields, respectively, they then satisfy the local but delayed relation $\mathbf{D}(\mathbf{r}) = \varepsilon_{\mathrm{eff}}\mathbf{E}(\mathbf{r})$. Turning to the transport equation (1.3), the dependence of $\mathbf{D}(\mathbf{r})$ on $\mathbf{E}(\mathbf{r})$ (at a given frequency) becomes moreover *non-local.* Indeed, elimination of $\mathbf{J}$ and ρ between (1.3, 1.4) and the conservation equation $\mathrm{div}\mathbf{J} = \mathrm{i}\omega\rho$ leads to the relation (7.2) below between $\mathbf{D}$ and $\mathbf{E}$. For an infinite homogeneous medium, it is convenient to perform a spatial Fourier transform, where we denote by $\mathbf{q}$ the conjugate of $\mathbf{r}$, which simplifies (7.2) into

$$\mathbf{D}(\mathbf{q}) = \left(\varepsilon + \frac{\mathrm{i}\sigma}{\omega}\right)\mathbf{E}(\mathbf{q}) + \mathbf{q}\,\frac{\sigma^2\lambda^2}{\omega^2\varepsilon + \mathrm{i}\omega\sigma\lambda^2 q^2}\left[\mathbf{q}\cdot\mathbf{E}(\mathbf{q})\right]. \tag{1.5}$$

This introduces a $(\mathbf{q},\omega)$-dependent effective permittivity tensor $\varepsilon_{\mathrm{eff}}(\mathbf{q},\omega)$, which exhibits a non-local character in its longitudinal component. Our problem thus enters the general framework of spatial dispersion [2]. Unfortunately, since our aim is to explore wave propagation near interfaces, we have to face boundary effects, which prevents us from using spatial Fourier transforms. The concept of effective permittivity thus becomes useless here since the system is not only non-local, but also non-homogeneous.

In order to deal, in the $\mathbf{r}$-space, with *local equations* only, we shall not try to eliminate $\mathbf{J}$ and ρ as we did to obtain (1.5). Instead, we shall keep $\rho(\mathbf{r})$ as one of our basic fields, together with the electric field $\mathbf{E}(\mathbf{r})$. Using this procedure, we shall see in Section 2 that the constitutive equation (1.3), together with Maxwell's equations, give rise at a given frequency to *two complex characteristic lengths* in the material. Beside the wavelength k^{-1}, given by $k^2 = \omega^2\mu_0\varepsilon + \mathrm{i}\omega\mu_0\sigma$ as in a metal, we shall find a dynamical screening length β^{-1}, of the same order of magnitude as λ, which governs the space variations of the charge density. The distribution of e.m. fields will in general depend on both lengths k^{-1} and β^{-1}. For a bulk material, these two complex lengths are associated with *two poles* in the $(\mathbf{q},\omega)$ Fourier transform of the propagator for $\mathbf{E}$, namely $\mathbf{q}^2 = k^2 = \omega^2\mu_0\varepsilon + \mathrm{i}\omega\mu_0\sigma$ for its transverse components and $\mathbf{q}^2 = -\beta^2 = -\lambda^{-2}\left(1 - \mathrm{i}\omega\varepsilon\sigma^{-1}\right)$ for its longitudinal component. The first pole also occurs in $\mathbf{D}$, in $\mathbf{H}$, and in the transverse part of $\mathbf{J}$, while the second pole occurs in ρ and in the longitudinal part of $\mathbf{J}$.

Let us now turn to the boundary conditions at the interfaces. At the surface of a metal, the normal component $J_\perp$ of the electric current does not vanish; according to (1.1), it is equal to the time-derivative of the surface charge. When λ is finite, the material cannot sustain any infinite charge density so that there is no surface charge. The conservation equation (1.1) then implies that $J_\perp$ vanishes at the interfaces. This property will appear as a boundary condition, supplementing the usual boundary conditions for the fields. Actually the partial differential equations for the fields, the currents and the charges are here of higher order than for metals, due to the occurrence of the gradient term in (1.3), and the additional boundary condition $J_\perp = 0$ is needed to ensure the unicity of their solution. This aspect of our problem, the so-called "*additional boundary conditions*", is discussed in Section 4.2 of reference [2]. It is related both to the occurrence of two poles instead of a single one in the propagators, and to the introduction of ρ as an additional field in the set of basic equations. The same problem has also been encountered by several authors [3–6] who dealt with spheres having a nonlocal dielectric constant or a metallic behaviour in the optical regime.

After having analyzed the general equations which govern the behaviour of the e.m. fields in our two-component system as well as the energy exchanges between field and matter (Sect. 2), we study the absorption of e.m. waves by a semiconductor or an ionic conductor in the simplest geometries. We begin with a thick plane wall, which leads to the simplest equations (Sect. 3); we discuss these equations in some detail (Sect. 4 and Appendix A) so as to explore the new features brought in by the finiteness of the screening length, which depending

on the circumstances may either enhance or reduce the absorption of e.m. waves. We then exhibit similar effects for a spherical inclusion in a dielectric medium (Sect. 5). Finally, we study the transmission through a semiconducting plane slab embedded in a dielectric and the reflection from it (Sect. 6). The Section 5 devoted to a sphere can be read independently.

The calculations in Sections 3 to 6 are rather tedious. We therefore resume their results in the conclusion (Sect. 7). The reader only interested in the experimental implications of the finiteness of the screening length may thus directly jump to Section 7, where the main expected phenomena are described and the main equations are listed.

2 General properties

2.1 Basic equations

As indicated in the introduction, we consider a system made of two materials, an insulator characterized by the dielectric constant ε^{i}, and a semiconductor or an electrolyte characterized by the dielectric constant ε, the conductivity σ and the electrostatic screening length λ. Electromagnetic waves with angular frequency ω are issued from the region of the insulator. The time-dependence of the electric field is expressed by:

$$\mathbf{E}(\mathbf{r},t) = \mathrm{Re}\,\left[\mathbf{E}(\mathbf{r})\,\mathrm{e}^{-\mathrm{i}\omega t}\right], \tag{2.1}$$

and likewise for the magnetic field **H,** the charge density ρ and the current density **J**. In the insulator, the fields are governed by Maxwell's equations:

$$\begin{aligned} \mathrm{i}\omega\mu_0\mathbf{H}(\mathbf{r}) - \mathrm{curl}\ \mathbf{E}(\mathbf{r}) = 0, \\ \mathrm{i}\omega\varepsilon^{\mathrm{i}}\mathbf{E}(\mathbf{r}) + \mathrm{curl}\ \mathbf{H}(\mathbf{r}) = 0. \end{aligned} \tag{2.2}$$

In the conductor, these equations, namely

$$\begin{aligned} \mathrm{i}\omega\mu_0\mathbf{H}(\mathbf{r}) - \mathrm{curl}\ \mathbf{E}(\mathbf{r}) = 0, \\ \mathrm{i}\omega\varepsilon\mathbf{E}(\mathbf{r}) + \mathrm{curl}\ \mathbf{H}(\mathbf{r}) = \mathbf{J}(\mathbf{r}), \end{aligned} \tag{2.3}$$

are supplemented by the response equation

$$\mathbf{J}(\mathbf{r}) = \sigma\left[\mathbf{E}(\mathbf{r}) - \frac{\lambda^2}{\varepsilon}\nabla\rho\,(\mathbf{r})\right], \tag{2.4}$$

and the conservation equation

$$\mathrm{i}\omega\rho\,(\mathbf{r}) - \mathrm{div}\ \mathbf{J}(\mathbf{r}) = 0, \tag{2.5}$$

which implies:

$$\varepsilon\ \mathrm{div}\ \mathbf{E}(\mathbf{r}) = \rho\,(\mathbf{r}). \tag{2.6}$$

Finally, we have to write the continuity across the interfaces of the tangential components $\mathbf{H}_{/\!/}, \mathbf{E}_{/\!/}$ of the magnetic and electric fields, and the vanishing of the normal component $J_\perp$ of the current density. These boundary conditions also imply the continuity of $H_\perp$ and of $D_\perp$, with $\mathbf{D} = \varepsilon^{\mathrm{i}}\mathbf{E}$ in the insulator and $\mathbf{D} = \varepsilon\mathbf{E} + \mathrm{i}\omega^{-1}\mathbf{J}$ in the semiconductor.

In the insulator, the solution of (2.2) is a superposition of transverse plane waves, with wavevectors $\boldsymbol{\kappa}$ satisfying

$$\kappa = \sqrt{\omega^2\mu_0\varepsilon^{\mathrm{i}}}. \tag{2.7}$$

In the semiconductor, (2.3) and (2.4) imply

$$\left(\nabla^2 + k^2\right)\mathbf{H}(\mathbf{r}) = 0, \qquad \mathrm{div}\ \mathbf{H}(\mathbf{r}) = 0, \tag{2.8}$$

where the complex wavenumber k is given by:

$$k \equiv \sqrt{\omega^2\mu_0\varepsilon + \mathrm{i}\omega\mu_0\sigma}, \qquad \mathrm{Re}\ k > 0. \tag{2.9}$$

The magnetic field $\mathbf{H}(\mathbf{r})$ is thus, as usual, a superposition of transverse plane waves, with wavevectors $\mathbf{k}$ of length (2.9). Another simple consequence of (2.4, 2.5, 2.6) is the equation for the charge density ρ:

$$\left(\nabla^2 - \beta^2\right)\rho(\mathbf{r}) = 0, \tag{2.10}$$

$$\beta \equiv \frac{1}{\lambda}\sqrt{1 - \frac{\mathrm{i}\omega\varepsilon}{\sigma}}, \qquad \mathrm{Re}\ \beta > 0. \tag{2.11}$$

The quantity β^{-1} is a (complex) *dynamical screening length*, reducing to λ in the static limit $\omega = 0$. It characterizes the range of variations for ρ, which is a linear combination of exponentials $\mathrm{e}^{-\boldsymbol{\beta}\cdot\mathbf{r}}$. The electric field **E** and the current density **J** drawn from (2.3, 2.4),

$$\mathbf{E}(\mathbf{r}) = \mathbf{E}^{\mathrm{p}}(\mathbf{r}) + \mathbf{E}^{\mathrm{s}}(\mathbf{r}), \tag{2.12}$$

$$\mathbf{E}^{\mathrm{p}}(\mathbf{r}) = \frac{1}{\sigma - \mathrm{i}\omega\varepsilon}\mathrm{curl}\ \mathbf{H}(\mathbf{r}),$$

$$\mathbf{E}^{\mathrm{s}}(\mathbf{r}) = \frac{1}{\varepsilon\beta^2}\nabla\rho(\mathbf{r}), \tag{2.13}$$

$$\mathbf{J}(\mathbf{r}) = \mathbf{J}^{\mathrm{p}}(\mathbf{r}) + \mathbf{J}^{\mathrm{s}}(\mathbf{r}), \tag{2.14}$$

$$\mathbf{J}^{\mathrm{p}}(\mathbf{r}) = \sigma\mathbf{E}^{\mathrm{p}}(\mathbf{r}), \qquad \mathbf{J}^{\mathrm{s}}(\mathbf{r}) = \mathrm{i}\omega\varepsilon\ \mathbf{E}^{\mathrm{s}}(\mathbf{r}), \tag{2.15}$$

appear as a *sum of two terms*, associated with *propagation* and with *screening*, respectively. The characteristic length for the propagative terms $\mathbf{E}^{\mathrm{p}}$ and $\mathbf{J}^{\mathrm{p}}$ is k^{-1}, and $\mathbf{E}^{\mathrm{p}}$ has the usual form of a superposition of transverse plane waves. However, while for a single plane wave $\mathbf{E}^{\mathrm{p}}$ and $\mathbf{J}^{\mathrm{p}}$ are perpendicular to both the wavevector $\mathbf{k}$ and the magnetic field **H**, the screening terms $\mathbf{E}^{\mathrm{s}}$ and $\mathbf{J}^{\mathrm{s}}$ have a range β^{-1} and are longitudinal: for $\rho \propto \mathrm{e}^{-\boldsymbol{\beta}\cdot\mathbf{r}}$, the vectors $\mathbf{E}^{\mathrm{s}}$ and $\mathbf{J}^{\mathrm{s}}$ lie parallel to $\boldsymbol{\beta}$. The time-dependences of the propagative and screening terms also exhibit a difference: as shown by (2.15) $\mathbf{J}^{\mathrm{p}}$ oscillates in phase with $\mathbf{E}^{\mathrm{p}}$ whereas $\mathbf{J}^{\mathrm{s}}$ is in quadrature with $\mathbf{E}^{\mathrm{s}}$.

For each geometry considered below, we shall use the following procedure to determine the e.m. fields. (i) Write **E** and **H** in the insulator as the sum of an incident plane wave with the wavevector $\boldsymbol{\kappa}$ and of waves (with the same wavenumber κ) reflected or scattered by the semiconductor or transmitted through it. The reflection and transmission coefficients, or the scattering amplitudes, are taken as parameters to be found later on. (ii) Write **H** in

the semiconductor as the solution of (2.8, 2.9). It is entirely determined in terms of $\mathbf{H}$ outside, owing to the boundary condition, that is, the continuity of $\mathbf{H}_{\shortparallel}$ across the interfaces. (iii) Write ρ as a solution of (2.10, 2.11); it involves an unknown amplitude for each possible direction of $\boldsymbol{\beta}$. (iv) Express $\mathbf{E}$ and $\mathbf{J}$ in the semiconductor by means of (2.12–2.15), and determine the amplitudes in ρ by imposing that the normal component of $\mathbf{J}$ at the interfaces vanishes. (v) Finally, use the boundary condition on $\mathbf{E}$, namely the continuity across the interfaces of the tangential component of $\mathbf{E}$, to determine the parameters introduced in the step (i).

In the limit $\lambda \to 0$ of a metal, β becomes large. The charge density $\rho(\mathbf{r})$, concentrated in a thin shell of thickness β^{-1} at the interfaces, tends to a distribution of surface charges. If we denote by z the distance to the interface, we have $\rho(\mathbf{r}) \propto \beta \mathrm{e}^{-\beta z}\, \theta(z) \to \delta(z)$. Although the normal component of $\nabla\rho$ is large, $\mathbf{E}^{\mathrm{s}}$ and $\mathbf{J}^{\mathrm{s}}$ remain finite near the interface, due to the denominator β^2 in (2.13). The normal component $J^{\mathrm{s}}_{\perp}$, in particular, varies from 0 for $z \gg \beta^{-1}$ to $-J^{\mathrm{p}}_{\perp}$ for $z = 0$ (so that $J_{\perp}$ vanishes there); this creates a discontinuity in the limit $\lambda \to 0$. However, in the sense of distributions, $\mathbf{E}^{\mathrm{s}}$ and $\mathbf{J}^{\mathrm{s}}$ vanish, even at $z = 0$; when smoothed over ranges larger than β^{-1}, they are completely washed out. The standard model for a metal with $J_{\perp} \neq 0$ is thereby recovered, but not trivially.

The splitting of $\mathbf{E}$ and $\mathbf{J}$ into two contributions, which partly decouples the equations, would also be a valuable tool for theoretical treatments of propagation of e.m. waves in random composite media. The use in this problem of the replica trick [7] or of supersymmetric methods [8], for instance, requires to treat all materials on the same footing, with a unique set of equations involving random parameters, non-singular and valid everywhere including the interfaces. This is readily done by extending $\rho, \mathbf{E}^{\mathrm{s}}$ and $\mathbf{J}^{\mathrm{s}}$ to the dielectric, where the equations force them to vanish.

2.2 Energy exchanges

In a stationary regime, the *energy density* of the field in the semiconductor or ionic conductor, averaged on time over a period $2\pi/\omega$ by means of (2.1), and including the polarization energy, is:

$$\frac{1}{2}\left\langle \varepsilon\left[\mathbf{E}(\mathbf{r},t)\right]^2 + \mu_0\left[\mathbf{H}(\mathbf{r},t)\right]^2 \right\rangle = \frac{1}{4}\mathrm{Re}\left[\varepsilon\left|\mathbf{E}(\mathbf{r})\right|^2 + \mu_0\left|\mathbf{H}(\mathbf{r})\right|^2\right], \tag{2.16}$$

and likewise with ε^{i} in the dielectric. Accordingly, the average *energy flux* of the field is characterized by the Poynting vector

$$\mathbf{N}(\mathbf{r}) = \frac{1}{2}\mathrm{Re}\,\left[\mathbf{E}(\mathbf{r}) \times \mathbf{H}(\mathbf{r})^*\right], \tag{2.17}$$

and the *power* per unit volume *yielded to matter* by the field, averaged over time, is at each point:

$$w(\mathbf{r}) = \frac{1}{2}\mathrm{Re}\,\left[\mathbf{E}(\mathbf{r}) \cdot \mathbf{J}(\mathbf{r})^*\right] = -\mathrm{div}\,\mathbf{N}(\mathbf{r}). \tag{2.18}$$

In our model for the semiconductor, the Poynting vector comes out from (2.12, 2.13) as the sum of two terms, associated with propagation and with screening, respectively:

$$\mathbf{N}(\mathbf{r}) = \mathbf{N}^{\mathrm{p}}(\mathbf{r}) + \mathbf{N}^{\mathrm{s}}(\mathbf{r}), \tag{2.19}$$

$$\mathbf{N}^{\mathrm{p}}(\mathbf{r}) = \frac{1}{2}\mathrm{Re}\,\left[\mathbf{E}^{\mathrm{p}}(\mathbf{r}) \times \mathbf{H}(\mathbf{r})^*\right] = \frac{1}{2}\mathrm{Re}\,\left[\frac{1}{\sigma - \mathrm{i}\omega\varepsilon}\mathrm{curl}\,\mathbf{H}(\mathbf{r}) \times \mathbf{H}(\mathbf{r})^*\right], \tag{2.20}$$

$$\mathbf{N}^{\mathrm{s}}(\mathbf{r}) = \frac{1}{2}\mathrm{Re}\,\left[\mathbf{E}^{\mathrm{s}}(\mathbf{r}) \times \mathbf{H}(\mathbf{r})^*\right] = \frac{1}{2}\mathrm{Re}\,\left[\frac{1}{\varepsilon\beta^2}\nabla\rho(\mathbf{r}) \times \mathbf{H}(\mathbf{r})^*\right]. \tag{2.21}$$

The *propagative term* $\mathbf{N}^{\mathrm{p}}$ is as usual directed along the wavevector $\mathbf{k}$. The *screening term* $\mathbf{N}^{\mathrm{s}}$ is perpendicular to both the magnetic field and the direction $\boldsymbol{\beta}$ of the gradient of the screening charge.

Within the same model, the local dissipation rate (2.18) can be written, using (2.4) and (2.5), as:

$$w(\mathbf{r}) = \frac{1}{2\sigma}\left|\mathbf{J}(\mathbf{r})\right|^2 + \frac{\lambda^2}{2\varepsilon}\mathrm{divRe}\,\left[\rho(\mathbf{r})\,\mathbf{J}(\mathbf{r})^*\right]. \tag{2.22}$$

While the first term, which has a usual form, is obviously positive at each point, the second term may have either sign. Moreover its positive and negative contributions cancel each other when we integrate $w(\mathbf{r})$ over the whole material, since $J_{\perp}$ vanishes at the interfaces. The overall dissipation rate thus reduces to

$$W = \frac{1}{2\sigma}\int d^3r\,\left|\mathbf{J}(\mathbf{r})\right|^2. \tag{2.23}$$

An alternative, more detailed form of the *local dissipation rate* (2.18) is associated with the two contributions (2.19–2.21) to the Poynting vector. The *propagative* contribution to $w(\mathbf{r})$ keeps the usual form:

$$w^{\mathrm{p}}(\mathbf{r}) = -\mathrm{div}\,\mathbf{N}^{\mathrm{p}}(\mathbf{r}) = \frac{1}{2}\mathrm{Re}\,\left[\mathbf{E}^{\mathrm{p}}(\mathbf{r}) \cdot \mathbf{J}^{\mathrm{p}}(\mathbf{r})^*\right] = \frac{\sigma}{2\left(\sigma^2 + \omega^2\varepsilon^2\right)}\left|\mathrm{curl}\,\mathbf{H}(\mathbf{r})\right|^2. \tag{2.24}$$

The contribution associated with *screening* is found from (2.13, 2.15) as:

$$w^{\mathrm{s}}(\mathbf{r}) = -\mathrm{div}\,\mathbf{N}^{\mathrm{s}}(\mathbf{r}) = \frac{1}{2}\mathrm{Re}\,\left[\mathbf{E}^{\mathrm{p}}(\mathbf{r}) \cdot \mathbf{J}^{\mathrm{s}}(\mathbf{r})^* + \mathbf{E}^{\mathrm{s}}(\mathbf{r}) \cdot \mathbf{J}^{\mathrm{p}}(\mathbf{r})^*\right] = \frac{1}{2}\mathrm{Re}\,\left[\frac{1}{\varepsilon\beta^2}\nabla\rho(\mathbf{r}) \cdot \mathrm{curl}\,\mathbf{H}(\mathbf{r})^*\right] = \frac{1}{2}\mathrm{divRe}\,\left[\frac{1}{\varepsilon\beta^2}\rho(\mathbf{r})\,\mathrm{curl}\,\mathbf{H}(\mathbf{r})^*\right]. \tag{2.25}$$

The term $\frac{1}{2}\mathrm{Re}\,\left[\mathbf{E}^{\mathrm{s}}(\mathbf{r}) \cdot \mathbf{J}^{\mathrm{s}}(\mathbf{r})^*\right]$ from (2.18) vanishes, due to the phase shift $\frac{\pi}{2}$ between $\mathbf{E}^{\mathrm{s}}$ and $\mathbf{J}^{\mathrm{s}}$. The total dissipation rate $W = W^{\mathrm{p}} + W^{\mathrm{s}}$, the integral of $w^{\mathrm{p}} + w^{\mathrm{s}}$

over the whole material, is checked to be the flux of the Poynting vector which enters through the interfaces; the contribution W^{s} is also the flux of $\frac{1}{2}\mathrm{Re}\left[\varepsilon^{-1}\beta^{-2}\rho\ \mathrm{curl}\ \mathbf{H}^{*}\right]$ according to (2.25) or that of $\frac{1}{2}\mathrm{Re}\left[\mathrm{i}\omega\beta^{-2}\rho\mathbf{E}^{*}\right]$, where we made use of (2.3) and $J_{\perp}=0$. Nothing forces it to be positive, contrary to W^{p}, the incoming flux of $\mathbf{N}^{\mathrm{p}}$, which is obviously positive since it is the integral of (2.24).

The occurrence of two types of contributions to the dissipation rate can be traced back to a qualitative microscopic analysis of the phenomena. In a region of space where $\rho=0$, the electric force $q\mathbf{E}^{\mathrm{p}}$ exerted on a carrier with charge q gives it an acceleration between two successive collisions on the inhomogeneities of the medium (impurities, phonons, solvent molecules in a ionic conductor, *etc.*); at the next collision, the distribution of velocities tends to recover its isotropy. These two combined types of processes result in a flux $\mathbf{J}^{\mathrm{p}}/q$ of carriers in the same direction as the force $q\mathbf{E}^{\mathrm{p}}$: Ohm's law. Energy is yielded by the field to the carriers through the successive accelerations, and hence to the medium through the collisions: the Joule effect (2.24). However, when the density ρ is not uniform, an additional contribution $\mathbf{J}^{\mathrm{s}}/q$ to the particle flux is generated by a diffusion process, whatever the field $\mathbf{E}$; it arises from the drift term in the Boltzmann equation and is directed along the gradient $\nabla\rho/q$ of the particle density. In case the angle between the instantaneous average flow $\mathbf{J}^{\mathrm{s}}(\mathbf{r},t)/q$ and the force $q\mathbf{E}^{\mathrm{p}}(\mathbf{r},t)$ exerted by the field exceeds $\frac{\pi}{2}$, this force *slows down the carriers* between two collisions, a property which can hold after time-averaging over a period. The average power $\frac{1}{2}\mathrm{Re}\ [\mathbf{E}^{\mathrm{p}}\cdot\mathbf{J}^{\mathrm{s}*}]$ yielded by the field to the carriers can then be negative. Thus, depending on the direction of the diffusion current $\mathbf{J}^{\mathrm{s}}$ with respect to the field $\mathbf{E}^{\mathrm{p}}$ at the considered point, the contribution $\frac{1}{2}\mathrm{Re}\ [\mathbf{E}^{\mathrm{p}}\cdot\mathbf{J}^{\mathrm{s}*}]$ to w^{s} corresponds locally either to a *cooling* or an *overheating* of matter by the field, added to the Joule heating.

Finally, the second term $\frac{1}{2}\mathrm{Re}\ [\mathbf{E}^{\mathrm{s}}\cdot\mathbf{J}^{\mathrm{p}*}]$ of (2.25) is associated with the field $\mathbf{E}^{\mathrm{s}}$ which is created by the diffusion current due to the motion of the screening charges. The main flow $\mathbf{J}^{\mathrm{p}}$ of carriers may, here again, be heated or cooled, depending on its direction, by this additional field $\mathbf{E}^{\mathrm{s}}$ which lies along $\nabla\rho$.

Such a local cooling or overheating of carriers is known in another context, that of the Landau damping in the collisionless regime [9]. However this phenomenon is found here in the opposite limit $\omega\tau\ll 1$. In order to discuss the possibility of observing it in practice, our model needs to be completed. Actually, apart from the above energy exchanges between the field and the carriers, and apart from the local thermalization associated with the scattering of the carriers in the medium, a realistic description should include the other mechanisms of heat transfer that we disregarded, in particular the heat conduction. In the local equilibrium regime which we considered, we should thus add to (1.3) a thermoelectric term proportional to the temperature gradient, express the total heat flux in terms of the gradients of T and μ, and solve the resulting coupled equations. Moreover we should also take into account the temperature dependence of the screening length, which arises mainly through the variation of the density of charge carriers. In this paper, and in particular in Sections 4.1 and 4.3, we shall restrict ourselves to the primary phenomenon, the energy transfer between field and carriers, keeping aside the subsequent heat transfers.

3 Plane wall: generalities

3.1 Influence of incidence and polarization

We consider here and in Section 4 a single plane interface which separates a dielectric material in the region $z<0$ and a semiconductor or ionic conductor in the region $z>0$. We wish to study the absorption and the reflection of a plane electromagnetic incident wave with wavevector $\boldsymbol{\kappa}=(\kappa_x,0,\kappa_z)$. Translational invariance implies that the x-component of all the wavevectors is the same, namely κ_x, so that the wavevectors (2.9) and (2.11) in the semiconductor have the form $\mathbf{k}=(\kappa_x,0,k_z)$ and $\boldsymbol{\beta}=(-\mathrm{i}\kappa_x,0,\beta_z)$. Their z-components are accordingly given by:

$$\kappa_z=\sqrt{\omega^2\mu_0\varepsilon^{\mathrm{i}}-\kappa_x^2}=\sqrt{\kappa^2-\kappa_x^2},\quad \kappa_z>0, \tag{3.1}$$

$$\begin{aligned} k_z&=\sqrt{\omega^2\mu_0\varepsilon+\mathrm{i}\omega\mu_0\sigma-\kappa_x^2}\\ &=\sqrt{k^2-\kappa_x^2},\quad \mathrm{Re}\ k_z>0, \end{aligned} \tag{3.2}$$

$$\begin{aligned} \beta_z&=\frac{1}{\lambda}\sqrt{1-\frac{\mathrm{i}\omega\varepsilon}{\sigma}+\kappa_x^2\lambda^2}\\ &=\sqrt{\beta^2+\kappa_x^2},\quad \mathrm{Re}\ \beta_z>0, \end{aligned} \tag{3.3}$$

while the reflected wave has the wavevector $(\kappa_x,0,-\kappa_z)$.

Consider first a TE wave, polarized in a direction parallel to the interface, *i.e.*, such that the incident electric field has only the component E_y. It is easy to check from Section 2.1 that this property also holds within the conductor for $\mathbf{E}$, and hence for $\mathbf{J}$; these quantities have only one component E_y or J_y, which depends on x and z. Since then $\mathrm{div}\ \mathbf{J}=0$, no free charges appear; in particular, for a metal with $\lambda=0$, there is no surface charge. Nothing is therefore changed in the distribution of fields and currents when λ becomes finite. This can be checked from the equations (2.2–2.15), in which we have $\rho=0$ everywhere. Thus $\mathbf{E}(\mathbf{r})$ and $\mathbf{J}(\mathbf{r})$ reduce to their propagative contributions $\mathbf{E}^{\mathrm{p}}(\mathbf{r})$ and $\mathbf{J}^{\mathrm{p}}(\mathbf{r})$, and the material behaves exactly as a metal with perfect screening which would have the same dielectric constant and the same conductivity.

We shall thus focus below on a TM wave with an oblique incidence $(\kappa_x\neq 0)$. The electric field lies in the incidence plane; for perfect screening $(\lambda=0)$, the normal components of $\mathbf{D}$ and of $\mathbf{J}$ are discontinuous and a surface charge is generated. For $\lambda\neq 0$, this charge is spread off, and we expect the e.m. field to be modified accordingly.

3.2 Distribution of fields and currents for TM waves

Since all the quantities that we are considering here depend on time and on the coordinate x only through

the factors $\mathrm{e}^{\pm \mathrm{i}(\kappa_x x-\omega t)}$, and since they do not depend on y, we can replace the convention (2.1) by

$$\mathbf{E}(\mathbf{r},t) = \mathrm{Re}\,\left[\mathbf{E}\,(z)\,\mathrm{e}^{\mathrm{i}(\kappa_x x-\omega t)}\right], \tag{3.4}$$

and likewise for $\mathbf{H}$, $\mathbf{J}$ and ρ. In the insulating region $z<0$, the non-vanishing components of the field have according to (2.2) the form:

$$H_y = \frac{\kappa E_0}{\omega\mu_0}\left(\mathrm{e}^{\mathrm{i}\kappa_z z} - R\mathrm{e}^{-\mathrm{i}\kappa_z z}\right), \tag{3.5}$$

$$E_x = \frac{\kappa_z}{\kappa}E_0\left(\mathrm{e}^{\mathrm{i}\kappa_z z} + R\mathrm{e}^{-\mathrm{i}\kappa_z z}\right),$$

$$E_z = -\frac{\omega\mu_0\kappa_x}{\kappa^2}H_y\,, \tag{3.6}$$

where κ_z is defined by (3.1) and κ by (2.7). The reflection coefficient R remains to be determined. For the incident wave, the component of the Poynting vector (2.17) normal to the interface is:

$$N_z^{\mathrm{i}} = \frac{\kappa_z}{2\omega\mu_0}\left|E_0\right|^2. \tag{3.7}$$

We use the procedure sketched in Section 2.1 to determine the field on the conducting side $z>0$. We first obtain the magnetic field, by using (2.8, 3.2) and by matching its value at $z=0$ with that of (3.5), as

$$H_y = \frac{\kappa E_0}{\omega\mu_0}\left(1-R\right)\mathrm{e}^{\mathrm{i}k_z z}. \tag{3.8}$$

The charge density, obtained from (2.10), has the form

$$\rho = c\,\mathrm{e}^{-\beta_z z}, \tag{3.9}$$

where β_z is defined by (3.3), and we find the coefficient c by writing that J_z, given by (2.14, 2.15), vanishes at $z=0$. This yields, using (3.8, 3.9),

$$c = \frac{\sigma}{\sigma-\mathrm{i}\omega\varepsilon}\,\frac{\kappa_x\kappa\beta^2}{\omega^2\mu_0\beta_z}\,E_0\left(1-R\right). \tag{3.10}$$

Altogether $\mathbf{E}$ and $\mathbf{J}$ are obtained by means of (2.12–2.15), using the definitions (3.1–3.3), as:

$$\frac{E_x^{\mathrm{p}}}{k_z} = \frac{E_z^{\mathrm{p}}}{-\kappa_x} = \frac{J_x^{\mathrm{p}}}{k_z\sigma} = \frac{J_z^{\mathrm{p}}}{-\kappa_x\sigma} = \frac{\kappa}{k^2}\,E_0\left(1-R\right)\mathrm{e}^{\mathrm{i}k_z z}, \tag{3.11}$$

$$\frac{E_x^{\mathrm{s}}}{-\mathrm{i}\kappa_x} = \frac{E_z^{\mathrm{s}}}{\beta_z} = \frac{J_x^{\mathrm{s}}}{\omega\varepsilon\kappa_x} = \frac{J_z^{\mathrm{s}}}{\mathrm{i}\omega\varepsilon\beta_z} = \frac{\sigma\kappa_x\kappa}{\mathrm{i}\omega\varepsilon k^2\beta_z}E_0\left(1-R\right)\mathrm{e}^{-\beta_z z}. \tag{3.12}$$

Finally, the reflection coefficient R is found by expressing the continuity of E_x across the interface. From (3.6), (3.11) and (3.12) we thus obtain:

$$R = \frac{C+D-B^*}{C+D-B}\,, \tag{3.13}$$

where we introduced the dimensionless quantities

$$B \equiv \frac{\mathrm{i}\kappa_z\kappa_x}{\kappa^2} = \mathrm{i}\left|B\right| = -B^*\,, \tag{3.14}$$

$$C \equiv -\frac{\mathrm{i}k_z\kappa_x}{k^2}\,, \tag{3.15}$$

$$D \equiv \frac{\mathrm{i}\sigma\kappa_x^3}{\omega\varepsilon k^2\beta_z} = \frac{\kappa_x^3}{\omega^2\mu_0\varepsilon\lambda^2\beta^2\beta_z}. \tag{3.16}$$

Remember that k, k_z, β and β_z given by (2.9, 3.2) and (3.3) are complex. We might have simplified the expression (3.13) by dividing out the numerator and denominator by $B=-B^*$ or by C, but (3.13) better exhibits the following structure that we shall encounter again for other geometries: the parameter B is associated with the dielectric region, the parameters C and D with the semiconductor; the effects of propagation and of screening are separated since C does not depend on the screening length and D vanishes with it.

The explicit expressions for the field and the current result from the replacement of $1-R$ by $-2B/\left(C+D-B\right)$ in equations (3.8–3.12). In the limit of a vanishingly short static screening length λ, D disappears and we can check on the expressions (3.11, 3.12) the features described at the end of Section 2.1. Note that the occurrence of a finite screening length not only produces the screening contributions (3.12) to $\mathbf{E}$ and $\mathbf{J}$ in a region of thickness λ near the interface, but also *modifies the propagative contributions* (3.5, 3.6, 3.8) and (3.11) in both materials through the parameter D which enters the reflection coefficient (3.13).

3.3 Expressions for energy exchanges

Let us write the energy flux $\mathbf{N}$ of the field and the power $w\left(\mathbf{r}\right)$ that it yields to the carriers at each point, using the expressions of Section 2.2. We normalize the incident flux perpendicular to the interface, thus choosing the amplitude E_0 in (3.5, 3.6) so as to let (3.7) be equal to 1. Taking the time-average over a period suppresses, according to (3.4), the oscillations in the x-direction.

In the insulating region $z<0$, we have

$$N_x = \frac{\kappa_x}{\kappa_z}\left|1-R\mathrm{e}^{-2\mathrm{i}\kappa_z z}\right|, \tag{3.17}$$

which displays interferences between the incident and reflected waves, and

$$N_z = 1-\left|R\right|^2, \tag{3.18}$$

which does not depend on z. For $z>0$ the *energy flux* of the e.m. wave is given by:

$$N_x^{\mathrm{p}} = \frac{4\left|B\right|\kappa_x^2\mathrm{Re}\;k^{-2}}{\left|C+D-B\right|^2}\;\mathrm{e}^{-2\mathrm{Im}\;k_z z}\,, \tag{3.19a}$$

$$N_x^{\mathrm{s}} = \frac{4\left|B\right|}{\left|C+D-B\right|^2\kappa_x}\;\mathrm{Re}\;\left[D\beta_z\mathrm{e}^{-(\beta_z+\mathrm{i}k_z^*)z}\right], \tag{3.19b}$$

$$N_z^{\rm p} = \frac{4\,|B|\,{\rm Im}\ (-C)}{|C+D-B|^2}\,{\rm e}^{-2{\rm Im}\ k_z z}\,, \tag{3.20a}$$

$$N_z^{\rm s} = \frac{-4\,|B|}{|C+D-B|^2}\,{\rm Im}\ \left[D\,{\rm e}^{-(\beta_z+{\rm i}k_z^*)z}\right]. \tag{3.20b}$$

The tangential component has at the interface a discontinuity

$$N_x\,(+0) - N_x\,(-0) = |1-R|^2\,\frac{\kappa_x}{\kappa_z}\left(\frac{\varepsilon^{\rm i}}{\varepsilon}-1\right), \tag{3.21}$$

which vanishes only if $\varepsilon^{\rm i}=\varepsilon$, while we check from (3.13), (3.18) that the normal component N_z is continuous.

The *local dissipation rate* per unit volume and unit incident flux is readily found from (2.24), (2.25) and (3.20) as

$$w^{\rm p}\,(z) = \frac{8\,|B|\,{\rm Im}\ (-C)}{|C+D-B|^2}\,{\rm Im}\ k_z\,{\rm e}^{-2{\rm Im}\ k_z z}, \tag{3.22}$$

$$w^{\rm s}\,(z) = \frac{-4\,|B|}{|C+D-B|^2} \times{\rm Im}\ \left[D\,(\beta_z+{\rm i}k_z^*)\,{\rm e}^{-(\beta_z+{\rm i}k_z^*)z}\right], \tag{3.23}$$

and the *total power absorbed* by the material is checked to be

$$W = N_z\,(+0) = \frac{4\,|B|}{|C+D-B|^2} \times{\rm Im}\ (-C-D) = 1-|R|^2\,, \tag{3.24}$$

simply expressing the energy conservation.

The equations (3.23–3.24) illustrate the general properties exhibited in Section 2.2, and we shall discuss some of their physical consequences in Section 4. Let us simply note here that, according to (3.2) and (3.3), Re k_z, Im k_z, Re β_z and $-$Im β_z are positive. Note also the bounds

$$-\frac{3\pi}{4} < \arg C < 0, \quad 0 < \arg D < \frac{3\pi}{4}, \\ -\frac{\pi}{4} < \arg\,(-DC^*) < \frac{\pi}{2}, \tag{3.25} \\ -\frac{3\pi}{4} < \arg\,(C+D) < 0,$$

$$0 < \arg\,[D\,(\beta_z+{\rm i}k_z^*)] < \frac{5\pi}{4}, \tag{3.26}$$

on the phases of the various coefficients which appear in the above equations.

4 Plane wall: discussion

4.1 Increase or decrease of the overall absorption

Let us first consider the total absorption (3.24), also equal to (2.23). Using (3.26) we readily check that it is positive. As a consequence of (3.25), its two contributions

$$W^{\rm p} = \frac{4\,|B|\,{\rm Im}\ (-C)}{|C+D-B|^2}, \quad W^{\rm s} = -\frac{4\,|B|\,{\rm Im}\ D}{|C+D-B|^2}\,, \tag{4.1}$$

have opposite signs. Through the introduction of the parameter D, the finiteness of the screening length has thus two consequences on the total absorption. On the one hand it produces the *negative screening term* $W^{\rm s}$ which always reduces the absorption. On the other hand the appearance of D in the reflection coefficient *indirectly affects the propagative term* $W^{\rm p}$ through its denominator. This term $W^{\rm p}$ is reduced if:

$$|D|^2 - 2{\rm Re}\ D^*\,(B-C) > 0; \tag{4.2}$$

it is otherwise enhanced. Note that (3.25) implies Re $D^*B>0$ and Re $(-D^*C)>0$.

Both effects therefore concur to reduce the absorption when the condition (4.2) is satisfied; they compete when it is violated. In order to discuss the latter case, we shall compare the total absorption W with the absorption W_0 that would take place in a material where $\lambda=0$, all other parameters remaining the same. We find

$$\frac{W-W_0}{W_0} = \frac{1}{|C+D-B|^2}\left[2{\rm Re}\ (-DC^*) - |D|^2 - \left(|B|^2+|C|^2\right)\frac{{\rm Im}\ D}{{\rm Im}\ (-C)}\right], \tag{4.3}$$

where each term in the bracket is positive on account of (3.25, 3.26).

We shall find convenient in the present section to discuss the equations in terms of the four real dimensionless parameters,

$$t \equiv \frac{2\kappa_z\kappa_x}{\kappa^2}\,, \quad \text{or} \quad t \equiv \sin 2\theta^{\rm i}\,, \quad {\rm tg}\ \theta^{\rm i} = \frac{\kappa_x}{\kappa_z}\,, \tag{4.4}$$

which is directly related to the incidence angle $\theta^{\rm i}$ of the incoming wave, u and s defined by

$$u \equiv \frac{\omega^2\mu_0\varepsilon}{\kappa_x^2}\,, \quad s \equiv \frac{\sigma}{\omega\varepsilon}\,, \tag{4.5}$$

which characterize the dielectric constant and the conductivity of the material for given ω and κ_x, and

$$v \equiv \frac{1}{\lambda^2\kappa_x^2}\,, \tag{4.6}$$

which characterizes its static screening length. The independent parameters s,t,u,v are positive, and $t\leqslant 1$. The normal wavenumbers k_z and β_z are then given by:

$$k_z = \kappa_x\sqrt{u\,(1+{\rm i}s)-1}\,, \\ \beta_z = \kappa_x\sqrt{v\,(1-{\rm i}s^{-1})+1}\,, \tag{4.7}$$

and the three complex parameters B, C and D introduced by (3.14–3.16) are expressed by:

$$B = \frac{{\rm i}t}{2}\,, \quad C = \frac{-{\rm i}\sqrt{u\,(1+{\rm i}s)-1}}{u\,(1+{\rm i}s)}, \\ D = \frac{{\rm i}s}{u\,(1+{\rm i}s)\,\sqrt{v\,(1-{\rm i}s^{-1})+1}}\cdot \tag{4.8}$$

We also introduce the notations

$$U \equiv \sqrt{(u-1)^2 + u^2 s^2} = \frac{|k_z|^2}{\kappa_x^2},$$
$$V \equiv \sqrt{(v+1)^2 + v^2 s^{-2}} \equiv \frac{|\beta_z|^2}{\kappa_x^2}, \tag{4.9}$$

which allow us to write:

$$\sqrt{2}\, k_z = \kappa_x \left(\sqrt{U+u-1} + \mathrm{i}\sqrt{U-u+1}\right), \tag{4.10a}$$
$$\sqrt{2}\, \beta_z = \kappa_x \left(\sqrt{V+v+1} - \mathrm{i}\sqrt{V-v-1}\right). \tag{4.10b}$$

We can then express the change (4.3) in the total absorption as:

$$\frac{W-W_0}{W_0} |C+D-B|^2 \frac{u^2 V}{s} [\sqrt{U+u-1} + s\sqrt{U-u+1}] = \frac{1}{\sqrt{V+v+1}} \times \left[\left(u - \frac{t^2u^2}{4}\right)(V+v+1) - \frac{V+1}{1+s^2} - \frac{t^2u^2}{4} v\right] - \frac{s^2(U+1)}{(1+s^2)\sqrt{U-u+1}}. \tag{4.11}$$

Let us first discuss the onset of the phenomenon, when the screening length λ *begins to increase*, starting from zero. If it is sufficiently small so that $\lambda\kappa_x \ll 1$ and $\lambda\kappa_x^2\sqrt{s} \ll |k_z|$, we have $v \gg 1$, hence $V \sim v\sqrt{1+s^{-2}}$. As $|D| \sim s^{3/2}\kappa_x^3 \lambda \left(1+s^2\right)^{-1/4} / |k|^2$ is then small, the inequality (4.2) is violated and we are in a situation of competition between the reduction of the absorption due to W^{s} and its enhancement due to the denominator in W^{p}. The last term of (4.11) can be neglected since $v \gg u$, so that the effect has the sign of:

$$W - W_0 \propto u\left(\frac{\sqrt{1+s^2}}{s} + 1\right) - \frac{1}{s\sqrt{1+s^2}} - \frac{t^2u^2}{4}\left(\frac{\sqrt{1+s^2}}{s} + 2\right). \tag{4.12}$$

Thus, depending on the positive parameters s, t, u defined by (4.4) and (4.5), with $t \leqslant 1$, the introduction of a finite (but small) screening length may either enhance the absorption if (4.12) is positive, or reduce it if (4.12) is negative. For given s, if u is smaller than $1 - s/\sqrt{1+s^2}$, the absorption is reduced for any t, that is, for any incidence angle; on the contrary if u takes a larger value, lying in the interval

$$\left|\frac{1}{2}u(1+s\sqrt{1+s^2}-s^2) - 1\right| < s\sqrt{2 - 2s(1+s^2)^{-1/2}}, \tag{4.13}$$

the absorption is enhanced for any $t\,(0 < t \leqslant 1)$; in the other two ranges of u, the enhancement takes place for values of t smaller than some bound. In particular, for $s \gg 1$, the region of enhancement is:

$$ut^2 < \frac{8}{3}, \tag{4.14}$$

which yields an upper bound for t if $u > \frac{8}{3}$, while enhancement takes place for any incidence angle if $u < \frac{8}{3}$. For $s \ll 1$, the absorption is enhanced if u lies between the bounds:

$$\frac{1}{\cos^2\theta^{\mathrm{i}}} \lesseqgtr u \lesseqgtr \frac{1}{\sin^2\theta^{\mathrm{i}}}, \qquad \text{for} \qquad \theta^{\mathrm{i}} \lesseqgtr \frac{\pi}{4}; \tag{4.15}$$

it is otherwise reduced.

Increasing values of λ, for which v is no longer large, make the negative term in $|D|^2$ of (4.3), or equivalently the last term of (4.11), significant. A typical case is the limit when the screening length is much larger than the skin depth, that is,

$$\mathrm{Re}\ \beta_z \ll \mathrm{Im}\ k_z, \tag{4.16}$$

or equivalently:

$$\sqrt{V+v+1} \ll \sqrt{U-u+1}. \tag{4.17}$$

This takes place in particular for $s \gg 1$ with finite u and v, or for $u \gg 1$ with finite s and v. We can readily check that (4.11) is then negative (at least if t is not too small). Hence, when the *screening length exceeds the skin depth,* the absorption becomes eventually *smaller* than for a vanishing screening length if (4.16) is satisfied, all other parameters being kept fixed.

Let us analyse this effect for $s \gg 1$ with finite u and v. The asymptotic forms

$$C \sim -\sqrt{\frac{\mathrm{i}}{us}}, \quad \mathrm{Re}\ D \sim \frac{1}{u\sqrt{v+1}}, \quad \mathrm{Im}\ D \sim \frac{3v+2}{2us\,(v+1)^{3/2}}, \tag{4.18a}$$

$$|C+D-B|^2 \sim \frac{t^2}{4} + \frac{1}{u^2\,(v+1)} \tag{4.18b}$$

provide as contributions (4.1) to the total absorption

$$\frac{W^{\mathrm{p}}}{W_0} \sim \left[1 + \frac{4}{t^2u^2\,(v+1)}\right]^{-1} = \left[1 + \left(\frac{\varepsilon^{\mathrm{i}}}{\varepsilon}\right)^2 \frac{\lambda^2\kappa_x^4}{\kappa_z^2\,(1+\lambda^2\kappa_x^2)}\right]^{-1}, \tag{4.19a}$$

$$\frac{W^{\mathrm{s}}}{W^{\mathrm{p}}} \sim \frac{-(3v+2)}{\sqrt{2us\,(v+1)^3}} = \frac{-\lambda\kappa_x^2\left(3+2\lambda^2\kappa_x^2\right)}{\sqrt{2\omega\mu_0\sigma\,(1+\lambda^2\kappa_x^2)^3}}, \tag{4.19b}$$

$$W_0 \sim \frac{4\sqrt{2}}{t\sqrt{us}} = \frac{2\sqrt{2}\kappa^2}{\kappa_z\sqrt{\omega\mu_0\sigma}}, \tag{4.19c}$$

where W_0 is the corresponding value for $\lambda = 0$. Due to the large value of s, the absorption coefficient W_0 is small; the reflection, of metallic type, is strong. However, *when* λ *becomes finite*, the absorption W further decreases, *the reflection* $|R|$ *further increases*, for two reasons:

(i) The contribution W^{p} is smaller than W_0 (Eq.(4.19a)), because the wave penetrates the medium with a *smaller amplitude* than for $\lambda = 0$. This can be seen from the increase (4.18b) of the factor $|C + D - B|^2$ which divides all the expressions of Section 3.3 giving the energy of the field in the medium. We can also see that the expressions (3.8–3.12) for the field itself contain the factor $1 - R = -2B/(C + D - B)$ which for $s \gg 1$ has a smaller modulus for finite v than for large v. Note that W^{p}/W_0 given by (4.19a) becomes small as $\left(\frac{\pi}{2} - \theta^{\mathrm{i}}\right)^2$ for grazing incidences, while W_0 increases as $\left(\frac{\pi}{2} - \theta^{\mathrm{i}}\right)^{-1}$.

(ii) The *direct effect* W^{s} of screening is *negative.* This term is, however, small compared to W^{p}, as shown by (4.19b). It is equal to the space-integral of the oscillatory contribution (3.23) to the local absorption $w^{\mathrm{s}}(z)$, and its sign indicates that the negative parts of $w^{\mathrm{s}}(z)$ slightly overcome its positive parts. Although locally $w^{\mathrm{s}}(z)$ can be larger than $w^{\mathrm{p}}(z)$ (Sect. 4.3), the dominant overall contribution is that of W^{p}.

4.2 Complete absorption

The fact that in some circumstances the finiteness of the screening length can enhance the absorption suggests us to look for the possibility of a complete absorption of a wave by a semiconductor or an ionic conductor. In such a situation, the incoming wave is *not reflected at all*, its whole energy being dissipated through the conductivity of the wall. We thus require $W = 1$ in (3.24), or $R = 0$, that is, from (3.13),

$$C + D = B^*. \tag{4.20}$$

Note first that, in a metal where the screening length λ vanishes we have $D = 0$, and C cannot equal B^*, since the equation $C = B^*$ implies either $k_z = \kappa_z$ or $k_z = \kappa_x^2/\kappa_z$ but k_z is not real if $\sigma \neq 0$. The condition (4.20) cannot then be satisfied, and the incident wave is always partly reflected (fully for $\sigma \to \infty$). On the other hand, if both materials are dielectrics, the reflection coefficient may vanish since $\sigma = 0$ allows the equation $C = B^*$ to have a solution: we then recover, through $\kappa_z/\kappa_x = \kappa_x/k_z$ the Brewster incidence angle. The extinction that we shall find, for finite values of the conductivity and the screening length, is of a different nature.

We shall discuss this problem in terms of the four independent dimensionless parameters s, t, u, v defined by (4.4–4.6). As functions of these variables, B, C and D are given by (4.8). In order to express that the reflection coefficient R vanishes, we have to impose on the four real variables s, t, u, v the two real equations (4.20), together with inequalities expressing that s, u, v must be positive and that $0 < t \leqslant 1$, not to speak of physical limitations about practical feasibility. We write the explicit form of the equations to be solved by multiplying (4.20) with $u(1 + \mathrm{i}s)$, then by using (4.10) to separate the real and imaginary parts. This yields:

$$\frac{tu}{\sqrt{2}} = \sqrt{U + u - 1} - \frac{s}{V}\sqrt{V + v + 1} = \frac{1}{s}\sqrt{U - u + 1} - \frac{1}{V}\sqrt{V - v - 1}, \tag{4.21}$$

where U and V were defined by (4.9).

We work out the solution of (4.21) and discuss the required inequalities in Appendix A, equations (A.1–A.20). The final solution is conveniently written by introducing the positive combinations

$$X \equiv \frac{1}{V\sqrt{2}}\sqrt{V + v + 1 + 2v^2 s^{-2}}, \tag{4.22a}$$

$$Y \equiv \frac{1}{V\sqrt{2}}\sqrt{V - v - 1}, \quad Z \equiv \frac{v}{V - v - 1}. \tag{4.22b}$$

We then find t and u as functions of s and v in the form

$$t = \frac{X - Y}{X(X - Y + YZ)}, \tag{4.23}$$

$$u = 2X(X - Y + YZ), \tag{4.24}$$

and the region of the plane (s, v) where this solution exists is characterized by

$$(X - Y)(X - 1) + XYZ \geqslant 0, \tag{4.25}$$

which expresses that $t \leqslant 1$. The other inequalities expressing that s, t, u, v are positive are automatically satisfied. It is shown in Appendix A that the condition (4.25) has the form:

$$v \leqslant v_{\max}(s), \tag{4.26}$$

where the curve $v = v_{\max}(s)$ is shown in Figure 1.

Thus, although the phenomenon is permitted, it requires special relations (4.22–4.25) between the various data to be satisfied. *For each pair* of variables $s \equiv \sigma/\omega\varepsilon$ and $v \equiv 1/\lambda^2\kappa_x^2$ lying in the region (4.26), we obtain *a single solution* for $t \equiv \sin 2\theta^{\mathrm{i}} = 2\kappa_z\kappa_x/\kappa^2$ and $u \equiv \omega^2\mu_0\varepsilon/\kappa_x^2$. For given λ and ε we can therefore determine in the region (4.26) a transverse wavelength (from v), a frequency ω (from u), a conductivity σ (from s), and a value of t such that the incident wave is fully absorbed. Actually, each $t < 1$ provides two solutions, associated with complementary angles of incidence θ^{i} and $\frac{\pi}{2} - \theta^{\mathrm{i}}$, and hence with two values for ε^{i} (or for $\kappa_z = \sqrt{\omega^2\mu_0\varepsilon^{\mathrm{i}} - \kappa_x^2}$), given by:

$$\frac{\varepsilon}{\varepsilon^{\mathrm{i}}} = u\sin^2\theta^{\mathrm{i}}, \quad \sin 2\theta^{\mathrm{i}} = t. \tag{4.27}$$

The boundary $t = 1$ of the allowed domain, that is, $s = 0$ and $v = v_{\max}(s)$, corresponds to an incidence angle of $\frac{\pi}{4}$.

A systematic analytic study of these equations is presented in Appendix A. There we give in particular

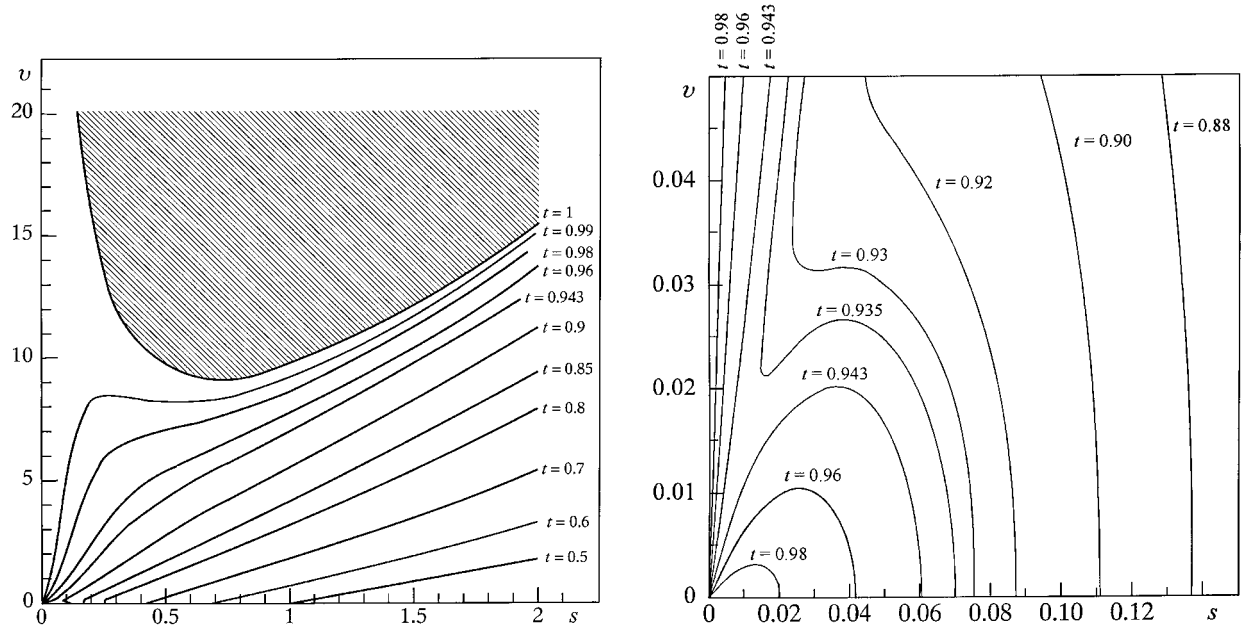

Fig. 1. Complete absorption in a wall. (i) The reflection coefficient R may vanish for any pair of values of $s \equiv \sigma/\omega\varepsilon$ and $v \equiv 1/\lambda^2\kappa_x^2$ such that $v \leqslant v_{\max}(s)$, provided t and u take the values (4.23, 4.24). We have drawn here, in the plane (s, v), the corresponding level lines for $t = \sin 2\theta^{\mathrm{i}}$, where the incidence angle θ^{i} is close to $\frac{\pi}{4}$ for $t \lesssim 1$, close to 0 or to $\frac{\pi}{2}$ for t small. The v -axis is a level line with $t = 1$. The shaded region, for which t would exceed 1, is forbidden. For $t < \frac{2}{3}\sqrt{2} \simeq 0.943$, each level line starts from the point $s = t^{-1} - 1$ of the s-axis. The plot on the right shows the vicinity of the origin; it exhibits the bending of the lines $t < \frac{2}{3}\sqrt{2}$, which eventually produces a kink directed towards the origin. For $1 > t \geqslant \frac{2}{3}\sqrt{2}$, two branches are issued from the origin (for $t = \frac{2}{3}\sqrt{2}$, their common slope is $\sqrt{3}$); the lower branch ends up on the s-axis, while the upper one passes round the forbidden region then goes on as $v \sim t^2 s^2$.

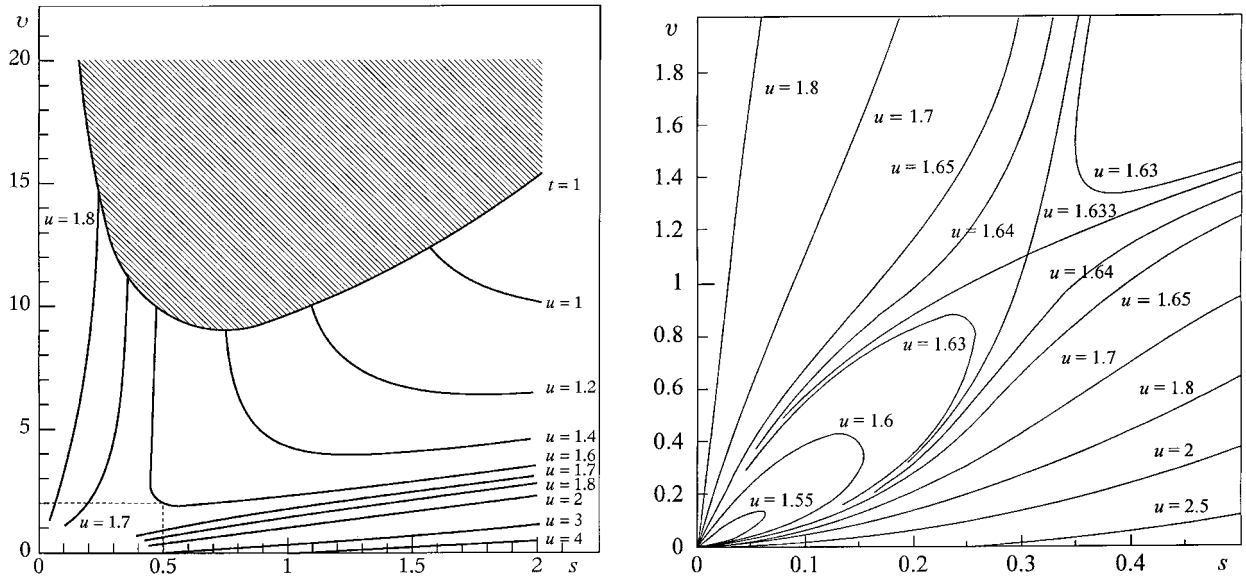

Fig. 2. Complete absorption in a wall. (ii) The level lines for $u = \omega^2\mu_0\varepsilon/\kappa_x^2 = \varepsilon/\varepsilon^{\mathrm{i}}\sin^2\theta^{\mathrm{i}}$ such that $R = 0$ are drawn in the plane (s, v). For $u > 2$, the level line starts from the point $s = \frac{u}{2} - 1$ of the s-axis. The level line $u = 2$ is tangent to the s-axis at the origin; furthermore, the v-axis is another level line with $u = 2$. The rectangle $s < 0.5, v < 2$ is enlarged on the right side. It shows that, as u decreases below 2, the two level lines, issued from the origin, get closer to each other so as to generate a saddle point for $u = 1.633$. For $1.633 > u > 1.5$, the two level lines consist of a closed loop and an open branch; only the latter survives for $u < 1.5$.

the asymptotic expressions of the various quantities, in the limits where s or v are either small or large (Eqs. (A.21–A.34)). Here we content ourselves with showing the maps (Figs. 1 and 2) which represent equations (4.23) and (4.24). The boundary (4.26) of the domain in which the reflection coefficient may vanish has a hyperbolic branch $v \sim 2.9 s^{-1}$ for $s \to 0$ and a parabolic branch $v \approx s^2 + 3.5 s$ for $s \to \infty$. The function $v_{\max}(s)$ has a minimum $v \simeq 9.0$ for $s \simeq 0.7$, so that total absorption is always possible when the screening length is sufficiently large so that $\lambda \kappa_x \gtrsim 0.33$. The range of values for the physical parameters which provide a vanishing reflection coefficient seems wide, so that it should be possible to exhibit the phenomenon experimentally.

We can easily check that the above results are compatible with those of Section 4.1, to wit, that the change (4.11) of the absorption with λ is positive when (4.23), (4.24) are satisfied. In particular, the ratio of the normal component of the screening length to the skin depth,

$$\frac{\text{Im } k_z}{\text{Re } \beta_z} = \sqrt{\frac{U-u+1}{V+v+1}}, \tag{4.28}$$

is expressed for $R = 0$ by

$$\begin{aligned} \frac{\text{Im } k_z}{\text{Re } \beta_z} &= \frac{s}{V}\sqrt{\frac{V+v+1+2v^2 s^{-2}}{V+v+1}} \\ &= \frac{s}{V}\sqrt{2V-2v-1}, \end{aligned} \tag{4.29}$$

where we used (A.19), (4.22a). In the plane (s, v), (4.29) is small as $\sqrt{2s^3/v}$ for $s \ll v$. It behaves as

$$\frac{\text{Im } k_z}{\text{Re } \beta_z} \approx \frac{1}{v+1}\sqrt{s^2 + \frac{v^3}{(v+1)^2}}$$

in both regions $v \ll 1$, finite s, and $s \gg 1$, arbitrary v. It may thus become large, as $s/(v+1)$, only in the region $s \gg v+1$. There t is small as $\sqrt{v+1}/s$ and u is large as $2s/(v+1)$ (see Eq.(A.33)). This is in agreement with Section 4.1, where we showed that the absorption cannot be larger than W_0 when $s \gg 1$ for fixed values of t, u and v.

4.3 Possibility of local cooling

We have seen in Section 3.3 that the time-averaged power given by the field to the charge carriers is at each point the sum of two contributions. The first one, $w^{\mathrm{p}}(z)$ given by (3.22), has the same exponential decrease $\exp[-2\text{Im } k_z z]$ as when the screening length vanishes, over a range equal to half the skin depth $[\text{Im } k_z]^{-1} \equiv \chi^{-1}$. Its coefficient may, however, be smaller or larger, depending whether the inequality (4.2) holds or not. The additional term, $w^{\mathrm{s}}(z)$ given by (3.23), which decreases exponentially as $\exp[-(\text{Im } k_z + \text{Re } \beta_z)\ z]$, displays moreover oscillations with the wavelength $2\pi(\text{Re } k_z + |\text{Im } \beta_z|)^{-1}$.

A remarkable situation occurs when the screening length $[\text{Re } \beta_z]^{-1}$ is much larger than the skin depth χ^{-1}, a property expressed by the condition (4.17). In this case, the decrease in $\mathrm{e}^{-\chi z}$ of $|w^{\mathrm{s}}(z)|$ is slower than that in $\mathrm{e}^{-2\chi z}$ of $w^{\mathrm{p}}(z)$; there exists a range where $|w^{\mathrm{s}}(z)|$ is larger than $w^{\mathrm{p}}(z)$, while remaining sizeable. Hence, we expect the occurrence of layers with thickness $\pi(\text{Re } k_z + |\text{Im } \beta_z|)^{-1}$ where $w(z)$ is *alternately positive and negative*. Thus, although on the whole the positive fraction $W = 1 - |R|^2$ of the power of the e.m. wave is dissipated in the medium, there are regions where the *carriers are cooled down* on average, under the action of the incident wave, instead of being heated. This is compensated for by the *overheating* of the intermediate layers. On the one hand, the diffusion current $\mathbf{J}^{\mathrm{s}}$ produced indirectly by the e.m. field may flow in a direction opposite to that of the propagating electric field $\mathbf{E}^{\mathrm{p}}$. On the other hand, the electric field $\mathbf{E}^{\mathrm{s}}$ produced by the motion of the screening charges may be directed against the ohmic current $\mathbf{J}^{\mathrm{p}}$. For such contributions to $w(z)$, the carriers are slowed down in their motion by an electric force. If (4.16) is satisfied, the expressions (3.22, 3.23) show the possibility of existence of regions where $w^{\mathrm{s}}(z)$ dominates $w^{\mathrm{p}}(z)$, that is, where this deceleration process is more efficient than the usual ohmic acceleration.

The same phenomenon can also be seen on the normal component (3.20) of the Poynting vector. Since $w(z) = -\partial N_z/\partial z$ (Eq. (2.18)), the existence of oscillations in $w(z)$ and the form of $N_z(z)$ imply that $N_z(z)$ is negative (positive) around values of z where $w(z)$ changes its sign by decreasing (increasing). At points z_1 where $N_z(z_1) < 0$, the *flow of energy* of the e.m. field is *opposite to the original direction* of propagation, due to a local predominance over $\mathbf{E}^{\mathrm{p}}$ of $\mathbf{E}^{\mathrm{s}}$, which is there both larger than $\mathbf{E}^{\mathrm{p}}$ and oriented differently. The matter lying in the region $z > z_1$ then receives on average a *negative power* from the field.

We have discussed so far only the exponential dependences on z of $w^{\mathrm{p}}, w^{\mathrm{s}}$, N_z^{p} and N_z^{s}, keeping aside the *amplitudes*. The ratio of the prefactors of N_z^{s} and N_z^{p} in (3.20) is

$$\frac{|D|}{\text{Im } (-C)} = \frac{\sqrt{2}\sqrt{1+s^2}\sqrt{U-u+1}}{(U+1)\sqrt{V}}, \tag{4.30}$$

and the ratio of the prefactors of w^{s} and w^{p} in (3.22), (3.23) is

$$\begin{aligned} \frac{|D(\beta_z + \mathrm{i}k_z^*)|}{2\text{Im } (-C)\,\text{Im } k_z} &= \frac{\sqrt{1+s^2}}{(U+1)\sqrt{V}}\Big[U+V \\ &+ \sqrt{(U-u+1)(V+v+1)} \\ &- \sqrt{(U+u-1)(V-v-1)}\Big]^{1/2}. \end{aligned} \tag{4.31}$$

For $s \gg 1$ with finite u and v, a typical situation where $\text{Re } \beta_z \ll \text{Im } k_z$, the ratio (4.30) behaves as $\sqrt{2s/u(v+1)}$ and (4.31) as $\sqrt{s/u(v+1)}$. These quantities are large, and hence the contributions $N_z^{\mathrm{s}}(z)$ and $w^{\mathrm{s}}(z)$ emerge still better. They may be important even at places where $N_z^{\mathrm{p}}(z)$ and $w^{\mathrm{p}}(z)$ have not yet been sunk by their exponential decrease. An example is shown in Figure 3.

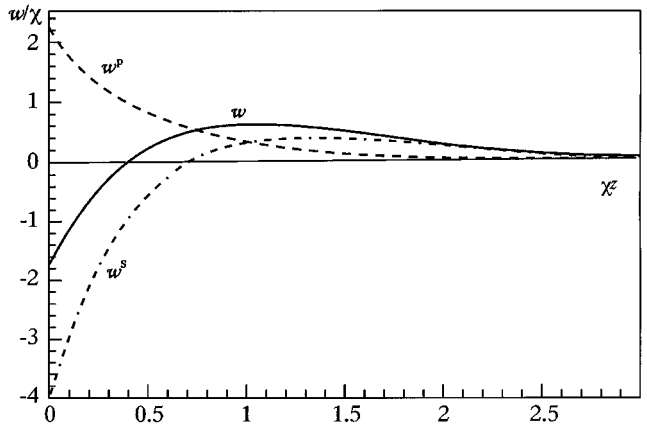

Fig. 3. Local exchanges of power between the field and the carriers. The dashed line shows the contribution $w^{\rm p}$ given by (3.22), which decreases as $\mathrm{e}^{-2\chi z}$ as function of the distance z to the interface, where $\chi = \mathrm{Im}\ k_z$ is the skin depth. The contribution $w^{\rm s}$ due to screening, given by (3.23) and shown by a dashed-dotted line, oscillates. The carriers are cooled in the regions where $w = w^{\rm p} + w^{\rm s}$, in solid line, is negative. The curves have been drawn for $s = 8,\ t = 1,\ u = 1,\ v = \frac{1}{2}$, which correspond to $\sigma = 8\omega\varepsilon,\ \theta^{\rm i} = \frac{\pi}{4},\ \varepsilon^{\rm i} = 2\varepsilon,\ \kappa\lambda = 2$, and the wavenumbers are $k_z/\kappa_x = 2 + 2\mathrm{i},\ \beta_z/\kappa_x = 1.23 - 0.03\mathrm{i}$.

Consider in particular the vicinity of the *interface*. The energy flux, expressed by (3.24), is there positive. However, the power yielded locally by the field to the carriers, given by (3.22, 3.23) as

$$\begin{aligned} w^{\rm p}(0) + w^{\rm s}(0) &= \frac{4\,|B|}{|C+D-B|^2} \\ &\times \{2\mathrm{Im}\ k_z \mathrm{Im}\ (-C) - \mathrm{Im}\ [D\,(\beta_z + \mathrm{i}k_z^*)]\} \\ &= \frac{4\left|BC^2\right| us\kappa_x}{|C+D-B|^2} \\ &\times \left[1 - \mathrm{Re}\ \frac{(s+\mathrm{i})}{\sqrt{u\,(1+\mathrm{i}s)-1}\sqrt{v\,(1-\mathrm{i}s^{-1})+1}}\right], \end{aligned} \quad (4.32)$$

may have either sign. As expected, it is positive if the screening length is short since $w^{\rm s} = 0$ for $v \gg 1$. However, it can be negative if v is finite. In particular, for $s \gg 1$ with fixed u and v, the negative screening term $w^{\rm s}(0)$ dominates the first one, so that the carriers are *cooled near the interface*, at the rate:

$$w(0) \sim -t\kappa_x \sqrt{\frac{2us}{v+1}} \left[\frac{t^2 u}{4} + \frac{1}{u\,(v+1)}\right]^{-1}. \quad (4.33)$$

As a consequence $N_z(z)$ *increases with* z near $z = 0$ in this case. The energy flux of the e.m. wave is enhanced there due to the field generated by the charges moving within the material. This excess of radiated energy balances for the local cooling of the layer below the interface.

Let us study more explicitly the local power exchange in the limit $s \gg 1$, with t, u, v remaining finite. Although in this case most of the energy is reflected, as shown by (4.19), the absorption is expected to take place anomalously. Indeed the energy flux (3.20) is then expressed by:

$$N_z^{\rm p}(z) \sim W^{\rm p}\mathrm{e}^{-2\chi z}, \quad \chi \equiv \sqrt{\frac{1}{2}us\kappa_x}, \quad (4.34a)$$

$$N_z^{\rm s}(z) \sim W^{\rm p}\sqrt{\frac{2s}{u\,(v+1)}}\mathrm{e}^{-\chi z}\sin\chi z, \quad (4.34b)$$

where the factor $W^{\rm p}$ is given by (4.19) and where the incident flux is taken as unity. We recover at $z = 0$ the value $N_z(0) \sim W \sim W^{\rm p}$, in agreement with (3.24) and (4.19). However, within the material, in the region where z is not too large compared to the skin depth, the flux is dominated by $N_z^{\rm s}$ which is much larger than $N_z^{\rm p}$. Its coefficient,

$$W^{\rm p}\sqrt{\frac{2s}{u\,(v+1)}} = \frac{8tu\sqrt{v+1}}{t^2u^2\,(v+1)+4},$$

is finite for $s \gg 1$, and smaller than 2, a value reached for $tu\sqrt{v+1} = 2$. As indicated above, it first *increases* with z in conjunction with the negative sign of $w(z)$. It reaches for $\chi z = \frac{\pi}{4}$ a maximum, which can be as high as $2e^{-\pi/4}\sin\frac{\pi}{4} \simeq 0,65$. Although the incident flux is nearly completely reflected and does not penetrate the medium, a significant fraction of this flux appears again at a distance from the interface equal to $\pi/4$ of the skin depth. Farther, between $\pi < \chi z < 2\pi$, the flux becomes *negative*, and the next oscillations are damped by the exponential factor.

The power $w(z)$ exchanged with the carriers is accordingly dominated in this limit by

$$w^{\rm s}(z) \sim 2W^{\rm p}\sqrt{\frac{s}{u\,(v+1)}}\chi\mathrm{e}^{-\chi z}\sin\left(\chi z - \frac{\pi}{4}\right), \quad (4.35)$$

which is much larger than the local Joule heating $w^{\rm p}(z) \sim 2W^{\rm p}\chi e^{-2\chi z}$. We recover the negative value (4.33) at $z = 0$. *Cooling* takes place for $\chi z < \pi/4$, then for $\frac{5\pi}{4} < \chi z < \frac{9\pi}{4}$, and so on, *heating* in the other intervals, in alternative layers. The prefactor in (4.35) is large as $\sqrt{s}$, so that the transfer of energy between field and carriers within each layer is of zeroth order in s, whereas the total Joule transfer $W^{\rm p}$ to the whole material is much smaller, in $1/\sqrt{s}$. In fact the integral of (4.35) from 0 to ∞ vanishes (it is equal to $N_z^{\rm s}(0)$). The phenomenon thus corresponds to a mere *transfer of heat* within the material, from the layers $\left(0, \frac{\pi}{4}\right)$, $\left(\frac{5\pi}{4}, \frac{9\pi}{4}\right)$, *etc.*, to the layers $\left(\frac{\pi}{4}, \frac{5\pi}{4}\right)$, *etc.* This transfer is *induced by the incoming wave,* which, however, hardly participates in the energy balance.

Let us further analyse the phenomenon by examining the configuration of the field and of the electric current in the considered limit $s \gg 1$, finite t, u, v. As for a metal, the wavevector $\mathbf{k} = (\kappa_x, 0, k_z)$ is nearly perpendicular to the interface since $k_z \sim \sqrt{\mathrm{i}us}\ \kappa_x \sim (1+\mathrm{i})\,\chi$. However the wavevector $\boldsymbol{\beta} = (-\mathrm{i}\kappa_x, 0, \beta_z)$ is oblique, with the finite ratio $\beta_z/\kappa_x \sim \sqrt{v+1}$; it is associated with propagation in the x-direction, damping in the z-direction. According to (3.11), (3.12) the electric field $\mathbf{E} = \mathbf{E}^{\rm p} + \mathbf{E}^{\rm s}$ and the

current density $\mathbf{J} = \mathbf{J}^{\mathrm{p}} + \mathbf{J}^{\mathrm{s}}$ have as components:

$$E_x^{\mathrm{p}} = J_x^{\mathrm{p}}/\sigma \propto \mathrm{e}^{\mathrm{i}k_z z}, \tag{4.36a}$$

$$E_x^{\mathrm{s}} = \frac{\kappa_x E_z^{\mathrm{s}}}{\mathrm{i}\beta_z} = \frac{J_x^{\mathrm{s}}}{\mathrm{i}\omega\varepsilon} = -\frac{\kappa_x J_z^{\mathrm{s}}}{\omega\varepsilon\beta_z} \propto \frac{D}{C}\mathrm{e}^{-\beta_z z}, \tag{4.36b}$$

where we dropped a common factor $\varepsilon^{\mathrm{i}} E_0 (1-R) k_z/\varepsilon (1+\mathrm{i}s)\kappa$ on the right-hand side; the components E_z^{p} and J_z^{p} are negligible. Since DC^{-1}, given by (4.18), is large as $\sqrt{s}$, and since $\mathrm{Im}\ k_z \gg \beta_z$, $\mathbf{E}^{\mathrm{s}}$ is much larger than $\mathbf{E}^{\mathrm{p}}$. Hence, the field $\mathbf{E} \simeq (E_x^{\mathrm{s}}, 0, E_z^{\mathrm{s}})$ is a longitudinal plane wave with its wavevector in the direction $\boldsymbol{\beta}$ of $\nabla\rho$. The current $\mathbf{J}$ is dominated within the skin $\chi z < \frac{1}{2}\ln us\,(v+1)$ by the contribution $\mathbf{J}^{\mathrm{p}} \simeq (J_x^{\mathrm{p}}, 0, 0)$, which has the same configuration as in a metal, namely flow in the x-direction and oscillations with damping in the z -direction; beyond, it has a tail $\mathbf{J} \simeq \mathrm{i}\omega\varepsilon\mathbf{E}$ in quadrature with $\mathbf{E}$. The dominant contribution to the local power transfer from the field to the carriers is then:

$$\begin{aligned} w(z) &\sim \mathrm{Re}\ \left(E_x^{\mathrm{s}}\ J_x^{\mathrm{p}*}\right) \propto \mathrm{Re}\ DC^{-1}\mathrm{e}^{-(\beta_z + \mathrm{i}k_z^*)z} \\ &\propto \mathrm{Re}\ \ \exp\left[-\sqrt{\mathrm{i}us}\ \kappa_x z - \mathrm{i}\frac{\pi}{4}\right], \end{aligned} \tag{4.37}$$

where we neglected $\beta_z \sim \kappa_z\sqrt{v+1}$ compared to k_z. We thus recover the behaviour (4.35). Likewise, the Poynting vector, which reduces to $\mathbf{N}(z) \sim \frac{1}{2}\mathrm{Re}\ [\mathbf{E}^{\mathrm{s}} \times \mathbf{H}^*]$, is not directed along $\mathbf{k}$, which is nearly in the z-direction as in a metal, but is perpendicular to $\boldsymbol{\beta}$ in the incidence plane. Among the various contributions to $w(z)$, the dominant one, (4.37), can be interpreted as follows. The charge carriers, characterized by the quasi-ohmic current $\mathbf{J} \sim \mathbf{J}^{\mathrm{p}}$, flow on average back and forth in the x-direction, with an exponential profile $\mathrm{e}^{-\chi z}$. They are submitted to the electric field $\mathbf{E} \sim \mathbf{E}^{\mathrm{s}}$, which is mainly produced by the diffusive motion of the screening charges, and which is oscillating like $\mathbf{J}$ as function of time and of x, but which is practically independent of z in the active region. There exists therefore a relative phase, varying as $\mathrm{i}k_z z$, between the oscillations of $\mathbf{E}$ and $\mathbf{J}$. Thus, depending on the value of z, the charge carriers are on average accelerated or decelerated in their motion along x by the screening electric field. This interpretation of the dominant contribution (4.37) to the power exchanges should, however, not hide the fact that E_x^{s} and J_x^{p} are coupled by the equations of Section 2.1 to the other components of $\mathbf{E}$ and $\mathbf{J}$ which, although smaller, contribute to control the effect.

Note finally that local cooling may take place for other values of the parameters than in the case $s \gg 1$, finite t, u, v that we just studied. This effect does not even require the total absorption rate W to be smaller than the value W_0 associated with a vanishing screening length. In particular, it can occur in the extreme case $W = 1$ of a complete absorption (Sect. 4.2), at least in the region $s \gg v+1,\ t \sim \sqrt{v+1}/s,\ u \sim 2s/(v+1)$ where (4.29) is large. Although the whole energy flux of the incoming wave then enters the material and is dissipated inside, the flux for $z > 0$,

$$N_z(z) \sim \mathrm{e}^{-2\chi z} + \mathrm{e}^{-\chi z}\sin\chi z, \tag{4.38}$$

where $\chi \equiv \kappa_x\sqrt{us/2} = s\kappa_x/\sqrt{v+1}$, and the local dissipation rate

$$w(z) \sim 2\chi\mathrm{e}^{-2\chi z} + \chi\sqrt{2}\mathrm{e}^{-\chi z}\sin\left(\chi z - \frac{\pi}{4}\right), \tag{4.39}$$

may again become negative at places. However the coefficients of both contributions have here comparable sizes; moreover the effect is expected to take place only at a distance from the interface larger than $z = 3.95\chi^{-1}$, where the damping is already strong.

5 Spherical inclusion

5.1 Determination of the fields and scattering amplitudes

We now turn to another simple geometry, a spherical piece of semiconductor or ionic conductor embedded in a dielectric medium. The case of a metallic sphere in the optical regime, near the main plasma resonance, has some mathematical similarity with the forthcoming analysis; it has been dicussed in reference [6]. We shall study the scattering and the absorption of a plane wave by this sphere. We shall take advantage of the rotational invariance by means of an angular momentum analysis, using for the vector spherical harmonics the conventions:

$$\begin{aligned} \mathbf{X}_{lm} &= -\frac{\mathrm{i}\mathbf{r}\times\nabla Y_{lm}}{\sqrt{l(l+1)}}, \\ \mathbf{Y}_{lm}^{\mathrm{t}} &= \frac{r\nabla Y_{lm}}{\sqrt{l(l+1)}}, \\ \mathbf{Y}_{lm}^{\mathrm{r}} &= \frac{\mathbf{r}}{r}Y_{lm}. \end{aligned} \tag{5.1}$$

We dropped for shorthand the argument $(\theta, \varphi) \equiv \hat{\mathbf{r}}$ in the scalar spherical harmonics Y_{lm} and in the vector ones $\mathbf{X}_{lm}, \mathbf{Y}_{lm}^{\mathrm{t}}$ and $\mathbf{Y}_{lm}^{\mathrm{r}}$. The latter quantities constitute an orthonormal basis for the vector fields on the unit sphere, and are related to the standard vector spherical harmonics $\mathbf{Y}_{jm}^{l}$ by:

$$\begin{aligned} \mathbf{Y}_{lm}^{\mathrm{t}} &= \sqrt{\frac{l+1}{2l+1}}\mathbf{Y}_{lm}^{l-1} + \sqrt{\frac{l}{2l+1}}\mathbf{Y}_{lm}^{l+1}, \\ \mathbf{Y}_{lm}^{\mathrm{r}} &= \sqrt{\frac{l}{2l+1}}\mathbf{Y}_{lm}^{l-1} - \sqrt{\frac{l+1}{2l+1}}\mathbf{Y}_{lm}^{l+1}. \end{aligned} \tag{5.2}$$

The vector harmonics $\mathbf{Y}_{lm}^{\mathrm{r}}\,(l \geqslant 0)$ are radial, while $\mathbf{X}_{lm}$ and $\mathbf{Y}_{lm}^{\mathrm{t}}\,(l \geqslant 1)$ are transverse, perpendicular at each point to $\mathbf{r}/r$. Their parities are $(-)^{l+1}$ for $\mathbf{X}_{lm}, (-)^{l}$ for $\mathbf{Y}_{lm}^{\mathrm{r}}$ and $\mathbf{Y}_{lm}^{\mathrm{t}}$. We shall also use the following equations of differential calculus, where f denotes any function of

the radial coordinate r:

$$\begin{aligned}&\text{div } \mathbf{X}f = 0,\\ &\text{curl } \mathbf{X}f = \mathrm{i}\mathbf{Y}^{\mathrm{t}}\left(f' + \frac{f}{r}\right) + \mathrm{i}\sqrt{l\,(l+1)}\mathbf{Y}^{\mathrm{r}}\,\frac{f}{r},\end{aligned} \tag{5.3a}$$

$$\begin{aligned}&\text{div } \mathbf{Y}^{\mathrm{t}}f = -\sqrt{l\,(l+1)}Y\frac{f}{r},\\ &\text{curl } \mathbf{Y}^{\mathrm{t}}f = \mathrm{i}\mathbf{X}\left(f' + \frac{f}{r}\right),\end{aligned} \tag{5.3b}$$

$$\begin{aligned}&\text{div } \mathbf{Y}^{\mathrm{r}}f = Y\left(f' + \frac{2f}{r}\right),\\ &\text{curl } \mathbf{Y}^{\mathrm{r}}f = -\mathrm{i}\sqrt{l\,(l+1)}\mathbf{X}\,\frac{f}{r};\end{aligned} \tag{5.3c}$$

for shorthand, we dropped the coordinates $\hat{\mathbf{r}}$ and r as well as the double index lm, which is the same in (5.3) for the scalar spherical harmonics Y and the three vector harmonics. Spherical waves with (real or complex) wavenumber k will be expressed in terms of the spherical Bessel functions $j_l\,(kr)\,, h_l^{(\pm)}\,(kr)$, defined with the conventions:

$$\begin{aligned}j_l\,(z) &= \sqrt{\frac{\pi}{2x}}\,J_{l+\frac{1}{2}}\,(z)\\ &= \frac{1}{2\mathrm{i}}\left[h_l^{(+)}\,(z) - h_l^{(-)}\,(z)\right],\end{aligned} \tag{5.4a}$$

$$\begin{aligned}h_l\,(z) &\equiv h_l^{(+)}\,(z)\,,\\ h_l^{(\pm)}\,(z) &= \sum_{p=0}^{l}\frac{(\mp\mathrm{i})^{l-p}\,(l+p)!}{2^p p!\,(l-p)!}\,\frac{\mathrm{e}^{\pm\mathrm{i}z}}{z^{p+1}}.\end{aligned} \tag{5.4b}$$

Let us first write the multipolar expansion of the incident plane wave, together with the outgoing wave scattered by the conducting sphere with radius R. We assume the incident wave to propagate in the z-direction, as $\mathrm{e}^{\mathrm{i}\kappa z}$ where κ is defined by (2.7), and to be circularly polarized; the polarization is denoted by $\epsilon = +1$ (or -1) for the right (or left) direction. We normalize the electric field of the plane wave in such a way that its time-dependent value in the plane $z = 0$ is $\left(\frac{1}{\sqrt{2}}E_0\cos\omega t, \epsilon\frac{1}{\sqrt{2}}E_0\sin\omega t, 0\right)$ and the incident energy flux is $\kappa E_0^2/2\omega\mu_0$. The corresponding solution of (2.2) for the e.m. field in the dielectric region $r > R$ has then the general form:

$$\mathbf{E}(\mathbf{r}) = E_0\sum_{l\geqslant 1}\,\mathrm{i}^l\,\sqrt{2\pi\,(2l+1)}\,\left[\mathbf{E}_{l\epsilon\mathrm{e}}(\mathbf{r}) + \mathbf{E}_{l\epsilon\mathrm{m}}(\mathbf{r})\right], \tag{5.5a}$$

$$\mathbf{E}_{l\epsilon\mathrm{e}}(\mathbf{r}) = \epsilon\kappa^{-1}\mathrm{curl}\left\{\mathbf{X}_{l\epsilon}\,(\hat{\mathbf{r}})\,\left[j_l\,(\kappa r) + A_{l\mathrm{e}}h_l\,(\kappa r)\right]\right\}, \tag{5.5b}$$

$$\mathbf{E}_{l\epsilon\mathrm{m}}(\mathbf{r}) = \mathbf{X}_{l\epsilon}\,(\hat{\mathbf{r}})\,\left[j_l\,(\kappa r) + A_{l\mathrm{m}}h_l\,(\kappa r)\right], \tag{5.5c}$$

$$\mathbf{H}(\mathbf{r}) = \frac{\kappa E_0}{\mathrm{i}\omega\mu_0}\,\sum_{l\geqslant 1}\,\mathrm{i}^l\,\sqrt{2\pi\,(2l+1)}\,\left[\mathbf{H}_{l\epsilon\mathrm{e}}(\mathbf{r}) + \mathbf{H}_{l\epsilon\mathrm{m}}(\mathbf{r})\right], \tag{5.6a}$$

$$\mathbf{H}_{l\epsilon\mathrm{e}}(\mathbf{r}) = \epsilon\mathbf{X}_{l\epsilon}\,(\hat{\mathbf{r}})\,\left[j_l\,(\kappa r) + A_{l\mathrm{e}}h_l\,(\kappa r)\right], \tag{5.6b}$$

$$\mathbf{H}_{l\epsilon\mathrm{m}}(\mathbf{r}) = \kappa^{-1}\,\mathrm{curl}\,\mathbf{E}_{l\epsilon\mathrm{m}}(\mathbf{r})\,. \tag{5.6c}$$

The terms in $j_l\,(\kappa r)$ describe the plane wave, those in $h_l\,(\kappa r)$ the outgoing partial waves. We denote by the indices $l\epsilon\mathrm{e}$ with $\epsilon \pm 1$ the electric 2^l -polar contribution; its magnetic field (5.6b) is transverse (TM mode), while the corresponding electric field (5.5b) is a combination of radial and transverse vector harmonics $\mathbf{Y}^{\mathrm{r}}$ and $\mathbf{Y}^{\mathrm{t}}$ given by (5.3a). Symmetrically, for the magnetic 2^l-polar contribution, denoted $l\epsilon\mathrm{m}$, the electric field (5.5c) is transverse (TE mode), while the magnetic field (5.6c) is oblique. The specific angular dependence of the outgoing waves and the fact that their coefficients $A_{l\mathrm{e}}$ and $A_{l\mathrm{m}}$ are the same for both polarizations result from the symmetries of the problem. These amplitudes are related to the eigenvalues of the S-matrix by $S = 1 + 2\mathrm{i}A$. We show below that they are given by (5.14), (5.15).

We determine the scattering amplitudes $A_{l\mathrm{e}}$ and $A_{l\mathrm{m}}$ by proceeding along the lines of Section 2.1. We first write the magnetic field within the semiconductor or ionic conductor which lies in $r < R$. Its multipolar expansion is identical with (5.6a), and the coefficient of each term is obtained by matching its tangential components with (5.6b) or (5.6c) at $r = R$:

$$\begin{aligned}\mathbf{H}_{l\epsilon\mathrm{e}}(\mathbf{r}) &= \epsilon b_{l\mathrm{e}}\,\mathbf{X}_{l\epsilon}\,(\hat{\mathbf{r}})\,j_l\,(kr)\,,\\ b_{l\mathrm{e}} &= \frac{j_l\,(\kappa R) + A_{l\mathrm{e}}\,h_l\,(\kappa R)}{j_l\,(kR)},\end{aligned} \tag{5.7a}$$

$$\mathbf{H}_{l\epsilon\mathrm{m}}(\mathbf{r}) = \kappa^{-1}\,b_{l\mathrm{m}}\,\mathrm{curl}\,\mathbf{X}_{l\epsilon}\,(\hat{\mathbf{r}})\,j_l\,(kr)\,, \tag{5.7b}$$

$$b_{l\mathrm{m}} = \frac{\kappa R\,[j_l'\,(\kappa R) + A_{l\mathrm{m}}\,h_l'\,(\kappa R)] + j_l\,(\kappa R) + A_{l\mathrm{m}}\,h_l\,(\kappa R)}{kRj_l'\,(kR) + j_l\,(kR)}. \tag{5.7c}$$

The wavenumber k was defined in (2.9).

We next write the general form for the charge density for $r < R$, which is a solution of (2.10) where β is the dynamical screening length (2.11):

$$\rho\,(\mathbf{r}) = \epsilon\beta\varepsilon E_0\sum_{l\geqslant 1}\mathrm{i}^l\sqrt{2\pi\,(2l+1)}c_l Y_{l\epsilon}\,(\hat{\mathbf{r}})\,j_l\,(\mathrm{i}\beta r)\,. \tag{5.8}$$

The coefficients c_l will be obtained by cancelling the radial component $r = R$ of the current (2.14, 2.15). However, the contribution $\mathbf{J}^{\mathrm{p}}$ to this current, which is proportional to curl $\mathbf{H}$, has a radial component which arises solely from the electric multipolar terms (5.7a), because the magnetic term curl curl$\mathbf{X}_{l\epsilon}j_l$ generated by (5.7b) is equal to $k^2\mathbf{X}_{l\epsilon}j_l$ and is thus purely transverse. The coefficients c_l in (5.8) are therefore coupled to the amplitudes $A_{l\mathrm{e}}$ only. The scattering of the *magnetic multipolar* partial waves, for which

the electric field is transverse, *is not affected* by the occurrence of a finite screening length λ. The amplitudes $A_{l\mathrm{m}}$ are the same as for $\lambda = 0$, and the magnetic multipolar contributions to ρ, to $\mathbf{E}^{\mathrm{s}}$ and to $\mathbf{J}^{\mathrm{s}}$ vanish. The situation is the same as in Section 3.1, where a plane wave, linearly polarized in a direction parallel to the plane wall, did not feel the finiteness of the screening length because no charge density appeared anyhow. Here, instead of the polarization, it is the electric or magnetic multipolarity which governs the effect of screening.

Expressing $\mathbf{J}$ by means of (2.14, 2.15, 5.7a, 5.8) and using (5.1, 5.3) to impose that the radial component of $\mathbf{J}$ vanishes at $r = R$, we find:

$$c_l = \frac{\mathrm{i}\sqrt{l\,(l+1)}s\kappa}{k^2 R} \times \frac{j_l\,(\kappa R) + A_{l\mathrm{e}} h_l\,(\kappa R)}{j_l'\,(\mathrm{i}\beta R)}, \tag{5.9}$$

where β was defined in (2.11) and $s \equiv \sigma/\omega\varepsilon$ as in (4.5). The determination of the parameters $A_{l\mathrm{e}}$ and $A_{l\mathrm{m}}$ is achieved by imposing the continuity at $r = R$ of the tangential components of the electric field (2.12, 2.13), itself expressed in terms of (5.7) and (5.8). Using again (5.1) and (5.3) we obtain:

$$\frac{\kappa^2}{k^2} b_{l\mathrm{e}} \left[kRj_l'\,(kR) + j_l\,(kR)\right] + \frac{\sqrt{l\,(l+1)}\,\kappa}{\mathrm{i}\beta} c_l j_l\,(\mathrm{i}\beta R)$$
$$= \kappa R\left[j_l'\,(\kappa R) + A_{l\mathrm{e}} h_l'\,(\kappa R)\right] + j_l\,(kR) + A_{l\mathrm{e}} h_l\,(\kappa R)\,,$$

$$b_{l\mathrm{m}} j_l\,(kR) = j_l\,(\kappa R) + A_{l\mathrm{m}} h_l\,(\kappa R)\,.$$

The replacement of $b_{l\mathrm{e}}, b_{l\mathrm{m}}$ and c_l by (5.7a, 5.7c) and (5.9) yields:

$$\frac{j_l'\,(\kappa R) + A_{l\mathrm{e}} h_l'\,(\kappa R)}{\kappa R\left[j_l\,(\kappa R) + A_{l\mathrm{e}} h_l\,(\kappa R)\right]} + \frac{1}{(\kappa R)^2} = C_l + D_l, \tag{5.10}$$

$$\frac{\kappa R\left[j_l'\,(\kappa R) + A_{l\mathrm{m}} h_l'\,(\kappa R)\right]}{j_l\,(\kappa R) + A_{l\mathrm{m}} h_l\,(\kappa R)} = \frac{kRj_l'\,(kR)}{j_l\,(kR)}, \tag{5.11}$$

where we defined

$$C_l \equiv \frac{j_l'\,(kR)}{kRj_l\,(kR)} + \frac{1}{(kR)^2}, \tag{5.12}$$

$$D_l \equiv \frac{l\,(l+1)\,s}{(kR)^2\,\beta R}\,\frac{j_l\,(\mathrm{i}\beta R)}{j_l'\,(\mathrm{i}\beta R)}. \tag{5.13}$$

Hence, using the Wronskian relation (B.3) recalled in Appendix B, we find:

$$A_{l\mathrm{e}} = -\frac{j_l\,(\kappa R)}{h_l\,(\kappa R)} + \frac{1}{(\kappa R)^3\left[h_l\,(\kappa R)\right]^2} \times \frac{1}{C_l + D_l - B_l}, \tag{5.14}$$

$$A_{l\mathrm{m}} = -\frac{j_l\,(\kappa R)}{h_l\,(\kappa R)} + \frac{1}{(\kappa R)\left[h_l\,(\kappa R)\right]^2} \times \frac{1}{(kR)^2 C_l - (\kappa R)^2 B_l}, \tag{5.15}$$

with

$$B_l \equiv \frac{h_l'\,(\kappa R)}{\kappa R h_l\,(\kappa R)} + \frac{1}{(\kappa R)^2}\,. \tag{5.16}$$

The fields are thus completely determined for $r > R$ by (5.5, 5.6, 5.14, 5.15). For $r < R$, the magnetic field is given by (5.6a, 5.7, 5.14, 5.15). The electric multipolar components of the electric field for $r > R$, including both propagative and screening contributions are obtained from (5.7–5.9, 5.14) as:

$$\mathbf{E}^{\mathrm{p}}_{l\epsilon\mathrm{e}}\,(\mathbf{r}) = \frac{\epsilon R\ \mathrm{curl}\left[\mathbf{X}_{l\epsilon}\,(\hat{\mathbf{r}})\,j_l\,(kr)\right]}{(\kappa R)^2\,h_l\,(\kappa R)\,(kR)^2\,j_l\,(kR)\left[C_l + D_l - B_l\right]}, \tag{5.17}$$

$$\mathbf{E}^{\mathrm{s}}_{l\epsilon\mathrm{e}}\,(\mathbf{r}) = \frac{\epsilon \mathrm{i} R\ D_l\ \nabla\left[Y_{l\epsilon}\,(\hat{\mathbf{r}})\ \ j_l\,(\mathrm{i}\beta r)\right]}{(\kappa R)^2\ \ h_l\,(\kappa R)\,\sqrt{l\,(l+1)}\,j_l\,(\mathrm{i}\beta R)\left[C_l + D_l - B_l\right]}, \tag{5.18}$$

and its magnetic multipolar components, purely propagative, are obtained from (5.7, 5.15) as:

$$\mathbf{E}_{l\epsilon\mathrm{m}}\,(\mathbf{r}) = \frac{\mathbf{X}_{l\epsilon}\,(\hat{\mathbf{r}})\,j_l\,(kr)}{(\kappa R)\,h_l\,(\kappa R)\,j_l\,(kR)\left[(kR)^2 C_l - (\kappa R)^2 B_l\right]}\,. \tag{5.19}$$

The current density is expressed by $\mathbf{J}^{\mathrm{p}} = \sigma\mathbf{E}^{\mathrm{p}}$ and, for the electric multipolar contributions, $\mathbf{J}^{\mathrm{s}} = \mathrm{i}\omega\varepsilon\mathbf{E}^{\mathrm{s}}$.

5.2 Radiated and absorbed energy

The power of the e.m. wave scattered in each direction by the semiconducting sphere is found by writing the large distance limit of the field (5.5, 5.6) and building the Poynting vector. The resulting, differential and total, *scattering cross-sections* read:

$$\frac{d\sigma}{d\hat{\mathbf{r}}} = \frac{2\pi}{\kappa^2}\left|\sum_{l\geqslant 1} \mathrm{i}^l\sqrt{2l+1}\left(A_{l\mathrm{e}}\mathbf{Y}^{\mathrm{t}}_{l\epsilon} - \epsilon A_{l\mathrm{m}}\mathbf{X}_{l\epsilon}\right)\right|^2, \tag{5.20}$$

$$\sigma_{\mathrm{tot}} = \frac{2\pi}{\kappa^2}\sum_{l\geqslant 1}(2l+1)\left[|A_{l\mathrm{e}}|^2 + |A_{l\mathrm{m}}|^2\right]. \tag{5.21}$$

The cross-sections are the same for both polarizations $\epsilon = \pm 1$. The screening length occurs only through the term D_l entering the *electric multipolar amplitudes* $A_{l\mathrm{e}}$ expressed by (5.14).

The *local dissipation rate* within the sphere $r < R$, averaged on time, is given by (2.24, 2.25). Let us write its angular average $\langle w\,(r)\rangle$, for a unit incident power flux, using the expressions (5.17–5.19) for $\mathbf{E}$ and $\mathbf{J}$. Angular integration cancels the cross-terms between the different

multipoles. The electric multipoles provide the two contributions:

$$\langle w_{\rm e}^{\rm p}(r)\rangle = \frac{{\rm Im}\ k^2}{2|k|^2\kappa^5 R^4}\sum_{l\geqslant 1}(2l+1) \times\frac{|krj_l'(kr)+j_l(kr)|^2+l(l+1)|j_l(kr)|^2}{r^2|h_l(\kappa R)\,kRj_l(kR)\,(C_l+D_l-B_l)|^2}, \tag{5.22}$$

$$\langle w_{\rm e}^{\rm s}(r)\rangle = \frac{1}{2\kappa^5 R^4}{\rm Re}\sum_{l\geqslant 1}\frac{(2l+1)\,{\rm i}D_l}{r^2|h_l(\kappa R)\,(C_l+D_l-B_l)|^2} \times\frac{d}{dr}\frac{rj_l({\rm i}\beta r)\,j_l(k^*r)}{j_l({\rm i}\beta R)\,j_l(k^*R)}, \tag{5.23}$$

while the magnetic multipoles provide:

$$\langle w_{\rm m}(r)\rangle = \frac{{\rm Im}\ k^2}{2\kappa^3 R^2} \times\sum_{l\geqslant 1}\frac{(2l+1)|j_l(kr)|^2}{|kRj_l'(kR)\,h_l(\kappa R)-\kappa Rj_l(kR)\,h_l'(\kappa R)|^2}. \tag{5.24}$$

The features of $\langle w(r)\rangle$ are similar to those that we found in Section 4.3 for the plane geometry. The propagative contributions $\langle w_{\rm e}^{\rm p}(r)\rangle$ and $\langle w_{\rm m}(r)\rangle$ are everywhere positive. For $|kR|\gg 1$, they decrease from the surface of the sphere towards the interior, as near the surface of the plane wall, but moreover display here some weak oscillations due to the interference of ingoing and outgoing waves. The screening length enters $\langle w_{\rm e}^{\rm p}(r)\rangle$ through D_l only; depending whether ${\rm Re}\ D_l^*(C_l-B_l)$ is positive or negative, $\langle w_{\rm e}^{\rm p}(r)\rangle$ is smaller or larger than the dissipation rate which would take place for a vanishing screening length. The screening contribution $\langle w_{\rm e}^{\rm s}(r)\rangle$ presents much more severe oscillations, since it may alternatively be positive and negative in space due to the interplay between the wavenumbers k and β. We shall see below (Sect. 5.3) that it may here again dominate the other contributions, so that the material is then cooled down at places.

The *total dissipation rate* W is obtained from (2.27, 2.28) by evaluating the flux through the interface $r=R$ of the Poynting vector, itself expressed in terms of the transverse components of the electric and magnetic field through (5.17–5.19, 5.6). For a unit incident flux, W is the absorption cross-section, and it is found to be the sum of the three contributions

$$W_{\rm e}^{\rm p}=\frac{2\pi}{\kappa^5 R^3}\sum_{l\geqslant 1}(2l+1)\frac{{\rm Im}\ (-C_l)}{|h_l(\kappa R)|^2|C_l+D_l-B_l|^2}, \tag{5.25}$$

$$W_{\rm e}^{\rm s}=-\frac{2\pi}{\kappa^5 R^3}\sum_{l\geqslant 1}(2l+1) \times\frac{{\rm Im}\ D_l}{|h_l(\kappa R)|^2|C_l+D_l-B_l|^2}, \tag{5.26}$$

$$W_{\rm m}=\frac{2\pi}{\kappa^3 R}\sum_{l\geqslant 1}(2l+1) \times\frac{{\rm Im}\ \left[-(kR)^2 C_l\right]}{|h_l(\kappa R)|^2\left|(kR)^2 C_l-(\kappa R)^2 B_l\right|^2}. \tag{5.27}$$

By making use of the Wronskian relations (B.3) and of the integrals (B.5–B.7) given in Appendix B, we can readily check that the expressions (5.25–5.27) are, respectively, the space integrals of the contributions (5.22–5.24) to the local dissipation rate.

Transforming the expressions (5.14, 5.15) by use of (5.4) and of

$$\frac{1}{(\kappa R)^3|h_l(\kappa R)|^2}={\rm Im}\ B_l \tag{5.28}$$

(see Eq. B.8), we can also relate the absorption cross-section W to the eigenvalues

$$S_{l{\rm e}}=1+2{\rm i}A_{l{\rm e}}=\frac{h_l^*(\kappa R)}{h_l(\kappa R)}\,\frac{C_l+D_l-B_l^*}{C_l+D_l-B_l}, \tag{5.29}$$

$$S_{l{\rm m}}=1+2{\rm i}A_{l{\rm m}} =\frac{h_l^*(\kappa R)}{h_l(\kappa R)}\,\frac{(kR)^2 C_l-(\kappa R)^2 B_l^*}{(kR)^2 C_l-(\kappa R)^2 B_l} \tag{5.30}$$

of the S-matrix, which are the ratios of the outgoing to the incoming partial waves. Indeed, (5.25–5.27) together with (5.18, 5.29) yield

$$W=\frac{\pi}{2\kappa^2}\sum_{l\geqslant 1}(2l+1)\left[\left(1-|S_{l{\rm e}}|^2\right)+\left(1-|S_{l{\rm m}}|^2\right)\right]. \tag{5.31}$$

We prove in Appendix B the inequalities

$$\begin{aligned}&{\rm Im}\ B_l>0,\quad {\rm Re}\ B_l<0,\\ &{\rm Im}\ C_l<\frac{-(l+1)\,{\rm Im}\ (kR)^2}{|kR|^4}<0,\\ &{\rm Im}\ (kR)^2 C_l<0,\quad 0<{\rm Im}\ D_l<\frac{(l+1)\,{\rm Im}\ (kR)^2}{|kR|^4},\\ &0<{\rm Im}\ (kR)^2 D_l<(l+1)\,s,\end{aligned} \tag{5.32}$$

whence we can check that

$$W_{\rm e}^{\rm p}>0,\ W_{\rm e}^{\rm s}<0,\ W_{\rm e}=W_{\rm e}^{\rm p}+W_{\rm e}^{\rm s}>0,\ W_{\rm m}>0, \tag{5.33}$$

which imply $|S|<1$. An alternative check of the positivity of the dissipation $W_{\rm e}$ relies on the fact that this quantity is the integral (2.23); the electric multipolar contribution to the angular average of $|\mathbf{J}|^2$ at the radius r is given by (2.22) as:

$$\frac{1}{2\sigma}\left\langle|\mathbf{J}_{\rm e}|^2\right\rangle=\langle w_{\rm e}(r)\rangle + \frac{1}{2\kappa^5R^4}{\rm Re}\sum_{l\geqslant1}\frac{(2l+1)\,{\rm i}D_l}{r^2\left|h_l(\kappa R)\left(C_l+D_l-B_l\right)\right|^2} \times\frac{1+{\rm i}s}{1-{\rm i}s}\quad\frac{d}{dr}\left\{r j_l({\rm i}\beta r)\left[\frac{j_l(kr)}{j_l({\rm i}\beta R)}-\frac{r j_l'({\rm i}\beta r)}{R j_l'({\rm i}\beta R)}\right]^*\right\}. \tag{5.34}$$

Note that, as for the plane wall (Eq.(4.1)), the contribution $W_{\rm e}^{\rm s}$ associated with a finite screening length λ is *negative*, whereas the propagative contribution $W_{\rm e}^{\rm p}$, which depends on the screening length λ through the term D_l in the denominator, may be either larger or smaller than the quantity $W_{\rm e}$ evaluated for $\lambda=0$.

5.3 Possibility of local cooling and overheating

Let us first consider the local dissipation rate (5.22–5.24), in the limit ${\rm Im}\,kR\gg1$, $|\beta|\ll{\rm Im}\,k$. Not too deep within the sphere, for values of r such that ${\rm Im}\,kr\gg1$ and such that $j_l({\rm i}\beta r)$ does not differ much from $j_l({\rm i}\beta R)$, the expressions (5.22–5.24) reduce to:

$$\langle w_{\rm e}^{\rm p}(r)\rangle\sim\frac{{\rm Im}\,k^2}{2|k|^2\kappa^5R^4} \times\sum_{l\geqslant1}\frac{(2l+1)\,{\rm e}^{-2{\rm Im}\;k(R-r)}}{\left|h_l(\kappa R)\left(C_l+D_l-B_l\right)\right|^2r^2}, \tag{5.35}$$

$$\langle w_{\rm e}^{\rm s}(r)\rangle\sim-\frac{1}{2\kappa^5R^3} \times{\rm Re}\sum_{l\geqslant1}\frac{(2l+1)\,k^*D_l{\rm e}^{-{\rm i}k^*(R-r)}}{\left|h_l(\kappa R)\left(C_l+D_l-B_l\right)\right|^2r^2}, \tag{5.36}$$

$$\langle w_{\rm m}(r)\rangle\sim\frac{{\rm Im}\,k^2}{2\kappa^3} \times\sum_{l\geqslant1}\frac{(2l+1)\,{\rm e}^{-2{\rm Im}\;k(R-r)}}{|h_l(\kappa R)|^2\left|(\kappa R)^2B_l+{\rm i}kR\right|^2r^2}. \tag{5.37}$$

As in the case of a plane wall (Sect. 4.3), the screening contribution (5.36) oscillates and decreases more slowly than the propagative contributions (5.35) and (5.37) when we penetrate the sphere, so that $w_{\rm e}(\mathbf{r})$ can be negative at places.

Here again, the phenomenon is especially marked if $s\gg1$. Assuming the other dimensionless parameters, $\omega^2\mu_0\varepsilon R^2, R/\lambda$ and κR to be finite, we then have

$$C_l\sim\frac{1}{{\rm i}kR},\quad D_l\sim\frac{l(l+1)}{\omega^2\mu_0\varepsilon R^2}\,\frac{\lambda j_l({\rm i}R/\lambda)}{{\rm i}Rj_l'({\rm i}R/\lambda)}, \tag{5.38}$$

so that $|C_l|\ll|D_l|$. Just below the surface of the sphere, for each l, the ratio of the screening and propagative contributions reads:

$$\frac{\langle w_{le}^{\rm s}(R)\rangle}{\langle w_{le}^{\rm p}(R)\rangle}\sim-{\rm Re}\;(k^*R\,D_l). \tag{5.39}$$

Here the quantity D_l is real and positive; according to (B.14), it is an increasing function of λ, with the two limits:

$$D_l\sim\frac{l(l+1)}{\omega^2\mu_0\varepsilon R^2}\,\frac{\lambda}{R},(\lambda\ll R); \qquad D_l\to\frac{l+1}{\omega^2\mu_0\varepsilon R^2},(\lambda\gg R). \tag{5.40}$$

Thus, under the considered conditions, the ratio (5.39) is a negative number and its absolute value is large. The electric to magnetic ratio, which for finite κR is equivalent to

$$\frac{\langle w_{le}^{\rm s}(R)\rangle}{\langle w_{l{\rm m}}(R)\rangle}\sim-\frac{1}{(\kappa R)^2\left|D_l-B_l\right|^2}{\rm Re}\;(k^*R\,D_l), \tag{5.41}$$

has also a large absolute value. Thus, the *local dissipation* near the surface, including both the electric and magnetic multipolar contributions, is *dominated by the screening contribution* (5.36) at least for $s\gg1$ and finite $\omega^2\mu_0\varepsilon R^2,\ R/\lambda,\ \kappa R$. For r not too deep within the sphere, the use of (5.28) in (5.36) yields the behaviour:

$$\langle w(r)\rangle\sim-\frac{1}{2\kappa^2}{\rm Re}\sum_{l\geqslant1}\frac{(2l+1)\,({\rm Im}\;B_l)\,k^*\;D_l{\rm e}^{-{\rm i}k^*(R-r)}}{\left|D_l-B_l\right|^2r^2}. \tag{5.42}$$

The material lying *in the superficial shell* of the sphere, ${\rm Re}\,k(R-r)<\frac{\pi}{4}$, is *cooled down* according to (5.42) under the effect of the incident e.m. wave. As in Section 4.2, this is compensated for by an overheating deeper inside.

Actually, after integration over space, the absorption cross-section (5.25–5.27) can be calculated in the above limit $s\gg1$, with $\omega^2\mu_0\varepsilon R^2,\ R/\lambda$ and κR finite, by expanding D_l in powers of $1/s$, using the Bessel equation (B.1). We thus find:

$$W_{\rm e}^{\rm p}\sim\frac{\pi\sqrt{2}}{|kR|\,\kappa^2}\sum_l\frac{(2l+1)\,{\rm Im}\;B_l}{\left|D_l-B_l\right|^2}, \tag{5.43}$$

$$W_{\rm e}^{\rm s}\sim-\frac{\pi}{|kR|\,\kappa^2}\sum_l\frac{(2l+1)\;l(l+1)\,{\rm Im}\;B_l}{\left|D_l-B_l\right|^2} \times\left\{\frac{\lambda j_l({\rm i}R/\lambda)}{{\rm i}Rj_l'({\rm i}R/\lambda)}-1-\frac{j_l^2({\rm i}R/\lambda)}{j_l'^2({\rm i}R/\lambda)}\left[1+\frac{l(l+1)\,\lambda^2}{R^2}\right]\right\}, \tag{5.44}$$

where according to (5.32) the curly bracket is a positive number smaller than $2/l$, and:

$$W_{\rm m}\sim\frac{\pi\sqrt{2}R^2}{|kR|}\sum_l(2l+1)\,{\rm Im}\;B_l. \tag{5.45}$$

As for the plane wall, the *screening contribution* $W_{\rm e}^{\rm s}$, of order $|kR|^{-2}$, *is negligible* compared to the propagative contribution $W_{\rm e}^{\rm p}$ and $W_{\rm m}$, of order $|kR|^{-1}$, although locally it is $\langle w_{\rm e}^{\rm p}(r)\rangle + \langle w_{\rm m}(r)\rangle$ which is negligible compared to $\langle w_{\rm e}^{\rm s}(r)\rangle$. The oscillations in (5.42) cancel one another upon integration, to the first two dominant orders in $|kR|$.

5.4 Inhibition of the scattering

The vanishing of the reflection coefficient that we studied for a plane wall in Section 4.2 has here two possible analogues, the minimization of the scattering, *i.e.*, the vanishing of some scattering amplitude, or the maximization of the absorption, *i.e.*, the vanishing of some elements of the S-matrix. Let us begin by searching whether a scattering amplitude can be cancelled. We can rewrite (5.10, 5.11), or equivalently (5.29, 5.30), using the wronkian (B.3), as

$$A_{l\rm e} = -\frac{j_l(\kappa R)}{h_l(\kappa R)}\,\frac{C_l + D_l - \hat{B}_l}{C_l + D_l - B_l}\,, \tag{5.46a}$$

$$A_{l\rm m} = -\frac{j_l(\kappa R)}{h_l(\kappa R)}\,\frac{(kR)^2 C_l - (\kappa R)^2 \hat{B}_l}{(kR)^2 C_l - (\kappa R)^2 B_l}\,, \tag{5.46b}$$

where we introduced the quantity

$$\hat{B}_l \equiv \frac{j_l'(\kappa R)}{\kappa R j_l(\kappa R)} + \frac{1}{(\kappa R)^2}\,, \tag{5.47}$$

which is real. However the inequalities (5.32) imply that $C_l + D_l$ as well as $(kR)^2 C_l$ have a negative imaginary part. Hence the right-hand sides of (5.46) and (5.47) can never vanish, and no scattering amplitude can exactly be zero.

Nevertheless, since Im D_l is positive, this discrepancy between the imaginary parts of $C_l + D_l$ and $\hat{B}_l$ in (5.46) is weaker than for the scattering amplitude $A_{l\rm e}^0$ which occurs when the screening length λ is negligible, and which is obtained from (5.46) by suppressing D_l. We thus expect a significant effect in case $C_l + D_l$ is nearly real. Let us therefore consider a *small sphere*, such that $\kappa R \ll |kR| \ll 1$. We have

$$\begin{aligned} B_l &\sim \frac{-l}{(\kappa R)^2}, \\ \hat{B}_l &\approx \frac{l+1}{(\kappa R)^2} - \frac{1}{2l+3}, \\ C_l &\approx \frac{l+1}{(kR)^2} - \frac{1}{2l+3}\,, \end{aligned} \tag{5.48}$$

and hence the amplitudes (5.46) behave for a vanishing screening length as:

$$A_{l\rm e}^0 \sim \frac{(\kappa R)^{2l+1}(l+1)}{(2l+1)!!\,(2l-1)!!} \times \frac{(kR)^2 - (\kappa R)^2}{l(kR)^2 + (l+1)(\kappa R)^2}\,, \tag{5.49a}$$

$$A_{l\rm m} \sim \frac{(\kappa R)^{2l+1}}{(2l+3)!!\,(2l+1)!!}\left[(kR)^2 - (\kappa R)^2\right]. \tag{5.49b}$$

Neither amplitude can be zero, since their imaginary parts are positive. Moreover, the magnetic multipolar contributions (5.49b) are small compared to the electric ones (5.49a). However, if the screening length λ, instead of being very short, is much larger than the size of the ball, the condition $|\beta R| \ll 1$ provides $D_l \sim (l+1)\,{\rm i}s/(kR)^2$, and hence the dominant electric multipolar amplitudes (5.46a) become:

$$A_{l\rm e} \sim \frac{(\kappa R)^{2l+1}(l+1)}{(2l+1)!!\,(2l-1)!!} \times \frac{{\rm Re}\ (kR)^2 - (\kappa R)^2}{l\,{\rm Re}\ (kR)^2 + (l+1)(\kappa R)^2}. \tag{5.49c}$$

Thus, if the dielectric constants ε and $\varepsilon^{\rm i}$ are equal, these amplitudes *approximately vanish for any value of the conductivity,* even if $s \equiv \sigma/\omega\varepsilon$ is large, and for any l. The cross-sections (5.20, 5.21) thus reduce to their second term, which for a vanishing screening length was much smaller than the first one. Small conducting spheres with a dielectric constant $\varepsilon \sim \varepsilon^{\rm i}$ illuminated by an e.m. wave (such that $\kappa R \ll 1$ and $|kR| \ll 1$) are therefore *much less visible* when the screening length is large ($\lambda \gg R$) than when it is small ($\lambda \ll R$), as the cross-sections are multiplied by a factor $|l(kR)^2 + (l+1)(\kappa R)^2|^2$. However, according to an above remark, $A_{l\rm e}$ can never vanish rigorously. We can find its lower bound by expanding C_l and D_l as

$$\begin{aligned} C_l &\approx \frac{(l+1)}{(kR)^2} - \frac{1}{2l+3} - \frac{(kR)^2}{(2l+3)^2(2l+5)}, \\ D_l &\approx \frac{(l+1)\,{\rm i}s}{(kR)^2}\left[1 - \frac{(\beta R)^2}{l(2l+3)} + \frac{(3l+5)(\beta R)^4}{l^2(2l+3)^2(2l+5)}\right], \end{aligned}$$

and likewise for $\hat{B}_l$. This yields, if we take

$$\frac{\varepsilon^{\rm i}}{\varepsilon} \approx 1 + \frac{R^2}{l(2l+3)\lambda^2} - \frac{R^4}{l(2l+3)^2(2l+5)\lambda^4},$$

the small value for the amplitude $A_{l\rm e}$:

$$A_{l\rm e} \sim \frac{{\rm i}s(\kappa R)^{2l+5}}{(2l+3)!!\,(2l+5)!!}\left[1 + \frac{(l+1)(3l+5)}{l^2 s^2 (\kappa\lambda)^4}\right]. \tag{5.50}$$

5.5 Enhancement of the absorption cross-section

We now explore the second analogy with Section 4.2 where we discovered the possibility of suppressing the reflection on a plane wall, and thus look for the *complete absorption of some partial wave* by a sphere. We show below that, for $\kappa R \gg 1$, the 2^l-polar electric wave is fully absorbed when the conductivity, the dielectric constant, the screening length and the frequency satisfy the two conditions

(5.60). More generally, for any κ, complete absorption is expressed by the vanishing of some eigenvalue (5.29), (5.30) of the S-matrix, that is:

$$C_l + D_l = B_l^*, \quad (S_{l\mathrm{e}} = 0)\,, \tag{5.51}$$

$$\frac{kRj_l'(kR)}{j_l(kR)} = \frac{\kappa R\, h_l'^*(\kappa R)}{h_l^*(\kappa R)}, \quad (S_{l\mathrm{m}} = 0)\,. \tag{5.52}$$

The signs of all the imaginary parts are now the same, which allows us to expect the occurence of solutions.

In fact, even when $\lambda = 0$, a possibility of complete absorption exists for both electric and magnetic multipolar partial waves. For instance, for electric dipolar waves with $\lambda = 0$, we can use (B.4) to write (5.51) for $l = 1$, that is $C_1 = B_1^*$, as

$$\frac{1}{1 - kR\,\mathrm{cotg}kR} - \frac{1}{(kR)^2} = \frac{1}{1 + \mathrm{i}\kappa R} - \frac{1}{(\kappa R)^2}, \tag{5.53}$$

a set of two real equations for three real variables. According to (5.32), the solutions satisfy:

$$\frac{1}{2} > \frac{\kappa R}{1 + (\kappa R)^2} > \frac{2\mathrm{Im}\ (kR)^2}{|kR|^4} = \frac{2s}{\omega^2\mu_0\varepsilon R^2\,(1 + s^2)}. \tag{5.54}$$

For $\kappa R \ll 1$, they lie near the zeroes of $j_1(z)$, *i.e.*, near the positive solutions ξ_n of $\mathrm{tg}\ \xi_n = \xi_n$, at values of k,

$$kR \approx \xi_n - \frac{(\kappa R)^2}{\xi_n} - \frac{(\kappa R)^4\left(\xi_n^2 + 1\right)}{\xi_n^3} + \mathrm{i}\frac{(\kappa R)^5}{\xi_n}, \tag{5.55}$$

which correspond to a *resonant complete absorption.* We also find, for $\kappa R \gg 1$, resonant solutions near the zeroes of $j_1'(z)$, at

$$kR \approx n\pi - \frac{1}{n\pi} + \mathrm{i}\frac{n\pi}{\kappa R}, \tag{5.56}$$

under the conditions $\kappa R \gg n\pi \gg 1$ for n.

In the presence of a finite screening length λ, which introduces the term D_l in (5.51), the cancellation of $S_{l\mathrm{e}}$ for given l is expressed as in Section 4.2 by two real equations for the four real dimensionless parameters $\kappa R, \omega^2\mu_0\varepsilon R^2 = \mathrm{Re}\ (kR)^2$, $s = \mathrm{Im}\ k^2/\mathrm{Re}\ k^2$ and R/λ. This opens the possibility of complete absorption *in new situations* of a type different from (5.55) or (5.56). For instance, for $\mathrm{Im}\ kR \gg 1, C_l$ is small as $1/\mathrm{i}kR$. For $\lambda = 0$, solving the equation $C_l = B_l^*$ would require in this case that B_l is small, hence from (B.8, B.9) that κR is large, and therefore

$$B_l^* \approx \frac{1}{\mathrm{i}\kappa R} + \frac{\mathrm{i}l\,(l+1)}{2\,(\kappa R)^3} - \frac{l\,(l+1)}{2\,(\kappa R)^4}; \tag{5.57}$$

we would then find $\mathrm{Re}\ k \sim \kappa$ and $\mathrm{Im}\ kR \sim l\,(l+1)\,/2\,(\kappa R)^2$, which is small, in contradiction to our hypothesis. Hence *no solution of* $S_{l\mathrm{e}} = 0$ *with* $\mathrm{Im}\ \kappa R \gg 1$ *can exist for* $\lambda = 0$. However, if the screening length is sufficiently large, the term D_l in $C_l + D_l = B_l^*$ may compensate for the smallness of the real part of (5.57). Indeed, if we assume for instance $\lambda \gg R$, we have

$$D_l \sim \frac{\mathrm{i}\,(l+1)\,s}{(kR)^2}, \tag{5.58}$$

and we find for $\kappa R \gg 1, \lambda \gg R$ the solution

$$s \sim \frac{\kappa R}{2\,(l+1)}, \quad k \sim \frac{1+\mathrm{i}}{2}\kappa \tag{5.59}$$

of $S_{l\mathrm{e}} = 0$.

This solution, for which $s \gg 1$ and $\omega^2\mu_0\varepsilon R^2 \gg 1$, is continued towards finite and even small values of λ/R provided κR remains large; in this more general case it reads

$$s \sim \frac{\kappa R}{2l\,(l+1)}\ \frac{\mathrm{i}Rj_l'(\mathrm{i}R/\lambda)}{\lambda j_l(\mathrm{i}R/\lambda)}, \quad k \sim \frac{1+\mathrm{i}}{2}\kappa, \quad (\kappa R \gg 1)\,, \tag{5.60}$$

where the second factor of s is a real positive number varying from l to R/λ as λ decrease. The dependence on l and λ is only through the expression of $s/\kappa R$ as long as $\kappa R \gg 1$ (Fig. 4). For smaller values of κR, the solution of $S_{l\mathrm{e}} = 0$ still exists but deviates from (5.60). Thus the occurrence of a non-vanishing screening length opens a new possibility: for suitably chosen parameters, some or other *electric multipolar incoming partial wave is completely absorbed* by a sphere of semiconductor or electrolyte with a radius larger than the wavelengths κ^{-1} and $(\mathrm{Re}\ k)^{-1}$ and with a sufficiently large conductivity.

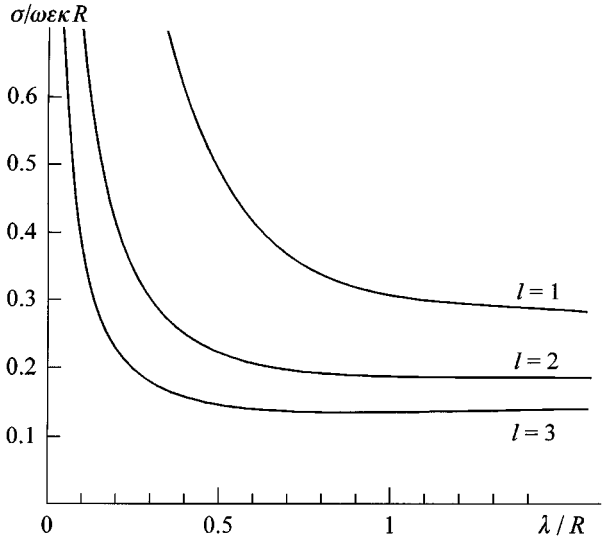

Fig. 4. Complete absorption by a sphere, for an incoming electric multipolar partial wave with small wavelength $(\kappa R \gg 1)$. The eigenvalue $S_{l\mathrm{e}}$ vanishes for an internal wavevector $k \sim \frac{1+\mathrm{i}}{2}\kappa$ and for a conductivity $\sigma \equiv \omega\varepsilon s$, which is drawn as function of the screening length λ.

6 Thin slab

6.1 General equations

We finally consider a slab of semiconductor or ionic conductor, lying in the domain $-\frac{l}{2} < z < \frac{l}{2}$, between two dielectric half-spaces $z < -\frac{l}{2}$ and $z > \frac{l}{2}$. We wish to study the *reflection and transmission coefficients* R and T for a plane wave with wavevector $(\kappa_x, 0, \kappa_z)$ issued from the region $z = -\infty$. As in Section 3.1 a transverse electric wave will be insensitive to the screening length, so that we focus on a wave with transverse magnetic polarization, $\mathbf{H} = (0, H_y, 0)$.

We take advantage of the symmetry $z \to -z$ of the system by solving beforehand the two problems where the electric field $\mathbf{E}$ is either symmetric or anti-symmetric, $\mathbf{H}$ being antisymmetric in the first case, symmetric in the second. In these two cases, denoted by the indices $\pm$, the non-vanishing components of the e.m. field, with the convention (3.4), have in the region $z > \frac{l}{2}$ the form:

$$E_{x\pm} = \frac{\kappa_z}{\kappa} E_\pm \left(\mathrm{e}^{-\mathrm{i}\kappa_z z} \pm S_\pm \mathrm{e}^{\mathrm{i}\kappa_z z}\right), \tag{6.1}$$

$$\begin{aligned} H_{y\pm} &= -\frac{\kappa E_\pm}{\omega\mu_0}\left(\mathrm{e}^{-\mathrm{i}\kappa_z z} \mp S_\pm \mathrm{e}^{\mathrm{i}\kappa_z z}\right) \\ &= -\frac{\kappa^2}{\omega\mu_0\kappa_x} E_{z\pm}. \end{aligned} \tag{6.2}$$

Since these components satisfy the symmetry properties

$$E_{x\pm}(z) = \pm E_{x\pm}(-z),$$

$$E_{z\pm}(z) = \mp E_{z\pm}(-z),$$

$$H_{y\pm}(z) = \mp H_{y\pm}(-z),$$

we obtain $\pm E_{x\pm}, \mp E_{z\pm}$ and $\mp H_{y\pm}$ in the $z < -\frac{l}{2}$ region by changing κ_z into $-\kappa_z$ in (6.1, 6.2). The coefficients $S_\pm$, the ratios of the outgoing to the incoming waves for given q, are the eigenvalues of the S-matrix. The signs have been chosen in such a way that $S_+ = S_- = 1$ for a uniform dielectric material.

The reflection and transmission coefficients are defined for an incident TM plane wave, normalized as in (3.6) according to $E_x = (\kappa_z/\kappa) E_0 \mathrm{e}^{\mathrm{i}\kappa_z z}$ for $z \to -\infty$, with a normal flux equal to (3.7). The corresponding complete field has thus the form

$$E_x = \frac{\kappa_z}{\kappa} E_0 \left(\mathrm{e}^{\mathrm{i}\kappa_z z} + R\ \mathrm{e}^{-\mathrm{i}\kappa_z z}\right) \quad \text{and} \quad E_x = \frac{\kappa_z}{\kappa} E_0 T \mathrm{e}^{\mathrm{i}\kappa_z z} \tag{6.3}$$

for $z < -\frac{l}{2}$ and $z > \frac{l}{2}$, respectively. This wave can be generated as a superposition of a symmetric wave (6.1) with amplitude $E_+ = \frac{1}{2}E_0$ and an antisymmetric wave (6.1) with amplitude $E_- = -\frac{1}{2}E_0$. Hence, we shall find the reflection and transmission coefficients as:

$$R = \frac{1}{2}(S_+ - S_-), \quad T = \frac{1}{2}(S_+ + S_-). \tag{6.4}$$

We determine S_+ and S_- by means of the general method of Section 2.1, while relying on the required symmetry properties. The magnetic field for $|z| < \frac{l}{2}$, matched with (6.2) at the interfaces, reads:

$$\begin{aligned} H_{y+} &= b_+ \sin k_z z, \\ b_+ &= \frac{\kappa \mathrm{e}_+ \left(S_+ \mathrm{e}^{\mathrm{i}\kappa_z l/2} - \mathrm{e}^{-\mathrm{i}\kappa_z l/2}\right)}{\omega\mu_0 \sin\frac{1}{2}k_z l}, \end{aligned} \tag{6.5a}$$

$$\begin{aligned} H_{y-} &= b_- \cos k_z z, \\ b_- &= -\frac{\kappa \mathrm{e}_- \left(S_- \mathrm{e}^{\mathrm{i}\kappa_z l/2} + \mathrm{e}^{-\mathrm{i}\kappa_z l/2}\right)}{\omega\mu_0 \cos\frac{1}{2}k_z l}, \end{aligned} \tag{6.5b}$$

with the same definitions (3.2) and (3.3) for the wave numbers k_z and β_z as in Section 3. The charge density, which satisfies the symmetry property $\rho_\pm(z) = \pm\rho_\pm(-z)$, has the form

$$\rho_+ = c_+ \cosh\beta_z z \quad , \quad \rho_- = c_- \sinh\beta_z z. \tag{6.6}$$

We obtain therefrom the propagative and screening contributions to $\mathbf{E}$ and $\mathbf{J}$ within the slab, by means of (2.13, 2.15):

$$\begin{aligned} E^{\mathrm{p}}_{x+} &= \frac{J^{\mathrm{p}}_{x+}}{\sigma} = \frac{-b_+ k_z}{\sigma - \mathrm{i}\omega\varepsilon} \cos k_z z, \\ E^{\mathrm{p}}_{z+} &= \frac{J^{\mathrm{p}}_{z+}}{\sigma} = \frac{\mathrm{i}b_+ \kappa_x}{\sigma - \mathrm{i}\omega\varepsilon} \sin k_z z, \end{aligned} \tag{6.7a}$$

$$\begin{aligned} E^{\mathrm{p}}_{x-} &= \frac{J^{\mathrm{p}}_{x-}}{\sigma} = \frac{b_- k_z}{\sigma - \mathrm{i}\omega\varepsilon} \sin k_z z, \\ E^{\mathrm{p}}_{z-} &= \frac{J^{\mathrm{p}}_{z-}}{\sigma} = \frac{\mathrm{i}b_- \kappa_x}{\sigma - \mathrm{i}\omega\varepsilon} \cos k_z z, \end{aligned} \tag{6.7b}$$

$$\begin{aligned} E^{\mathrm{s}}_{x+} &= \frac{J^{\mathrm{s}}_{x+}}{\mathrm{i}\omega\varepsilon} = \frac{\mathrm{i}c_+ \kappa_x}{\varepsilon\beta^2} \cosh\beta_z z, \\ E^{\mathrm{s}}_{z+} &= \frac{J^{\mathrm{s}}_{z+}}{\mathrm{i}\omega\varepsilon} = \frac{c_+ \beta_z}{\varepsilon\beta^2} \sinh\beta_z z, \end{aligned} \tag{6.8a}$$

$$\begin{aligned} E^{\mathrm{s}}_{x-} &= \frac{J^{\mathrm{s}}_{x-}}{\mathrm{i}\omega\varepsilon} = \frac{\mathrm{i}c_- \kappa_x}{\varepsilon\beta^2} \sinh\beta_z z, \\ E^{\mathrm{s}}_{z-} &= \frac{J^{\mathrm{s}}_{z-}}{\mathrm{i}\omega\varepsilon} = \frac{c_- \beta_z}{\varepsilon\beta^2} \cosh\beta_z z. \end{aligned} \tag{6.8b}$$

Expressing that $J_{z\pm}$ vanishes at the interfaces provides us with $c_\pm$ in terms of $b_\pm$, whence, using (6.5), in terms of $S_\pm$:

$$c_+ = \frac{-\sigma}{\sigma - \mathrm{i}\omega\varepsilon} \frac{\kappa_x \kappa \beta^2}{\omega^2 \mu_0 \beta_z} E_+ \frac{S_+ \mathrm{e}^{\mathrm{i}\kappa l/2} - \mathrm{e}^{-\mathrm{i}\kappa l/2}}{\sinh\frac{1}{2}\beta_z l}, \tag{6.9a}$$

$$c_- = \frac{\sigma}{\sigma - \mathrm{i}\omega\varepsilon} \frac{\kappa_x \kappa \beta^2}{\omega^2 \mu_0 \beta_z} E_- \frac{S_- \mathrm{e}^{\mathrm{i}\kappa l/2} + \mathrm{e}^{-\mathrm{i}\kappa l/2}}{\cosh\frac{1}{2}\beta_z l}\cdot \tag{6.9b}$$

Finally the continuity of E_x across the interfaces yields, by combination of (6.1, 6.5, 6.7, 6.8) and (6.9),

$$R = \mathrm{e}^{-\mathrm{i}\kappa_z l}\frac{C^2+D^2-B^2+2\mathrm{i}CD\,(\operatorname{cotg} k_z l\ \coth\beta_z l - \operatorname{cosec} k_z l \operatorname{cosech}\beta_z l)}{(C_+ + D_+ - B)\,(C_- + D_- - B)}\,. \tag{6.14}$$

$$T = \mathrm{e}^{-\mathrm{i}\kappa_z l}\frac{-2B\,(\mathrm{i}C \operatorname{cosec} k_z l + D \operatorname{cosech}\beta_z l)}{(C_+ + D_+ - B)\,(C_- + D_- - B)}. \tag{6.15}$$

the equations:

$$B\frac{S_+ + \mathrm{e}^{-\mathrm{i}\kappa_z l}}{S_+ - \mathrm{e}^{-\mathrm{i}\kappa_z l}} = \mathrm{i}C\operatorname{cotg}\frac{1}{2}k_z l + D\coth\frac{1}{2}\beta_z l, \tag{6.10a}$$

$$B\frac{S_- - \mathrm{e}^{-\mathrm{i}\kappa_z l}}{S_- + \mathrm{e}^{-\mathrm{i}\kappa_z l}} = \mathrm{i}C\mathrm{tg}\frac{1}{2}k_z l + D\tanh\frac{1}{2}\beta_z l, \tag{6.10b}$$

where we introduced the same notations

$$B \equiv \frac{\mathrm{i}\kappa_z\kappa_x}{\kappa^2}, \quad C \equiv \frac{-\mathrm{i}k_z\kappa_x}{k^2}, \quad D \equiv \frac{\mathrm{i}\sigma\kappa_x^3}{\omega\varepsilon k^2\beta_z} \tag{6.11}$$

as in (3.14–3.16). We thus have determined the S-matrix in the same form as (5.29) for a sphere, namely,

$$S_\pm = \pm\mathrm{e}^{-\mathrm{i}\kappa_z l}\frac{C_\pm + D_\pm - B^*}{C_\pm + D_\pm - B}, \tag{6.12}$$

where we introduced

$$C_+ \equiv \mathrm{i}C\operatorname{cotg}\frac{1}{2}k_z l, \quad D_+ \equiv D\coth\frac{1}{2}\beta_z l, \tag{6.13a}$$

$$C_- \equiv -\mathrm{i}C\mathrm{tg}\frac{1}{2}k_z l, \quad D_- \equiv D\tanh\frac{1}{2}\beta_z l, \tag{6.13b}$$

and where we noted that $B = -B^*$. (We establish in Appendix C.1 some inequalities satisfied by $C_\pm$ and $D_\pm$.) Hence, we obtain through (6.4) the reflection and transmission coefficients:

(see equations (6.14) and (6.15) above)

For a transverse electric incident wave, we would have obtained:

$$S_+ = \mathrm{e}^{-\mathrm{i}\kappa_z l}\frac{k_z^{-1}\operatorname{cotg}\frac{1}{2}k_z l + \mathrm{i}\kappa_z^{-1}}{k_z^{-1}\operatorname{cotg}\frac{1}{2}k_z l - \mathrm{i}\kappa_z^{-1}},$$

$$S_- = -\mathrm{e}^{-\mathrm{i}\kappa_z l}\frac{-k_z^{-1}\mathrm{tg}\frac{1}{2}k_z l + \mathrm{i}\kappa_z^{-1}}{-k_z^{-1}\mathrm{tg}\frac{1}{2}k_z l - \mathrm{i}\kappa_z^{-1}}. \tag{6.16}$$

This result has the same form as (6.12), within the replacement of C by $-\mathrm{i}\kappa_x/k_z$, of B by $\mathrm{i}\kappa_x/\kappa_z$, and the suppression of the terms in D. The situation is similar to the transverse electric fields for a sphere, which provided (5.30) as S-matrix elements. As we already noted in Sections 3.1 and 4.1, the screening plays no rôle in this case since there appears anyhow no charge density in the conductor. We readily check that (6.12) and (6.16) coincide for $\kappa_x = 0$, when the incidence is perpendicular to the slab.

We can also check that $S_+ = S_- = 1$ if the material of the slab is replaced by the surrounding material, in which case $\beta_z = \infty$, $D = 0$, $k_z = \kappa_z$, $B = -C$. As a further check, consider the limit of a thick slab, with $\mathrm{Im}\ k_z l \gg 1, \mathrm{Re}\ \beta_z l \gg 1$. The S-matrix (6.12) reduces to:

$$S_+ \sim -S_- \sim \mathrm{e}^{-\mathrm{i}\kappa_z l}\frac{C + D - B^*}{C + D - B} \sim R. \tag{6.17}$$

Hence the transmission coefficient T vanishes and the same expression (3.13) as for a plane wall is recovered for the reflection coefficient R, within a phase factor due to the fact that the wave is reflected here on the interface $z = -\frac{l}{2}$.

6.2 Energy exchanges

Since the local and global energy exchanges behave here as for a plane wall (Sect. 3.3) or for a sphere (Sect. 5.2), we shall not dwell upon them. The fields are obtained by inserting (6.12) into the equations (6.1, 6.2, 6.5–6.7). The resulting Poynting vector and the local dissipation rate are similar to those found for the plane wall, except for additional oscillations associated with the interference between waves propagating in both directions $\pm z$.

Whereas an incident wave of the form (6.3) generates a *local* dissipation rate and energy transfers within the conducting material which involve cross terms between the symmetric and antisymmetric contributions to the e.m. field, the *total* power W yielded by the field to matter can be decomposed as a sum of two terms W_+ and W_- arising from these two contributions. If W is defined as the total dissipation per unit area of the slab for a unit incident flux perpendicular to this slab, we find after integration over space, as expected from (6.4, 6.12),

$$W = 1 - |R|^2 - |T|^2 = W_+ + W_-, \tag{6.18}$$

$$W_\pm = \frac{1}{2}\left(1 - |S_\pm|^2\right) = \frac{2\,|B|\,\mathrm{Im}\ (-C_\pm - D_\pm)}{|C_\pm + D_\pm - B|^2}\,. \tag{6.19}$$

According to equations (C.5, C.7, C.10, C.12) established in Appendix C.1, we check that W_+ and W_- are positive, as well as their first term, the only one which survives when $\lambda = 0$, that is, when $D = 0$. Their second term, proportional to $-\mathrm{Im}\ D_\pm$, is however negative according to (C.14), and it substracts out from the first one, in the same way as W^{s} did for a wall (Eq.(4.1)) or $W_{\mathrm{e}}^{\mathrm{s}}$ for a sphere (Eq.(5.33)).

6.3 Enhancement of the transparency

As in Section 5.4 where we saw that a sufficiently large screening length λ can significantly reduce the scattering

cross-section of a sphere, we look whether the transmission coefficient $|T|^2$ of a slab can here become close to 1.

In the limit of a *thin slab* where $|k_z l| \ll 1$, all other dimensionless parameters being finite, we have $|C_-| \ll |B| \ll |C_+|$. Hence, if we first consider perfect screening, with $\lambda = 0,\ D = 0$, we find from (6.15) to lowest order in $|k_z l|$ a transmission coefficient

$$T_0 \approx \mathrm{e}^{-\mathrm{i}\kappa_z l}\left[1 - \frac{\mathrm{i}}{2}k_z l\left(\frac{B}{C} + \frac{C}{B}\right)\right]. \tag{6.20}$$

The corresponding attenuation

$$1 - |T_0|^2 \sim -\mathrm{Im}\ k_z l\left(\frac{B}{C} + \frac{C}{B}\right) = \left(\frac{\kappa_z}{\kappa^2} + \frac{\kappa^2\kappa_x^2}{\kappa_z |k|^4}\right) l\mathrm{Im}\ k^2 \tag{6.21}$$

is thus proportional to the thickness l. However, for finite λ, the expression (6.15) reads, to lowest order in $|k_z l|$,

$$T \approx \mathrm{e}^{-\mathrm{i}\kappa_z l}\left[1 - \frac{\mathrm{i}}{2}k_z l\left(\frac{B}{C - \frac{\mathrm{i}}{2}k_z l\ D\coth\frac{1}{2}\beta_z l} + \frac{C + 2\mathrm{i}\,(k_z l)^{-1} D\tanh\frac{1}{2}\beta_z l}{B - D\tanh\frac{1}{2}\beta_z l}\right)\right]. \tag{6.22}$$

In the resulting attenuation, expanded in powers of $|\beta_z l|$, the first term of (6.22) yields to lowest order

$$1 - |T|^2 \sim \frac{\kappa_z}{\kappa^2\left(1 + s^2\kappa_x^4\lambda^4\right)} l\mathrm{Im}\ k^2 + \mathcal{O}\left(l^2\right), \tag{6.23a}$$

where $s \equiv \sigma/\omega\varepsilon$; the second term provides a contribution,

$$\frac{\kappa^4}{4\kappa_z^2}\left|\frac{\mathrm{Re}\ k_z^2}{\mathrm{Re}\ k^2}\right|^2 l^2 + \frac{\kappa^2\kappa_x^4}{6\kappa_z |k|^4} l^3 \mathrm{Im}\ k^2, \tag{6.23b}$$

which does not depend on λ, but which has the same order as terms in l^2 that we have neglected in the expansion of T in powers of $|kl|$. The first part (6.23a) strongly decreases with the screening length. In the considered limit $|k_z l| \ll 1$, $\lambda \gg l$, we see from (6.23) that the attenuation $1 - |T|^2$ is not only *much smaller* than (6.21), but that it is moreover *proportional to the square l^2 of the thickness* rather than to the thickness l itself.

In the limit of a *thick slab*, $\mathrm{Im}\ k_z l \gg 1$, C_+ and C_- are approximately equal to C. The expression (6.15) of T provides, for a perfect screening where $\lambda = 0,\ D = 0$,

$$T_0 \sim \frac{-4BC\mathrm{e}^{-\mathrm{i}\kappa_z l}}{(C - B)^2}\mathrm{e}^{\mathrm{i}k_z l} = \frac{4\kappa^2\kappa_z k^2 k_z \mathrm{e}^{-\mathrm{i}\kappa_z l}}{\left(\kappa_z k^2 + k_z\kappa^2\right)^2}\mathrm{e}^{\mathrm{i}k_z l}, \tag{6.24}$$

which shows as expected that the transmitted power is exponentially small as $\mathrm{e}^{-2\mathrm{Im}\ k_z l}$. However, for a finite D and a *large screening length*, $\lambda \gg l$, the second term of (6.15) dominates since $|\beta_z l| \ll 1$, and we obtain, using $D/D_+ \sim D/D_- \sim \frac{1}{2}\beta_z l$,

$$T \sim \frac{-2BD\ \mathrm{e}^{-\mathrm{i}\kappa_z l}}{[2D + \beta_z l\,(C - B)]\left[C - B + \frac{1}{2}D\ \beta_z l\right]} \sim \frac{\kappa_z k^2\ \mathrm{e}^{-\mathrm{i}\kappa_z l}}{\kappa_z k^2 + k_z\kappa^2}. \tag{6.25}$$

Remarkably, since l enters (6.25) only through a phase factor, *the attenuation no longer depends on the thickness* l of the slab as long as l remains smaller than λ. The delocalization effect produced by the lack of screening allows the wave to pass easily through the slab. The expression (6.25) shows that $|T|^2$ can reach values significant compared to 1, so that the occurrence of a screening length much larger than the skin depth can *increase the transparency by many orders of magnitude.*

This strong discrepancy between the two transmission coefficients, T_0 in the regime $(\mathrm{Im}\ k_z)^{-1} \ll l,\ \lambda = 0$, and T in the regime $(\mathrm{Im}\ k_z)^{-1} \ll l \ll \lambda$, can be traced back to their expression (6.4) in terms of the S-matrix. For $D = 0$, we obtain from (6.12), in the limit $\mathrm{Im}\ k_z l \gg 1$ where $C_+ \sim C_- \sim C$,

$$S_+ \sim -S_- \sim \mathrm{e}^{-\mathrm{i}\kappa_z l}\frac{C + B}{C - B} \sim R_0. \tag{6.26}$$

Hence, from (6.4), the transmission coefficient T_0 is extremely small while the reflection coefficient R_0 is nearly equal to its value for a bulk plane wall, as expected. The absorption (6.18), (6.19), which reduces to

$$W_0 \sim \frac{4\mathrm{Re}\ BC}{|C - B|^2} \sim 1 - |R_0|^2, \tag{6.27}$$

may be small, especially in the metallic regime $s \gg 1$ where $|C| \ll |B|$. However, if $\lambda \gg l$, and if $|D|$ is comparable to $|B|$ and $|C|$, we have $|D_+| \gg |D| \gg |D_-|$, and hence:

$$S_+ \approx \mathrm{e}^{-\mathrm{i}\kappa_z l}\left(1 + \frac{B}{D}\beta_z l\right), \quad S_- \sim \mathrm{e}^{-\mathrm{i}\kappa_z l}\frac{C + B}{C - B}\cdot \tag{6.28}$$

In the symmetric channel, S_+ becomes nearly unitary, while S_- is practically unchanged. Actually, the weakness of the screening allows for *penetration of the field* through the slab, far beyond the skin. We find from equations (5.5–5.9) that $\mathbf{H}, \mathbf{E}^{\mathrm{p}}$ and $\mathbf{J}^{\mathrm{p}}$ are negligible within this region $\left(\frac{l}{2} - |z|\right)\mathrm{Im}\ k_z \ll 1$, while $\mathbf{E}^{\mathrm{s}}$ is dominated by its *symmetric contribution*

$$E_{x+}^{\mathrm{s}} \sim E_0\frac{\kappa_z}{\kappa}\mathrm{e}^{-\mathrm{i}\kappa_z l/2}\cosh\beta_z z,$$

$$E_{z+}^{\mathrm{s}} \sim -\mathrm{i}E_0\frac{\kappa_z\beta_z}{\kappa\kappa_x}\mathrm{e}^{-\mathrm{i}\kappa_z l/2}\sinh\beta_z z, \tag{6.29}$$

and the current $\mathbf{J} \sim \mathbf{J}^{\mathrm{s}} = \mathrm{i}\omega\varepsilon\mathbf{E}^{\mathrm{s}} = \mathrm{i}\omega\beta^{-2}\nabla\rho$ is *non-dissipative.* The absorption $W \sim \frac{1}{2}W_0$ is mainly due to the antisymmetric part of the wave, since $|S_+|^2 \sim 1$, and the *symmetric part* passes through the slab with a phase-shift, but *nearly without absorption.* The reflection and

transmission coefficients are given by (6.4) as:

$$R \sim \mathrm{e}^{-\mathrm{i}\kappa_z l}\frac{C}{C-B}, \quad T \sim \mathrm{e}^{-\mathrm{i}\kappa_z l}\frac{B}{B-C}; \tag{6.30}$$

we recover for T the significantly large value (6.25), owing to the difference which now occurs between the symmetric and antisymmetric parts of the wave. The reflection coefficient $|R|^2$ may be smaller or larger than $|R_0|^2$, depending on the sign of $\kappa_z\kappa^{-2} - 2\mathrm{Re}\, k_z k^{-2}$. A simultaneous increase of both coefficients $|T|^2 > |T_0|^2$ and $|R|^2 > |R_0|^2$ is made possible because the total absorption, $W = \frac{1}{2}W_0$, is divided by 2.

6.4 Suppression of the reflection or of the transmission

Among the new properties brought in by the finiteness of the screening length, we shall explore the possibility of cancelling either the reflection or the transmission coefficient R or T. Note first that T can never vanish for a material with perfect screening $(\lambda = 0)$, although it is exponentially small for a slab with increasing thickness as soon as the conductivity is non-zero. However, for $\lambda \neq 0$ (or $D \neq 0$) we see from (6.15) that T vanishes when

$$\mathrm{i}C \sinh \beta_z l + D \sin k_z l = 0. \tag{6.31}$$

In order to discuss this equation, we introduce the five real positive dimensionless parameters s, t, u, v, w which enter the problem:

$$s \equiv \frac{\sigma}{\omega\varepsilon},\ t \equiv \frac{2\kappa_z\kappa_x}{\kappa^2},\ u \equiv \frac{\omega^2\mu_0\varepsilon}{\kappa_x^2},\ v \equiv \frac{1}{\lambda^2\kappa_x^2}, \quad w \equiv \kappa_x l. \tag{6.32}$$

The first four (with $t \leqslant 1$) are the same as in Section 4, and the last one characterizes the thickness of the slab. The various quantities involved in the equations are expressed in terms of them as:

$$\begin{aligned} k_z l &= w\sqrt{u\,(1+\mathrm{i}s) - 1}, \\ \beta_z l &= w\sqrt{v\,(1-\mathrm{i}s^{-1}) + 1}, \end{aligned} \tag{6.33}$$

$$\begin{aligned} B &= \frac{\mathrm{i}t}{2}, \quad C = \frac{-\mathrm{i}\sqrt{u\,(1+\mathrm{i}s) - 1}}{u\,(1+\mathrm{i}s)}, \\ D &= \frac{\mathrm{i}s}{u\,(1+\mathrm{i}s)\,\sqrt{v\,(1-\mathrm{i}s^{-1}) + 1}}. \end{aligned} \tag{6.34}$$

The equation $T = 0$ then reads:

$$\begin{aligned} s\,\frac{\sin w\sqrt{u\,(1-\mathrm{i}s) - 1}}{\sqrt{u\,(1+\mathrm{i}s) - 1}} &= \mathrm{i}\sqrt{v\,(1-\mathrm{i}s^{-1}) + 1} \\ \times \sinh w\sqrt{v\,(1-\mathrm{i}s^{-1}) + 1}, \end{aligned} \tag{6.35}$$

a set of two real equations for the four positive variables s, u, v, w; the parameter $t \equiv \sin 2\theta^{\mathrm{i}}$ does not appear here.

We show the existence of solutions for (6.35) by determining, in the limiting case $s \gg 1$, the variables v and w in terms of s and u, supposed to be given, with $us \gg 1$. The argument of the complex number $\sin k_z l$ should then be $3\pi/4$, which is expressed by

$$\mathrm{tg}\ \chi l \sim -\tanh \chi l,\ \cos \chi l > 0, \quad \chi l \equiv w\sqrt{\frac{us}{2}}, \tag{6.36}$$

where χ is the wavevector $\mathrm{Im}\ k_z$. We find a sequence of values of χl, each one lying between $2n\pi - \frac{\pi}{4}$ and $2n\pi$, with $n \geqslant 1$, which for large n tend to $2n\pi - \frac{\pi}{4}$. Actually, even for $n = 1$, χl is fairly large and lies close to $2n\pi - \frac{\pi}{4}$, since it can be expanded as:

$$\chi l \equiv \mathrm{Im}\ k_z l \equiv w\sqrt{\frac{us}{2}} \approx 2n\pi - \frac{\pi}{4} + \mathrm{e}^{-4n\pi + \pi/2}. \tag{6.37}$$

Writing now that the modulus is the same on both sides of (6.35), we should satisfy:

$$\begin{aligned} \sqrt{v+1}\sinh w\sqrt{v+1} &\sim \sqrt{\frac{2s}{u}}\cos \chi l\ \mathrm{sh}\chi l \\ &\sim \frac{1}{2}\sqrt{\frac{s}{u}}\mathrm{e}^{2n\pi - \pi/4}. \end{aligned} \tag{6.38}$$

This equation determines v, provided the right-hand side is larger than $\sinh w$, *i.e.*,

$$\frac{1}{2}\sqrt{\frac{s}{u}}\mathrm{e}^{2n\pi - \pi/4} > \sinh\left(\sqrt{\frac{2}{us}}\left(2n\pi - \frac{\pi}{4}\right)\right). \tag{6.39}$$

We thus find a set of solutions of $T = 0$, labelled by n and expressed by (6.37, 6.38), for given $s \gg 1$ and given u, provided u is not smaller than the bound given by (6.39).

An expansion of (6.35) for $s \gg 1$ reveals that the condition $T = 0$ cannot be satisfied if s is too small. The solutions obtained for $s \gg 1$ thus cannot be continued down to $s = 0$.

The cancellation of the transmission coefficient T appears as a kind of *resonance effect*, which is *made possible only by the finiteness of the screening length.* It may occur for a wide range of values of the parameters s and u, the parameter t which characterizes the outside medium remaining arbitrary. For $s \gg 1$, in which case the wavenumber χ equals the skin depth, the phenomenon requires a tuning of both the wavelength, through (6.37), and the screening length, through (6.38).

Likewise, the cancellation of the reflection coefficient (6.14) is impossible for $\lambda = 0$ and $\sigma \neq 0$, since this is expressed by the same condition $C^2 = B^2$ as for a plane wall. While $C = B$ has no solution, $C = -B$ would provide only real values for k_z requiring $\sigma = 0$, namely the trivial one $k_z = \kappa_z$ and the Brewster angle $k_z = \kappa_x^2/\kappa_z$. However, the additional terms involving D in the numerator of (6.14) can now allow for the cancellation of R when the conductivity is finite. The equation to be solved is $(C_+ + D_+)(C_- + D_-) = B^2$. We have solved this equation in Section 4.2 in the limit $|k_z l| \gg 1, |\beta_z l| \gg 1$, where it reduces to $C + D = -B$, and nothing prevents R to vanish for a thinner slab.

6.5 Suppression of both the reflection and transmission

Since the reflection and transmission coefficients depend on the five parameters (6.32), we may look for their *simultaneous extinction*, in which case the wave is *completely absorbed*. Requiring that $R = T = 0$ is also expressed, on account of (6.4), by the cancellation of both S_+ and S_-. This condition is in turn expressed, using (6.12), by:

$$C_+ + D_+ = C_- + D_- = -B. \tag{6.40}$$

The imaginary parts of all these three quantities are negative, so that there is no a priori impossibility. By using the definitions (6.13) we can check that the first equation (6.40) is equivalent to (6.31). We can further symmetrize the remaining condition as $C_+ + C_- + D_+ + D_- = -2B$, that is,

$$\mathrm{i}C \operatorname{cotg} k_z l + D \coth \beta_z l = -B, \tag{6.41}$$

which reads in terms of the parameters (6.32):

$$\begin{aligned} &\mathrm{i}\sqrt{u\,(1+\mathrm{i}s)-1}\ \operatorname{cotg} w\sqrt{u\,(1+\mathrm{i}s)-1} \\ &- \frac{s \coth w\sqrt{v\,(1-\mathrm{i}s^{-1})+1}}{\sqrt{v\,(1-\mathrm{i}s^{-1})+1}} \\ &= \frac{tu}{2}\,(1+\mathrm{i}s)\,. \end{aligned} \tag{6.42}$$

By combining (6.31) and (6.41) we also obtain:

$$\begin{aligned} \mathrm{e}^{(\mathrm{i}k_z-\beta_z)l} &= \frac{C+D+B}{C+D-B}, \\ \mathrm{e}^{(\mathrm{i}k_z+\beta_z)l} &= \frac{C-D+B}{C-D-B}\cdot \end{aligned} \tag{6.43}$$

The four real equations for s, t, u, v, w which express that the wave is completely absorbed are thus written equivalently as (6.40), or as (6.31, 6.41), or as (6.35, 6.42), or as (6.43).

As we did for the cancellation of T alone, let us study the solution of these equations in the region $s \gg 1$. Apart from the equalities (6.37, 6.38) which give the solution of (6.31) or (6.35), we have to solve (6.42), which reduces for $s \gg 1$ to:

$$\frac{1}{\sqrt{\mathrm{i}us}} \operatorname{cotg} w\sqrt{\mathrm{i}us} + \frac{1}{u\sqrt{v+1}} \coth w\sqrt{v+1} \sim -\frac{\mathrm{i}t}{2}\,. \tag{6.44}$$

Since $\operatorname{Im} w\sqrt{\mathrm{i}us} = \chi l$, given by (6.37), is a rather large quantity, at least equal to the number 5.5, we can replace $\operatorname{cotg} w\sqrt{\mathrm{i}us}$ by $-\mathrm{i}$. The imaginary and the real parts of (6.44) then yield, respectively,

$$\frac{t}{2} \sim \frac{1}{\sqrt{2us}}, \quad \coth w\sqrt{v+1} \sim \sqrt{\frac{u\,(v+1)}{2s}}\cdot \tag{6.45}$$

Multiplication by (6.38) shows that

$$\cosh w\sqrt{v+1} \sim \frac{1}{2\sqrt{2}} \mathrm{e}^{2n\pi - \pi/4} \tag{6.46}$$

is large, even for $n = 1$, and hence we get from (6.45) and (6.46), within exponential corrections,

$$\frac{u\,(v+1)}{2s} \sim 1, \quad w\sqrt{v+1} \sim 2n\pi - \frac{\pi}{4} - \frac{1}{2}\ln 2. \tag{6.47}$$

We can check that the requirement (6.38) is satisfied. Altogether, combining (6.37, 6.44) and (6.47), and noting that v is large, we find for $s \gg 1$:

$$t \sim \frac{1}{\sqrt{s}}\sqrt{1-\eta}, \quad u \sim \frac{2}{1-\eta}, \quad v \sim s\,(1-\eta)\,, \tag{6.48}$$

$$w \sim \frac{2n\pi - \frac{\pi}{4}}{\sqrt{s}}\sqrt{1-\eta}, \quad \eta \equiv \frac{\ln 2}{4n\pi - \frac{\pi}{2}}\cdot \tag{6.49}$$

At least in the limit of large s, we have thus obtained for each s and for each $n \geqslant 1$ a set of parameters $t_n(s), u_n(s), v_n(s), w_n(s)$ approximately given by (6.48) *such that the wave is neither reflected by the slab nor transmitted through it.* The term η is small, since we have $\eta \sim 0.063$ for $n = 1$. The first three equations (6.48) characterize (for $\sigma \gg \omega\varepsilon$) the incidence angle θ^{i} and the properties of the two materials which should be realized to produce complete absorption, namely:

$$\begin{aligned} \sin 2\theta^{\mathrm{i}} \equiv \frac{2\kappa_z\kappa_x}{\kappa^2} &\sim \sqrt{\frac{\omega\varepsilon}{\sigma}}, \\ \omega^2\mu_0\varepsilon \sim 2\kappa_x^2, \quad \lambda^2 &\sim \frac{2}{\omega\mu_0\sigma}\cdot \end{aligned} \tag{6.50}$$

In this regime the incidence should be either close to normal, with $\theta^{\mathrm{i}} \sim \frac{1}{2}\sqrt{\omega\varepsilon/\sigma}$ and hence from (4.27) $2\sigma \sim \omega\varepsilon^{\mathrm{i}}$, or close to tangential, with $\frac{\pi}{2} - \theta^{\mathrm{i}} \sim \frac{1}{2}\sqrt{\omega\varepsilon/\sigma}$ and hence $\varepsilon \sim 2\varepsilon^{\mathrm{i}}$; in the first case, $\varepsilon^{\mathrm{i}}/\varepsilon \sim 2\sigma/\omega\varepsilon$ should be large. The conditions (6.50) imply that $k \sim k_z$ and that all quantities

$$\lambda^{-1} \sim \beta_z \sim \operatorname{Re} k_z \sim \operatorname{Im} k_z \sim \chi, \quad \chi = \kappa_x\sqrt{\frac{\sigma}{\omega\varepsilon}} \tag{6.51}$$

are approximately equal. This approximate *equality between the screening length and the skin depth* clearly shows that complete absorption requires a close fit between propagative and screening contributions. Finally, the last equation, (6.49), namely

$$\chi l \sim 2n\pi - \frac{\pi}{4}, \tag{6.52}$$

expresses a *resonance* condition that should be satisfied by the thickness l of the slab to ensure the cancellation of both R and T.

Note that, to lowest order in $1/s$, the conditions (6.45) or (6.48) imply:

$$t \sim \frac{\sqrt{v}}{s}, \quad u \sim \frac{2s}{v}\,. \tag{6.53}$$

We had encountered these behaviors of t and u in the end of Section 4.2 and in Appendix A (Eq. (A.33)), when we looked for complete absorption by a wall for given s and

v, in the regime $s \gg 1, v \ll s^2$. We recover here these same equations because (6.41) reduces approximately to $C + D \sim -B$, the very condition which was studied in Section 4.2 to express the extinction of the reflection from a wall. We must however satisfy here the additional constraint $v + \frac{1}{2} \simeq s$, which is represented asymptotically by a straight line with the slope 1 on the graph of Figures 1 and 2, not to speak of the condition (6.52) on the thickness.

When s becomes no longer very large, the above solutions of (6.35, 6.42) can be continued as sets of functions $t_n(s), u_n(s), v_n(s), w_n(s)$ labelled by the index $n = 1, n = 2, ...$, provided s, t, u, v, w remain positive and t less than 1. We write in Appendix C.2 a convenient approximate form (C.16, C.17) for the equations (6.35, 6.42), and exhibit a single equation (C.21) for $v_n(s)$, from which $t_n(s), u_n(s)$ and $w_n(s)$ are given explicitly by (4.23, 4.24) and (C.22), respectively. We show there that the condition which restricts the domain of variation of s is the positivity of v. For each n, $s \equiv \sigma/\omega\varepsilon$ should thus be larger than some number s_n close to 1 (Eq. (C.37)), and the function $v_n(s)$, where $v \equiv 1/\lambda^2\kappa_x^2$, grows from 0 to ∞, nearly linearly as $s - s_n$, when s varies from s_n to ∞. The resulting function $u_n(s)$, where $u \equiv \omega^2\mu_0\varepsilon/\kappa_x^2$, decreases from about 4 to 2, while $t_n(s)$, where $t \equiv \sin 2\theta^{\mathrm{i}}$, decreases from about $\frac{1}{2}$ to zero (as $s^{-1/2}$), and $w_n(s)$, where $w \equiv \kappa_x l$, starts from a value of order $n\pi$, reaches a maximum and tends to zero proportionally to $s^{-1/2}$. These results are plotted in Figure 5, which represents the outcome of a numerical solution of equations (6.35, 6.42). We derive analytically in Appendix C.2 the expansions of the solutions for large s (Eqs. (C.24–C.32)) and for s close to its lower bound s_n (Eqs. (C.37–C.43)).

We have also estimated, as functions of s, the values of the wavevectors k_z and β_z for which complete extinction of the reflected and transmitted waves takes place. They are represented by Figure 6, and their expansions are expressed by (C.33, C.34) for large s, and by (C.44–C.48) near the lower bound s_n of s. The dynamical screening length β_z^{-1} is nearly real at both ends of the interval. While Re k_z, Im k_z and Re β_z are nearly equal for large s, these quantities behave differently as s decreases down to s_n: the first one, Re k_z, slightly increases and passes through a maximum, whereas the last two, Im k_z and Re β_z, decrease by about a factor 2.

When $R = T = 0$, the trigonometric or hyperbolic functions which enter the expression (6.15) of the transmission coefficient T thus reach their largest moduli for the branch $n = 1$, corresponding to the thinnest possible slab, and for $s = s_1 \simeq 1.28$, corresponding to the largest possible frequency $\omega = 0.78\sigma/\varepsilon$ such that the phenomenon may take place. These values are

$$|\mathrm{cosec}\ k_z l| \simeq 0.08, \qquad |\mathrm{cosech}\ \beta_z l| \simeq 0.16, \tag{6.54}$$

but the numbers are much smaller for lower frequencies or for higher-order resonances ($n \geqslant 2$). Since anyhow $|T|^2$ is small in the range of parameters where we expect R and T to vanish, the best conditions under which the extinction $R = T = 0$ might be exhibited experimentally are thus associated with $n = 1$ and with s slightly larger than 1.28, or ω slightly lower than $0.78\sigma/\varepsilon$. The other parameters, given by $v_1(s), u_1(s), w_1(s)$ and $t_1(s)$ (Eqs. (C.39–C.43)), should be such that $\kappa_x\lambda$ is large, that κ_x lies close to $0.5\omega\sqrt{\mu_0\varepsilon}$, that $\kappa_x l$ lies close to 2.5, and that t lies close to 0.5. The latter condition means that either the incidence angle θ^{i} is close to $\frac{\pi}{12}$ and $\varepsilon^{\mathrm{i}}/\varepsilon$ (given by (4.27)) is close to 3.3, or that θ^{i} is close to $5\pi/12$ and $\varepsilon^{\mathrm{i}}/\varepsilon$ is close to 1/4.

7 Summary and conclusions

We have studied the propagation of electromagnetic waves in systems, one component of which is a material with a finite screening length such as a semiconductor or ionic conductor. We relied on a simple model where the current density

$$\mathbf{J} = \sigma\mathbf{E} - D\nabla\rho \tag{7.1}$$

contains, in addition to the ohmic contribution, a diffusion term proportional to the gradient of the charge density. The diffusion coefficient D is related to the static screening length λ by $D = \sigma\lambda^2/\varepsilon$. Although this model is crude, it is expected to be realistic at sufficiently low frequency, and it gives rise to several interesting predictions. The main new feature brought in by the additional term is non-locality. Indeed, while the displacement field defined by $\mathbf{D} \equiv \varepsilon\mathbf{E} + \mathrm{i}\omega^{-1}\mathbf{J}$ is, for a metal where $\lambda = 0$, proportional to the electric field at the same point, it is related here to the electric field by:

$$\left(1 - \frac{\mathrm{i}\sigma\lambda^2}{\omega\varepsilon}\mathrm{grad\ div}\right)(\mathbf{D} - \varepsilon\mathbf{E}) = \frac{\mathrm{i}\sigma}{\omega}\mathbf{E}, \tag{7.2}$$

an equation obtained by using the conservation law $\mathrm{div}\mathbf{J} = \mathrm{i}\omega\rho$ in (7.1) to eliminate ρ. Maxwell's equation $\omega^2\mu_0\mathbf{D} = \mathrm{curl\ curl}\ \mathbf{E}$ then leads to the simple standard equations $\mathrm{div}\mathbf{D} = 0, \nabla^2\mathbf{D} + k^2\mathbf{D} = 0$, where $k \equiv \sqrt{\omega^2\mu_0\varepsilon + \mathrm{i}\omega\mu_0\sigma}$ is the usual complex wavenumber. However, extracting $\mathbf{E}$ from $\mathbf{D}$ raises here intractable questions. On the one hand, (7.2) does not yield a unique solution for $\mathbf{E}$ when $\mathbf{D}$ is given. On the other hand its solutions are *non-local*. This is a nuisance for problems such as ours, since dealing with interfaces requires the use of boundary conditions for local quantities. A similar difficulty is currently encountered for spheres having a spatially dispersive dielectric constant or for metallic ones in the optical regime [2–6].

In this paper we have overcome this difficulty by increasing the number of basic fields, a standard technique to replace non-local field theories by local ones. In particle physics or in statistical mechanics, a new particle or quasiparticle with its own simple propagator is often introduced to account for a complex structure in the original propagator. In particular the various kinds of quasiparticles which occur in solid state or in plasma physics can be introduced as poles in the propagators for one or for several true particles, and their own propagators are simpler. Here we rely likewise on field equations, not only for the electric or magnetic field itself as usual, but also for a *scalar field*

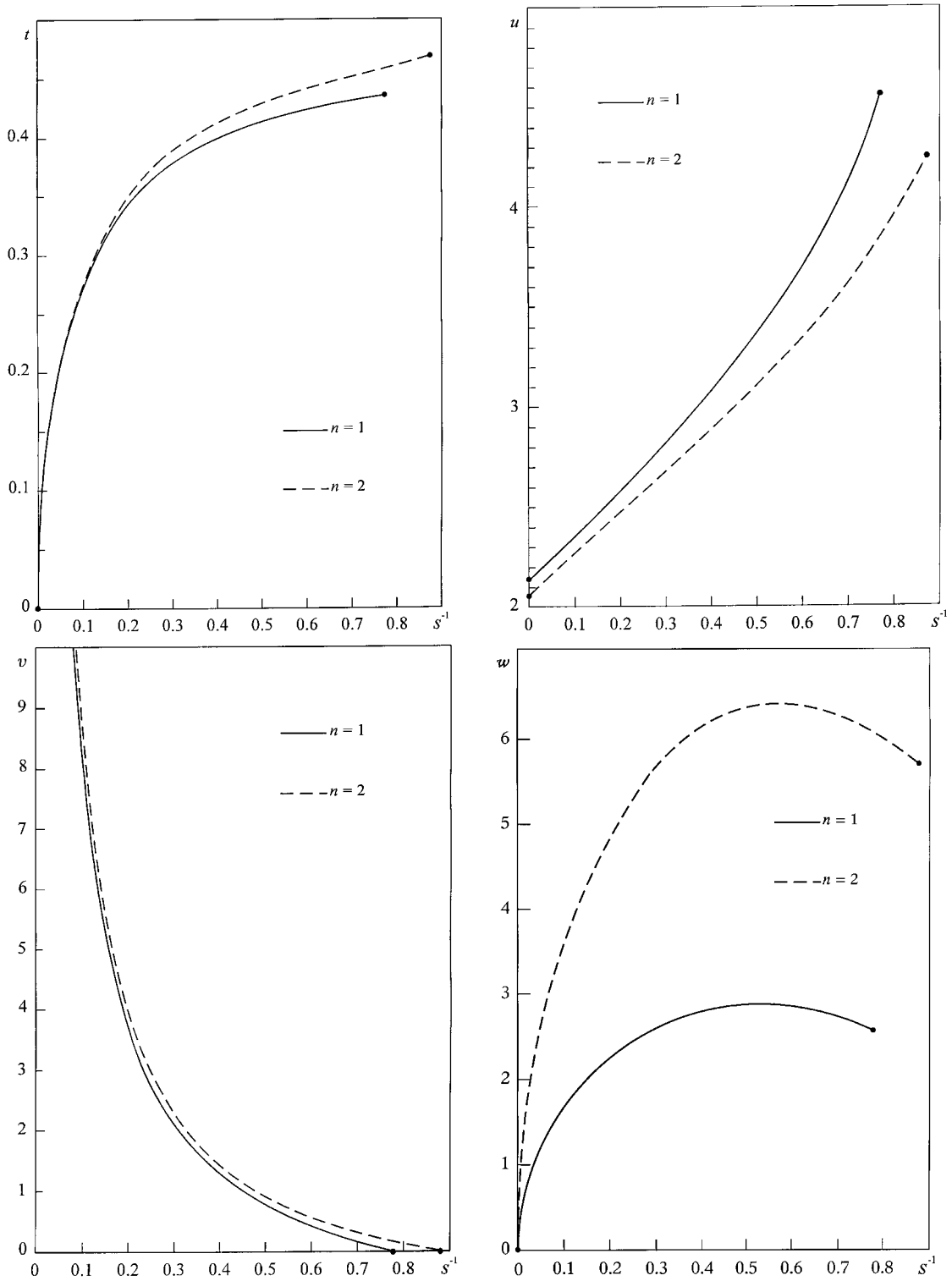

Fig. 5. Complete absorption by a slab. (i) Both the transmission and the reflection coefficients vanish when the four parameters $t \equiv \sin 2\theta^{\mathrm{i}}$ (where θ^{i} is the incidence angle), $u \equiv \omega^2 \mu_0 \varepsilon / \kappa_x^2 = \varepsilon / \varepsilon^{\mathrm{i}} \sin \theta^{\mathrm{i}}$, $v \equiv 1/\lambda^2 \kappa_x^2$ and $w \equiv \kappa_x l$ (where l is the thickness of the slab) take in terms of $s^{-1} \equiv \omega\varepsilon/\sigma$ the values which are represented here for the first two branches, $n = 1$ (full lines) and $n = 2$ (dashed lines). The variables s^{-1}, t, u and w have a finite range, in particular $s > 1.28$ for $n = 1$, $s > 1.13$ for $n = 2$.

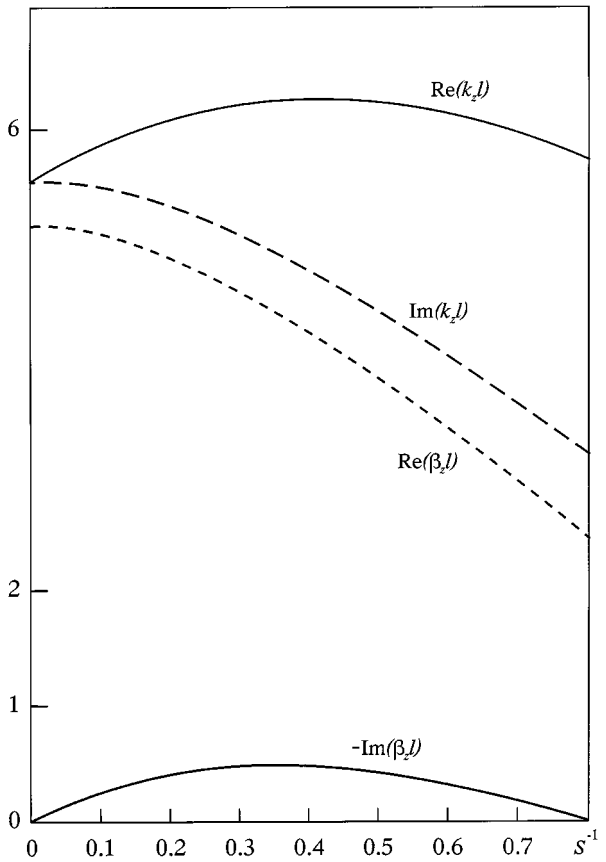

Fig. 6. Complete absorption by a slab. (ii) The normal components k_z and β_z of the complex wavevectors $\mathbf{k}$ and $\boldsymbol{\beta}$ for which complete absorption takes place are drawn as functions of $s^{-1} \equiv \omega\varepsilon/\sigma$, for the first branch $n = 1$ of solutions. The transverse component κ_x is represented by the curve $w\left(s^{-1}\right)$ of Figure 5.

describing the *charge density.* Actually, due to the gradient in (7.1), the partial differential equation for $\mathbf{E}$ alone would be of fourth-order, whereas the procedure that we described in Section 2.1 relies on *two second-order* usual Helmholtz field equations, one for the vector field $\mathbf{H}$ with the wavevector k (Eq. (2.8)), the other for the scalar field ρ with a dynamical screening length $\lambda\left(1 - \mathrm{i}\omega\varepsilon\sigma^{-1}\right)^{-1/2}$ (Eq. (2.10)). This neatly separates the two characteristic lengths of the problem, which play here the same rôle as the masses of elementary particles in field theory. Accordingly $\mathbf{E}$ and $\mathbf{J}$ are separated as a sum of two parts (which for $\mathbf{J}$ do not coincide with the two terms in (7.1)). The first one,

$$\mathbf{E}^{\mathrm{p}} = \frac{1}{\varepsilon + \mathrm{i}\sigma\omega^{-1}}\mathbf{D} = \frac{1}{\sigma}\mathbf{J}^{\mathrm{p}} = \frac{1}{\sigma - \mathrm{i}\omega\varepsilon}\mathrm{curl}\ \mathbf{H}, \qquad (7.3)$$

has the usual propagative form. The second one,

$$\mathbf{E}^{\mathrm{s}} = \frac{1}{\mathrm{i}\omega\varepsilon}\mathbf{J}^{\mathrm{s}} = \frac{\lambda^2\sigma}{\varepsilon}\frac{1}{\sigma - \mathrm{i}\omega\varepsilon}\nabla\rho, \qquad (7.4)$$

arises from the finite size of the screening length λ. The contribution $\mathbf{J}^{\mathrm{s}}$ to the current describes the motion of the screening charges, located within a distance λ from the interfaces, whereas the characteristic distance for the contribution $\mathbf{J}^{\mathrm{p}}$ is the usual skin depth. The boundary conditions are implemented by expressing the continuity at the interfaces of the tangential components of $\mathbf{H}$ and $\mathbf{E}$ and the vanishing of the normal component of $\mathbf{J}$, in agreement with the absence of a surface charge. The propagative and screening contributions are *coupled by these boundary conditions*, although they satisfy independent field equations.

We have studied a few elementary geometries, for which a polarized plane wave issued from a dielectric region impinges on a piece of conductor with a finite screening length. In the three cases considered, an explicit solution was obtained by separation of variables, and a remarkable structure, always the same, emerged for the S-matrix which relates the outgoing to the incoming waves. For a plane wall, S is identified with the reflection coefficient; for a sphere, it is related through (5.29, 5.30) to the scattering amplitudes and hence to the cross-sections (5.20, 5.21); for a plane slab, it is related through (6.4) to the reflection and transmission coefficients. In all three cases, the eigenvalues of S were cast (Eqs. (3.13, 5.29, 5.30, 6.12)) into the form

$$S = \mathrm{e}^{\mathrm{i}\Phi}\frac{C + D - B^*}{C + D - B}, \qquad (7.5)$$

which clearly *separates the parameters* governing the behaviour of the wave. The phase factor $\mathrm{e}^{\mathrm{i}\Phi}$ and the term B depend only on the wavevector in the external dielectric medium (Eqs. (3.14, 5.16, 6.11)). The term C depends only on the wavenumber k in the conductor, and not on the intensity of screening (Eqs. (3.15, 5.12, 6.13)). Finally $k^2 D$ is merely a function of the dynamical screening length $\lambda\left(1 - \mathrm{i}\omega\varepsilon\sigma^{-1}\right)^{-1/2}$; it is given by (3.16, 5.13, 6.13). It vanishes for $\lambda = 0$, and also for waves with transverse electric polarization, both for planar and spherical geometries; in this case, the currents induced by the wave have no divergence and thus no screening charge appears. Each element Φ, B, C, D of (7.5) depends on the geometry, and they always satisfy the inequalities

$$\begin{aligned} &\mathrm{Im}\ B > 0, \qquad \mathrm{Im}\ (-C) > \mathrm{Im}\ D > 0, \\ &\mathrm{Im}\ k^2 C < 0 < \mathrm{Im}\ k^2 D. \end{aligned} \qquad (7.6)$$

The power dissipated by each partial wave within the medium is given in all three cases by:

$$W = 1 - |S|^2 = \frac{4\mathrm{Im}\ B\,(-C - D)}{|C + D - B|^2} \qquad (7.7)$$

(Eqs. (3.24, 5.31, 6.19)). The inequalities (7.6) ensure that it is positive, and also imply that the term D in the *numerator* of (7.7) contributes to *reduce* the absorption rate. The screening length λ, however, also occurs in the *denominator* of (7.7) through D, and this occurrence may *either enhance or reduce* the absorption. We have discussed in detail the interplay of these two occurrences of D and their influence on the overall dissipation rate in the case of a plane wall (Sect. 4.1).

The presence in the S-matrix (7.5) of the two terms D, which arise from the finiteness of the screening length, has remarkable consequences. Several effects, which are *forbidden for metal–dielectric interfaces, become possible* when the screening becomes imperfect.

A first class of such unusual phenomena are related to a possible *enhancement of the absorption,* which may even become *complete.* Namely, for some values of the physical and geometrical parameters, some eigenvalues (7.5) of the *S-matrix may vanish.* This is expressed by the possibility of finding solutions to the equation $C + D = B^*$, whereas the equation $C = B^*$ which would arise for $\lambda = 0$ never has solutions for a metal–dielectric interface in the geometries considered above. We have studied three examples of such effects. We have first seen (Sect. 4.2) that the *reflection coefficient from a semiconducting plane wall may vanish* for a TM wave with appropriate incidence and frequency, for suitably chosen dielectric constants, conductivity and screening length (Figs. 1 and 2). In contrast, it is well known that a metallic plane wall (with $\lambda = 0$) *always* reflects partly any incident wave. Similarly we have shown that for a spherical semiconductor or ionic conductor embedded in a dielectric medium *the absorption cross-section* (5.31) *may reach its largest possible value* corresponding to $S_{l\mathrm{e}} = 0$ for some incoming multipolar electric partial wave. This wave is thus *fully captured* (Sect. 5.5, Eq. (5.60) and Fig. 4). Finally, an effect which we find even more surprising is the possibility of *complete absorption* of a TM wave *by a slab* (Sect. 6.5): *both the reflection and the transmission coefficients can vanish* for some set of physical and geometrical parameters shown by Figures 5 and 6. In the limit $\sigma \gg \omega\varepsilon$, this effect requires in particular the screening length to lie close to the skin depth, and the thickness of the slab to satisfy a resonance condition.

A second class of effects generated by the finiteness of the screening length, and which may take place for other ranges of the parameters, correspond to a possible *reduction of the absorption.* The *reflection* from a plane wall is thus significantly *enhanced* by an imperfect screening for large $\sigma/\omega\varepsilon$, all other dimensionless parameters being finite (end of Sect. 4.1). We have also shown that *a small sphere scatters much less* the e.m. waves when the screening length is larger than its radius than when it is smaller (Sect. 5.4). Likewise, the *transparency of a thin slab increases with* λ (Sect. 6.3). If the slab is thinner than the skin depth and the screening length, we saw that its transparency is not proportional to its thickness as usual but to the *square of its thickness* (Eq. (6.23)). If on the other hand it is thicker than the skin depth, the transmission coefficient, which is exponentially small when $\lambda = 0$, may increase by many orders of magnitude when λ becomes larger than the thickness of the slab, all other parameters being kept fixed; its value (6.25) is then nearly independent of the thickness.

A last type of effects are associated with *local heat transfers* between the wave and the charge carriers. We have shown in Section 2.2 that both the Poynting vector and the local dissipation rate $w(\mathbf{r}) = \frac{1}{2}\mathrm{Re}\ \mathbf{E}\cdot\mathbf{J}^*$ are here the sum of two contributions, the normal dissipative one $w^{\mathrm{p}}(\mathbf{r})$ which is everywhere positive, plus a cross-term $w^{\mathrm{s}}(\mathbf{r}) = \frac{1}{2}\mathrm{Re}\ (\mathbf{E}^{\mathrm{p}}\cdot\mathbf{J}^{\mathrm{s}*} + \mathbf{E}^{\mathrm{s}}\cdot\mathbf{J}^{\mathrm{p}*})$ between the propagative and screening contributions to $\mathbf{E}$ and $\mathbf{J}$. This second term oscillates in space, due to the fact that $\mathbf{E}^{\mathrm{p}}, \mathbf{J}^{\mathrm{p}}$ on the one hand, $\mathbf{E}^{\mathrm{s}}, \mathbf{J}^{\mathrm{s}}$ on the other hand propagate with different wavenumbers. In some circumstances, illustrated by Figure 3, the amplitude of these oscillations may be larger than the ordinary dissipative term $w^{\mathrm{p}}(\mathbf{r})$. Then, at places where $w^{\mathrm{s}}(\mathbf{r}) < -w^{\mathrm{p}}(\mathbf{r})$, energy is pumped on average from the carriers by the field, while energy is released by the field in the regions where $w(\mathbf{r})$ is positive. We have discussed in Sections 2.2 and 4.3 why it is not unreasonable to expect such an effect. In particular, we predicted for a plane wall (Sect. 4.3) and for not too small a sphere (Sect. 5.3) that for $\sigma \gg \omega\varepsilon$ and λ larger than the skin depth the conductor should *be cooled by the wave just below the interface,* and overheated further inside, at a distance of the order of the skin depth. In these circumstances the Joule heat is expected to be small compared to these odd energy transfers.

Although we gather from discussions with experimentalists that some of these effects might have already been seen, the influence of a finite screening length on the propagation of electromagnetic waves near interfaces does not seem to have been systematically investigated by experiments. Admittedly, our predictions rely on a very crude model, the validity of which may be questioned. In particular, in our study of thermal effects, we have disregarded the heat conduction, focusing only on the energy exchanges between the e.m. wave and the charge carriers. This may render the observation of the cooling of the carriers difficult. Nevertheless our basic constitutive equation (7.1) should hold at sufficiently low frequencies, such that $\omega\tau \ll 1$.

Finally, as our purpose was merely exploratory and theoretical, we have left all the parameters free to vary. Many of the effects predicted here require, however, specific constraints on these parameters. For instance, materials for which the screening length λ is sizeable cannot have a very large conductivity σ, since the diffusion coefficient $\sigma\lambda^2/\varepsilon$, which is of the order of the product of the mean free path and the thermal velocity of carriers, cannot take values varying over a very wide range. If then the condition $\sigma \gg \omega\varepsilon$ that we encountered on several occurrences should hold, experiments should be performed at low frequency. Moreover, we saw that some effects occur only if the parameters are adjusted in a particular manner. In particular, the slab problem depends on five dimensionless parameters, and total absorption may take place only if they are related to one another by four equations (Sect. 6.5). We have even seen (end of Sect. 6.5) that the best conditions for detecting the simultaneous cancellation of the reflection and the transmission coefficients require rather well-defined values for all five dimensionless parameters. While the frequency and the geometrical parameters, that is, the incidence angle and the thickness of the slab, can easily be varied, the physical parameters, namely the dielectric constants of the two media, the conductivity and the screening length cannot be chosen at will. Hopefully,

the large variety of existing materials and the possibility of controlling some of their properties should render the experiments feasible.

Appendix A: Vanishing of the reflection coefficient

A.1. Solution of equations (4.21)

Our purpose is to solve the equations (4.21) so as to express t and u in terms of s and v. In order to find u, we start from the second of these equations,

$$\sqrt{U+u-1}-\frac{1}{s}\sqrt{U-u+1}=\frac{s}{V}\sqrt{V+v+1} - \frac{1}{V}\sqrt{V-v-1}, \tag{A.1}$$

which by use of the definitions (4.22) reads

$$\sqrt{U+u-1}-\frac{1}{s}\sqrt{U-u+1}=\sqrt{2}\,Y(Z-1). \tag{A.2}$$

Taking the square of (A.2) and using the definition (4.9) of U yields

$$\frac{s^2+1}{s^2}U+\frac{s^2-1}{s^2}(u-1)-2u=2\,Y^2\,(Z-1)^2\,,$$

or equivalently

$$U=\frac{2s^2}{s^2+1}\left[Y^2\,(Z-1)^2+1\right]+u-1. \tag{A.3}$$

Among the solutions of (A.3) we must select those for which both sides of (A.2) have the same sign, a condition expressed by

$$\left[\left(s^2-1\right)U+\left(s^2+1\right)(u-1)\right](Z-1)\geqslant 0. \tag{A.4}$$

Using the definitions (4.22), we can check that

$$\left(s^2+1\right)X^2-1=Y^2\,(Z-1)^2\,, \tag{A.5}$$

so that we can rewrite (A.3) as

$$U=2s^2X^2+u-1. \tag{A.6}$$

Taking now the square of (A.6), we find

$$u^2-4X^2u+4X^2\left(1-s^2X^2\right)=0, \tag{A.7}$$

to be supplemented with the new inequality

$$2s^2X^2+u-1>0. \tag{A.8}$$

The general solution of (A.7) reads

$$u=2X^2\pm 2XY\,(Z-1)\,, \tag{A.9}$$

where we used again (A.5). Both roots (A.9) satisfy the inequality (A.8), since (A.5) implies

$$2s^2X^2+u-1=\left[X\pm Y\,(Z-1)\right]^2+s^2X^2.$$

We thus have

$$U-u+1=2s^2X^2\quad,\quad U+u-1=\frac{u^2}{2X^2}, \tag{A.10}$$

which allow us to rewrite the conditions (A.4) in the form $\left(u^2-4X^4\right)(Z-1)\geqslant 0$, or equivalently

$$Y\,(Z-1)\pm 2X\geqslant 0. \tag{A.11}$$

A last inequality remains to be satisfied, namely $u>0$, that is,

$$X\pm Y\,(Z-1)>0. \tag{A.12}$$

The conditions (A.11) and (A.12) are incompatible for the lower sign since they then imply $X>2X$ (remember that X,Y,Z are positive). We must thus exclude the solution (A.9) with the minus sign. For the remaining solution,

$$u=2X\,(X-Y+YZ)\,, \tag{A.13}$$

the condition $Y\,(Z-1)+2X>0$ results from $X+Y\,(Z-1)>0$, and it thus suffices to check the positivity of u. This is readily done, since $X>Y$.

The next step consists in determining t from the first equation (4.21). We first find, from (A.10, A.13),

$$\sqrt{U+u-1}=\frac{u}{\sqrt{2}X}=\sqrt{2}\,(X-Y+YZ)\,. \tag{A.14}$$

We then note, from (4.22), that

$$\frac{s}{V}\sqrt{V+v+1}=\frac{v}{V\sqrt{V-v-1}}=\sqrt{2}\,YZ; \tag{A.15}$$

hence, we find:

$$t=\frac{2}{u}\,(X-Y)=\frac{X-Y}{X\,(X-Y+YZ)}\cdot \tag{A.16}$$

This solution is positive, but it is admissible only if it is less than 1, so that s and v should satisfy

$$(X-Y)\,(X-1)+XYZ\geqslant 0. \tag{A.17}$$

The parameters X,Y,Z can also be used to express the wavevectors $\mathbf{k}$ and $\boldsymbol{\beta}$ in terms of s and v. Indeed, we find from (4.10, 4.22) that

$$\kappa_x\mathrm{Im}\,\frac{1}{\beta_z}=Y,\quad \frac{\mathrm{Re}\;\beta_z}{|\mathrm{Im}\;\beta_z|}=\frac{Z}{s},\quad \frac{|\beta_z|^2}{\kappa_x^2}=V, \tag{A.18}$$

while (A.15) shows that $s\kappa_x\mathrm{Re}\;(1/\beta_z)=YZ$. We find also from (A.10, A.13) and (A.14) that, for a vanishing reflection coefficient,

$$\frac{1}{\kappa_x}\mathrm{Im}\;k_z=sX,\quad \frac{1}{\kappa_x}\mathrm{Re}\;k_z=X-Y+YZ,$$
$$\frac{|k_z|^2}{\kappa_x^2}=U=1+2Y\,(Z-1)\,(X-Y+YZ)\,. \tag{A.19}$$

These expressions allow us to check that

$$C = \frac{-B\left[X\left(1+\mathrm{i}s\right)+Y\left(Z-1\right)\right]}{\left(X-Y\right)\left(1+\mathrm{i}s\right)}$$

and

$$D = \frac{BY\left(Z+\mathrm{i}s\right)}{\left(X-Y\right)\left(1+\mathrm{i}s\right)} \tag{A.20}$$

sum up to $B^* = -B$. They also can be used to derive from the condition (A.17) some inequalities to be satisfied by the wavevectors.

A.2. Limiting cases

Let us now discuss the results (A.13, A.16, A.17) in terms of the variables s and v. We first note that (A.17) obviously holds for $X \geqslant 1$, that is, for

$$s^2 \leqslant \frac{v}{4\left(v+1\right)^3}\cdot \tag{A.21}$$

On the other hand, although the boundary of (A.17) is a portion of an algebraic curve of high degree, simple analytic results are available along the curve $Z = 1$ in the plane (s, v), that is,

$$v = \frac{2s^2}{1-3s^2}, \quad s < \frac{1}{\sqrt{3}}\cdot \tag{A.22}$$

We have there $V = 2v + 1$, and hence

$$t = \sqrt{s^2+1} - s\sqrt{1-3s^2}, \quad u = \frac{2}{s^2+1}, \quad U = 1. \tag{A.23}$$

The condition $t \leqslant 1$ thus yields along the curve (A.22):

$$\begin{aligned} s &\leqslant \sqrt{\frac{2^{4/3}-2^{2/3}}{3}} \simeq 0.56, \\ v &\leqslant \frac{8\left(1+2^{1/3}\right)}{3} + 2^{5/3} \simeq 9.2. \end{aligned} \tag{A.24}$$

We now turn to the asymptotic forms of equations (A.13, A.16, A.17) in the various limiting cases. Near the axis $v \ll 1$, we always find a solution. It is given, for finite or large s, by

$$\begin{aligned} t^{-1} &\approx (1+s) - \frac{vs}{2}, \\ u &\approx 2\left(1+s\right) - v\left(\frac{1}{s}+2+2s\right), \end{aligned} \tag{A.25}$$

and for s either comparable to v or smaller than v, by

$$\begin{aligned} t &\approx \frac{\sqrt{2}\,V}{\sqrt{\left(V+1\right)\left(2V-1\right)}}, \\ u &\approx \frac{\left(2V-1\right)\left(V+1\right) - vs^{-1}\sqrt{2V-1}}{V^2}, \end{aligned} \tag{A.26}$$

where $V = \sqrt{1+v^2s^{-2}}$. A cross-over between these two forms takes place for $v \ll s \ll 1$, in which case:

$$t^{-1} \approx 1 + s - \frac{vs}{2} + \frac{v^2}{8s^2}, \quad u \approx 2\left(1+s-\frac{v}{2s}\right). \tag{A.27}$$

Thus, for small fixed v, when s increases, t first decreases as $1 - s/4v$ for $s \ll v$, reaches a minimum slightly below $\frac{2}{3}\sqrt{2} \simeq 0.9428$ for $s \sim v/\sqrt{3}$, then returns to a maximum $1 - \frac{3}{2}\left(v/2\right)^{2/3}$ for $s = \left(v/2\right)^{2/3}$ and finally decreases down to zero as s^{-1} for $s \to \infty$. Likewise, u first decreases as $2 - \sqrt{2s/v}$ down to its minimum $\frac{3}{2}$ for $s = v/\sqrt{3}$, then increases, reaching 2 for $s = \sqrt{v/2}$, and tends to ∞ as $2s$ for $s \to \infty$.

Near the origin, (A.26) shows that t depends only on the ratio v/s. When v/s increases, from 0 to $\sqrt{3}$, $t = \sin 2\theta^{\mathrm{i}}$ decreases from 1 to $\frac{2}{3}\sqrt{2}$; then when v/s increases from$\sqrt{3}$ to ∞, t increases back to 1. The incidence angle θ^{i} thus remains in the vicinity of $\frac{\pi}{4}$ for v and s both small. The correction to (A.26) for $v \simeq s\sqrt{3},\ v \to 0$,

$$t \approx \frac{2\sqrt{2}}{3} + \frac{2\sqrt{2}}{9}\left[\frac{1}{32}\left(\frac{v}{s}-\sqrt{3}\right)^2 - v\right],$$

shows that two level lines with $t = \frac{2}{3}\sqrt{2}$ start from the origin $s = v = 0$ with the same slope $\sqrt{3}$. The quantity u given by (A.26) also depends near the origin on v/s only ; it decreases from 2 to $\frac{3}{2}$ when v/s increases from 0 to $\sqrt{3}$, then returns to 2 for $v/s \to \infty$. The correction to (A.26) for $v \simeq s\sqrt{3},\ v \to 0$,

$$u \approx \frac{3}{2} + \frac{1}{2}\left[\frac{1}{16}\left(\frac{v}{s}-\sqrt{3}\right)^2 + v\right],$$

shows that for values of u slightly larger than $\frac{3}{2}$, the level lines constitute closed loops which start from the origin $s = v = 0$ and return to it.

Near the axis $s \ll 1$, we find for v either finite or large,

$$\begin{aligned} t &\approx 1 + \frac{s^2}{2} - \sqrt{\frac{s^3}{2v}} - \frac{s}{4v} + \frac{s^2}{4v^2}\left(3v+1\right), \\ u &\approx 2 - \sqrt{\frac{2s}{v}}. \end{aligned} \tag{A.28}$$

The condition $t \leqslant 1$ requires that

$$v \leqslant v_{\max}\left(s\right) \sim \frac{\frac{3}{2}+\sqrt{2}}{s} \simeq \frac{2.9}{s}, \quad \left(s \ll 1\right). \tag{A.29}$$

We thus see that the allowed region is limited by a curve with the asymptote (A.29), too small values of the screening length being forbidden for s fixed. If for given $s \ll 1$, v increases, t and u also increase, starting as $1 - s/4v$ and $2 - \sqrt{2s/v}$, respectively, till v reaches $v_{\max}\left(s\right)$. While t remains close to 1, u remains close to 2, expressing that $k_z^{\mathrm{i}} \sim \kappa_x \sim k_z$: both the incidence and the refraction angle, are close to $\frac{\pi}{4}$ in this limit. The complex wavevector $\boldsymbol{\beta}$ is

nearly normal to the interface since $\beta_z/\kappa_x \sim \sqrt{-\mathrm{i}v/s}$ is large.

For $v \gg 1$, we have just seen that the region $1 \gg s > \left(\frac{3}{2}+\sqrt{2}\right)/v$ is forbidden. Finite values for s are also forbidden since (A.16) provides, for $v \gg 1$ and s finite, $t \sim \sqrt{1+s^2} > 1$. Let us then explore the region $v \gg 1,\ s \gg 1$. We then find from (A.13, A.16)

$$t^{-1} \approx \frac{s}{\sqrt{v}}\left(1+\frac{\frac{3}{2}+vs^{-2}}{s\sqrt{1+vs^{-2}}}\right),$$
$$u \approx \frac{2s}{v}\left(\sqrt{1+vs^{-2}}+\frac{1+vs^{-2}}{s}\right), \qquad \text{(A.30)}$$

where we dropped terms of relative order s^{-2} or v^{-1}. By expressing that $t^{-1} > 1$, we find a parabolic branch

$$v < v_{\max}(s) \approx s^2 + \frac{5s}{\sqrt{2}}, \quad (s \gg 1), \qquad \text{(A.31)}$$

for the curve which bounds the allowed region. Unless s is either sufficiently small or sufficiently large, short values for the screening length are incompatible with a total absorption. When s increases in the allowed region, starting from $s = \sqrt{v},\ t$ decreases from 1 to 0 while u remains small. The wavevectors satisfy

$$\frac{k_z}{\kappa_x} \sim \frac{s}{\sqrt{v}} + \mathrm{i}\sqrt{1+\frac{s^2}{v}}, \quad \frac{\beta_z}{\kappa_x} \sim \sqrt{v} \gg 1. \qquad \text{(A.32)}$$

Finally, for $s \gg 1$ and $v \ll s^2$, there is always a solution,

$$t \approx \frac{\sqrt{v+1}}{s}\left(1-\frac{3v+2}{2s(v+1)}\right), \quad u \approx \frac{2(s+1)}{v+1}, \quad \text{(A.33)}$$

which interpolates (A.27) and (A.30). Since t is small, the incidence should then be close to normal or to grazing, and the equations

$$\frac{k_z}{\kappa_x} \sim s\sqrt{\frac{2\mathrm{i}}{v+1}}, \quad \frac{\beta_z}{\kappa_x} \sim \sqrt{v+1} \qquad \text{(A.34)}$$

show that $\kappa_x \ll |k_z|$ while $\boldsymbol{\beta}$ is real.

Altogether, a solution is available for all points below the curve $v = v_{\max}(s)$, which has the hyperbolic behaviour (A.29) for $s \to 0$ and the parabolic behaviour (A.31) for $s \to \infty$. This curve passes through the point (A.24), and has a minimum, found numerically to lie at $s \simeq 0.696, \quad v \simeq 8.98$; at this point, where $t = 1, \quad u \simeq 1.42$, we find from (A.18), (A.19) that $k_z/\kappa_x = 0.87+0.57\mathrm{i}$ and $\beta_z/\kappa_x \simeq 3.63-1.78\mathrm{i}$. The maps of t and u in the plane (s, v) are shown in Figures 1 and 2; they are consistent with the above analytic results.

Appendix B: Some properties of Bessel functions

We gather below a few results that we use in the main text, Sections 5.2 and 5.3. Their proofs rely on properties of Bessel functions gathered in reference [10]. The spherical Bessel functions (5.4) are solutions of the differential equation

$$\left[\frac{d^2}{dz^2}+\frac{2}{z}\frac{d}{dz}+1-\frac{l(l+1)}{z^2}\right] j_l(z) = 0. \qquad \text{(B.1)}$$

They behave for $z \to 0$ as

$$j_l(z) \approx \frac{z^l}{(2l+1)!!}\left(1-\frac{z^2}{2(2l+3)}\right), \qquad \text{(B.2a)}$$
$$h_l(z) \approx \frac{(2l-1)!!}{z^{l+1}}\left(1+\frac{z^2}{2(2l-1)}\right). \qquad \text{(B.2b)}$$

Their Wronskians are

$$j_l'(z)\,h_l(z) - j_l(z)h_l'(z) = \frac{1}{z^2}$$
$$= \frac{1}{2\mathrm{i}}\left[h_l'(z)\,h_l^{(-)}(z) - h_l(z)\,h_l^{(-)'}(z)\right]. \qquad \text{(B.3)}$$

For $l = 1$, they reduce to

$$j_1(z) = \frac{\sin z}{z^2} - \frac{\cos z}{z}, \quad h_1(z) = \frac{1-\mathrm{i}z}{z^2}\mathrm{e}^{\mathrm{i}z}. \qquad \text{(B.4)}$$

We use in the text some integrals over products of spherical Bessel functions, namely

$$\left(k^2-k^{*2}\right)\int r^2\,|j_l(kr)|^2\,dr$$
$$= r^2\left[k^* j_l(kr)\,j_l'(k^*r) - k j_l'(kr)\,j_l(k^*r)\right], \qquad \text{(B.5)}$$

$$\left(k^2-k^{*2}\right)\int\left[l(l+1)\,|j_l(kr)|^2 + \left|kr j_l'\right|^2\right]dr$$

$$= |k|^2 r^2\left[k j_l(kr)\,j_l'(k^*r) - k^* j_l'(kr)\,j_l(k^*r)\right], \qquad \text{(B.6)}$$

$$\int\left[|j_l(kr)|^2 + 2\mathrm{Re}\ kr j_l'(kr)\,j_l(k^*r)\right]dr = r\,|j_l(kr)|^2. \qquad \text{(B.7)}$$

Let us now find a few inequalities satisfied by B_l, C_l and D_l. From the definition (5.16) of B_l, we obtain, letting $x \equiv \kappa R$,

$$\mathrm{Im}\ B_l = \frac{h_l'(x)\,h_l^{(-)}(x) - h_l(x)\,h_l^{(-)'}(x)}{2\mathrm{i}x\,|h_l(x)|^2}$$
$$= \frac{1}{x^3\,|h_l(x)|^2}, \qquad \text{(B.8)}$$

where we used the Wronskian (B.3). Hence Im B_l is positive. The real part of B_l reads

$$\mathrm{Re}\ B_l = \frac{1}{2x}\frac{d}{dx}\left[\ln x^2\,|h_l(x)|^2\right]$$
$$= \frac{1}{2x}\frac{d}{dx}\left\{\ln x\left[J^2_{l+\frac{1}{2}}(x) + N^2_{l+\frac{1}{2}}(x)\right]\right\}, \qquad \text{(B.9)}$$

and it is negative since $x\left[J_\nu^2(x)+N_\nu^2(x)\right]$ decreases monotonically for $\nu>\frac{1}{2}$.

The quantity C_l defined by (5.12) is the value for $z=kR$ of the meromorphic function of z^2,

$$\frac{j_l^{'}(z)}{zj_l(z)}+\frac{1}{z^2},$$

which has, as only singularities for finite z^2, a simple pole at $z=0$ around which it behaves as $(l+1)z^{-2}+\mathcal{O}(1)$, and a sequence of simple poles $z^2=\xi_n$ on the real positive axis, such that

$$\left|\sqrt{\xi_n}-n\pi-l\frac{\pi}{2}\right|<\frac{\pi}{2},\quad (n\geqslant 1),$$

the residues being equal to 2. It tends to zero for $z\to\pm\mathrm{i}\infty$, and its Mittag–Leffler expansion is therefore

$$\frac{j_l^{'}(z)}{zj_l(z)}+\frac{1}{z^2}=\frac{l+1}{z^2}+2\sum_{n\geqslant 1}\frac{1}{z^2-\xi_n}\cdot \tag{B.10}$$

Hence, introducing the notations

$$\tilde{k}\equiv|kR|^2,\quad \tilde{\beta}\equiv|\beta R|^2,$$
$$\psi\equiv \mathrm{tg}^{-1}s,\quad \left(0<\psi<\frac{\pi}{2}\right), \tag{B.11}$$

which imply that

$$(kR)^2=\tilde{k}\mathrm{e}^{\mathrm{i}\psi},\quad (\mathrm{i}\beta R)^2=\mathrm{i}\tilde{\beta}\mathrm{e}^{\mathrm{i}\psi}, \tag{B.12}$$

we find

$$\begin{aligned}\mathrm{Im}\ C_l&=-\frac{(l+1)\sin\psi}{\tilde{k}}\\&\quad-2\tilde{k}\sin\psi\sum_{n\geqslant 1}\frac{1}{\tilde{k}^2-2\tilde{k}\xi_n\cos\psi+\xi_n^2}\\&<-\frac{(l+1)\sin\psi}{\tilde{k}}<0.\end{aligned} \tag{B.13}$$

Instead of C_l, magnetic multipoles involve the function

$$\frac{zj_l^{'}(z)}{j_l(z)}=l+2\sum_{n\geqslant 1}\frac{z^2}{z^2-\xi_n} \tag{B.14}$$

taken at $z=kR$, which thus satisfies

$$\mathrm{Im}\ (kR)^2C_l=-2\sin\psi\sum_{n\geqslant 1}\frac{\xi_n}{\tilde{k}^2-2\tilde{k}\xi_n\cos\psi+\xi_n^2}<0. \tag{B.15}$$

The quantity D_l defined by (5.13) can be written by use of the notations (B.12) as

$$D_l=-\frac{l(l+1)s\tilde{\beta}}{\tilde{k}}\frac{j_l(z)}{z^3j_l^{'}(z)}, \tag{B.16}$$

where $z=\mathrm{i}\beta R$. From (B.14) and (B.12) we find

$$\begin{aligned}\mathrm{Im}\ \frac{z^3j_l^{'}(z)}{j_l(z)}&=\mathrm{Im}\ \left[lz^2+2\sum_{n\geqslant 1}\frac{z^4}{z^2-\xi_n}\right]\\&=l\tilde{\beta}\cos\psi\\&\quad+2\tilde{\beta}^2\sum_{n\geqslant 1}\frac{\tilde{\beta}\cos\psi+\xi_n\sin 2\psi}{\tilde{\beta}^2+2\tilde{\beta}\xi_n\sin\psi+\xi_n^2},\end{aligned}$$

and hence

$$\mathrm{Im}\ D_l>0. \tag{B.17}$$

An alternative representation of D_l is obtained by writing its Mittag-Leffler expansion. From (B.15) we see that $j_l^{'}(z)$ cannot vanish outside the real and imaginary axes, and the positivity of (B.14) on the imaginary axis then implies that all the poles of (B.16) lie on the real axis, at $z=0$, and at the extrema $z=\pm\sqrt{\zeta_n}$ of $j_l(z)$, which are intertwined with its zeroes ξ_n:

$$l(l+1)<\zeta_1<\xi_1<\zeta_2<...$$

At its simple poles $z=\pm\sqrt{\zeta_n}$ the residue of $j_l(z)/z^3j_l^{'}(z)$ is found from (B.1) to be

$$\frac{j_l\left(\sqrt{\zeta_n}\right)}{\zeta_n^{3/2}j_l^{''}\left(\sqrt{\zeta_n}\right)}=\frac{1}{\sqrt{\zeta_n}\left[l(l+1)-\zeta_n\right]};$$

around $z=0$, this function behaves as $1/lz^2+\mathcal{O}(1)$, and it tends to zero for $z\to\pm\mathrm{i}\infty$. Hence it is expanded as

$$\frac{j_l(z)}{z^3j_l^{'}(z)}=\frac{1}{lz^2}-2\sum_{n\geqslant 1}\frac{1}{\zeta_n-l(l+1)}\ \frac{1}{z^2-\zeta_n}, \tag{B.18}$$

which provides for (B.16), using (B.11, B.12):

$$\begin{aligned}\mathrm{Re}\ D_l&=\frac{(l+1)\sin^2\psi}{\tilde{k}\cos\psi}-\frac{2\tilde{\beta}\mathrm{tg}\psi}{\tilde{k}}\\&\quad\times\sum_{n\geqslant 1}\frac{l(l+1)}{\zeta_n-l(l+1)}\ \frac{\tilde{\beta}\sin\psi+\zeta_n}{\tilde{\beta}^2+2\tilde{\beta}\zeta_n\sin\psi+\zeta_n^2},\end{aligned} \tag{B.19}$$

$$\begin{aligned}\mathrm{Im}\ D_l&=\frac{(l+1)\sin\psi}{\tilde{k}}-\frac{2\tilde{\beta}^2\sin\psi}{\tilde{k}}\\&\quad\times\sum_{n\geqslant 1}\frac{l(l+1)}{\zeta_n-l(l+1)}\ \frac{1}{\tilde{\beta}^2+2\tilde{\beta}\zeta_n\sin\psi+\zeta_n^2}.\end{aligned} \tag{B.20}$$

As a consequence of (B.13) and (B.20) we have

$$\mathrm{Im}\ D_l<\frac{(l+1)\sin\psi}{\tilde{k}^2},\quad \mathrm{Im}\ (C_l+D_l)<0. \tag{B.21}$$

We can also check from (B.20) that $\mathrm{Im}\ D_l>0$. To this aim, we use the sum rule

$$\frac{1}{l}=2\sum_{n\geqslant 1}\frac{1}{\zeta_n-l(l+1)}, \tag{B.22}$$

which expresses that (B.18) tends to zero faster than z^{-2} for $z \to \pm i\infty$; we thus rewrite (B.20) as

$$\text{Im } D_l = \frac{2\sin\psi}{\tilde{k}} \times \sum_{n\geqslant 1} \frac{l(l+1)}{\zeta_n - l(l+1)} \frac{2\tilde{\beta}\zeta_n \sin\psi + \zeta_n^2}{\tilde{\beta}^2 + 2\tilde{\beta}\zeta_n \sin\psi + \zeta_n^2}, \quad \text{(B.23)}$$

which is obviously positive.

Finally, we can also write bounds on

$$(kR)^2 D_l = il(l+1)\, s \frac{j_l(z)}{z j_l'(z)}, \quad \text{(B.24)}$$

where $z = i\beta R$. From (B.14), we find, using $z^2 = i\tilde{\beta}e^{i\psi}$,

$$\left[(kR)^2 D_l\right]^{-1} = -\frac{1}{l(l+1)\, s} \times \left[il + 2\tilde{\beta}\sum_{n\geqslant 1} \frac{\xi_n \cos\psi + i\left(\tilde{\beta} + \xi_n \sin\psi\right)}{\tilde{\beta}^2 + 2\tilde{\beta}\xi_n \sin\psi + \xi_n^2}\right], \quad \text{(B.25)}$$

and hence

$$\text{Re}\left[(kR)^2 D_l\right] < 0, \quad \text{Im}\left[(kR)^2 D_l\right] > 0. \quad \text{(B.26)}$$

From (B.18) we also find

$$(kR)^2 D_l = l(l+1)\, s \times \left[\frac{i}{l} - 2\tilde{\beta}\sum_n \frac{1}{\zeta_n - l(l+1)} \frac{\zeta_n \cos\psi + i\left(\tilde{\beta} + \zeta_n \sin\psi\right)}{\tilde{\beta}^2 + 2\tilde{\beta}\zeta_n \sin\psi + \zeta_n^2}\right],$$

and hence

$$\text{Im}\left[(kR)^2 D_l\right] < (l+1)\, s. \quad \text{(B.27)}$$

Appendix C: Dissipation in a slab

C.1. Some inequalities

We gather here a few inequalities satisfied by the various terms of the S -matrix (6.12). We have already seen (Eqs.(3.25)) that C and D satisfy

$$-\frac{3\pi}{4} < \arg C < D, \quad 0 < \arg D < \frac{3\pi}{4}, \quad -\frac{\pi}{4} < \arg(-DC^*) < \frac{\pi}{2}. \quad \text{(C.1)}$$

We also readily find

$$\text{Im tg}\frac{1}{2}k_z l > 0, \qquad \text{Re tanh}\frac{1}{2}\beta_z l > 0. \quad \text{(C.2)}$$

In order to discuss the signs of the various terms in (6.19), we note that C_+ has the form

$$C_+ = \frac{w}{2z^2}\sqrt{z^2 - \frac{1}{4}w^2}\ \text{cotg}\ \sqrt{z^2 - \frac{1}{4}w^2},$$

where we used the definition (6.11, 6.13) of C_+, and where we set $z = \frac{1}{2}kl, w = \kappa_x l$. We proceed as for C_l in Appendix B, expanding this expression in terms of its poles $z^2 = 0$ and $z^2 = \xi_n \equiv n^2\pi^2 + \frac{1}{4}w^2\ (n \geqslant 1)$. We find

$$C_+ = \frac{w}{2z^2} + \frac{w\left(z^2 - \frac{1}{4}w^2\right)}{z^2}\sum_{n\geqslant 1}\frac{1}{z^2 - \xi_n} = \frac{1}{4z^2}w^2 \coth\frac{1}{2}w + w\sum_{n\geqslant 1}\frac{n^2\pi^2}{\xi_n}\frac{1}{z^2 - \xi_n}, \quad \text{(C.3)}$$

and hence, introducing as in (B.11) the notations $\tilde{k} \equiv \frac{1}{4}|kl|^2, \psi \equiv \text{tg}^{-1}s$, so that $z^2 = \tilde{k}e^{i\psi}$,

$$\text{Im } C_+ = -\frac{1}{4\tilde{k}}w^2 \coth\frac{1}{2}w\ \sin\psi - w\tilde{k}\sin\psi \times \sum_{n\geqslant 1}\frac{n^2\pi^2}{\xi_n}\ \frac{1}{\tilde{k}^2 - 2\tilde{k}\xi_n\cos\psi + \xi_n^2}. \quad \text{(C.4)}$$

This yields the inequality

$$\text{Im } C_+ < -\frac{\sin\psi\ w^2 \coth\frac{1}{2}w}{4\tilde{k}} < 0. \quad \text{(C.5)}$$

Likewise, C_- is expanded as

$$C_- = -\frac{1}{2}wz^{-2}\ \sqrt{z^2 - \frac{1}{4}w^2}\quad \text{tg}\sqrt{z^2 - \frac{1}{4}w^2} = \frac{1}{4z^2}w^2 \tanh\frac{1}{2}w + w\sum_{n\geqslant 1}\frac{\left(n - \frac{1}{2}\right)^2\pi^2}{\zeta_n}\frac{1}{z^2 - \zeta_n}, \quad \text{(C.6)}$$

where we introduced the notation $\zeta_n \equiv \left(n - \frac{1}{2}\right)^2\pi^2 + \frac{1}{4}w^2$, and its imaginary part satisfies

$$\text{Im } C_- < -\frac{w^2 \tanh\frac{1}{2}w\ \sin\psi}{4\tilde{k}} < 0. \quad \text{(C.7)}$$

The second term of (6.19) involves D_+, which we rewrite as we did for D_l in (B.16) in the form

$$D_+ = \frac{w^3\tilde{\beta}\text{tg}\psi}{8\tilde{k}}\frac{\text{cotg}\sqrt{z^2 - \frac{1}{4}w^2}}{z^2\sqrt{z^2 - \frac{1}{4}w^2}}, \quad \text{(C.8)}$$

where $z \equiv \frac{\mathrm{i}}{2}\beta l$ and $\tilde{\beta} \equiv \frac{1}{4}|\beta l|^2$, so that $z^2 = \mathrm{i}\tilde{\beta}\mathrm{e}^{\mathrm{i}\psi}$. The pole expansion of D_+ analogous to (C.3) reads

$$D_+ = -\frac{\tilde{\beta}\mathrm{tg}\psi}{4\tilde{k}z^2}w^2 \coth\frac{1}{2}w + \frac{\tilde{\beta}\mathrm{tg}\psi\ w^3}{8\tilde{k}}\left[\frac{1}{\xi_0\left(z^2-\xi_0\right)} + 2\sum_{n\geqslant 1}\frac{1}{\xi_n\left(z^2-\xi_n\right)}\right], \tag{C.9}$$

whence we find, using $z^2 = \mathrm{i}\tilde{\beta}\mathrm{e}^{\mathrm{i}\psi}$,

$$\mathrm{Im}\ D_+ < \frac{\sin\psi\ w^2\coth\frac{1}{2}w}{4\tilde{k}},$$
$$\mathrm{Re}\ D_+ < \frac{\sin^2\psi\ w^2\coth\frac{1}{2}w}{4\tilde{k}\cos\psi}. \tag{C.10}$$

Likewise, from

$$D- = -\frac{\tilde{\beta}\mathrm{tg}\psi w^3}{8\tilde{k}}\ \frac{\mathrm{tg}\sqrt{z^2-\frac{1}{4}w^2}}{z^2\sqrt{z^2-\frac{1}{4}w^2}} = -\frac{\tilde{\beta}\mathrm{tg}\psi}{4\tilde{k}z^2}w^2\tanh\frac{1}{2}w + \frac{\tilde{\beta}\mathrm{tg}\psi w^3}{4\tilde{k}}\sum_{n\geqslant 1}\frac{1}{\zeta_n\left(z^2-\zeta_n\right)}, \tag{C.11}$$

we obtain

$$\mathrm{Im}\ D_- < \frac{\sin\psi\ w^2\tanh\frac{1}{2}w}{4\tilde{k}},$$
$$\mathrm{Re}\ D_- < \frac{\sin^2\psi\ w^2\tanh\frac{1}{2}w}{4\tilde{k}\cos\psi}. \tag{C.12}$$

Finally, again as we did to find the sign of $\mathrm{Im}\ D_l$ in Appendix B, we can use the pole expansion of either $\left(D_\pm\right)^{-1}$ or $z^2D_\pm$. For instance the second method provides D_+ as a sum of terms (for $n \geqslant 0$) proportional to

$$\frac{1}{z^2\left(z^2-\xi_n\right)} = \frac{\left(\xi_n\sin\psi - \tilde{\beta}\cos 2\psi\right) + \mathrm{i}\left(\xi_n\cos\psi + \tilde{\beta}\sin 2\psi\right)}{\tilde{\beta}\left(\tilde{\beta}^2 + 2\tilde{\beta}\xi_n\sin\psi + \xi_n^2\right)}, \tag{C.13}$$

and similarly for D_- where ξ_n is changed into $\zeta_n\ (n \geqslant 1)$. Hence, we find

$$\mathrm{Im}\ D_+ > 0, \quad \mathrm{Im}\ D_- > 0. \tag{C.14}$$

Similar calculations using the above formulae also provide the inequalities

$$\mathrm{Im}\ \left(C_\pm k^2\right) < 0, \quad \mathrm{Im}\ \left(D_\pm k^2\right) > 0, \quad \mathrm{Re}\ \left(D_\pm k^2\right) < 0. \tag{C.15}$$

C.2. Explicit approximate conditions for complete absorption

We start from the equations (6.35) and (6.42) which express that the wave is completely absorbed, that is, $R = T = 0 = S_\pm$, in terms of the dimensionless variables s, t, u, v, w defined by (6.32).

We have found the solution (6.48, 6.49) of these coupled equations in the limit as $s \to \infty$. We saw that in this limit the quantities $\mathrm{Im}\ k_z l$ and $\mathrm{Re}\ \beta_z l$, of order $\chi l \sim w\sqrt{s} \sim 2n\pi - \frac{\pi}{4}$ were rather large, so that $\left|\mathrm{e}^{2\mathrm{i}k_z l}\right|$ and $\left|\mathrm{e}^{-2\beta_z l}\right|$ were at most equal to 1.7×10^{-5}. We were therefore entitled to replace $\sin k_z l$ by $\frac{\mathrm{i}}{2}\mathrm{e}^{-\mathrm{i}k_z l}$ and $\sinh\beta_z l$ by $\frac{1}{2}\mathrm{e}^{\beta_z l}$ in (6.35), which then simplifies into

$$\mathrm{i}\sqrt{u\left(1+\mathrm{i}s\right)-1} + \sqrt{v\left(1-\mathrm{i}s^{-1}\right)+1} = \frac{1}{w}\left[2n\mathrm{i}\pi + \ln s - \ln\sqrt{u\left(1+\mathrm{i}s\right)-1} - \ln\sqrt{v\left(1-\mathrm{i}s^{-1}\right)+1}\right], \tag{C.16}$$

and to replace $\mathrm{cotg}\ k_z l$ by $-\mathrm{i}$ and $\coth\beta_z l$ by 1 in (6.42), which simplies into

$$\sqrt{u\left(1+\mathrm{i}s\right)-1} - \frac{s}{\sqrt{v\left(1-\mathrm{i}s^{-1}\right)+1}} = \frac{tu}{2}\left(1+\mathrm{i}s\right). \tag{C.17}$$

The equations (C.16) and (C.17) might alternatively be found from the set (6.43), which provide within the same approximation the equation $C + D + B = 0$, identical to (C.17), and hence the equation $\mathrm{e}^{(\mathrm{i}k_z+\beta_z)l} = -D/C$, identical to (C.16).

Provided $\left|\mathrm{e}^{2\mathrm{i}k_z l}\right|$ and $\left|\mathrm{e}^{-2\beta_z l}\right|$ remain negligible, we can then replace the exact equations (6.35) and (6.42) for complete absorption by (C.16) and (C.17). The latter equation is the same as the one, (4.20), that we solved in Section 4.2 and Appendix A. We explicitly expressed t and u in terms of s and v by means of equations (4.23, 4.24), where X, Y and Z are functions of s and v defined by (4.9, 4.22). Inserting the expression thus found for u and hence for U into (C.16), and separating the real and imaginary parts, we find two real equations relating s, v and w:

$$\sqrt{U-u+1} - \sqrt{V+v+1} = \frac{1}{w\sqrt{2}}\ln\frac{UV}{s^2}, \tag{C.18}$$

$$\sqrt{U+u-1} - \sqrt{V-v-1} = \frac{\sqrt{2}}{w}\left[2n\pi - \frac{1}{2}\mathrm{tg}^{-1}\frac{us}{u-1} + \frac{1}{2}\mathrm{tg}^{-1}\frac{v}{s\left(v+1\right)}\right]. \tag{C.19}$$

We can eliminate w between (C.18) and (C.19), in the form:

$$\frac{\sqrt{U-u+1} - \sqrt{V+v+1}}{\sqrt{U+u-1} - \sqrt{V-v-1}} = \frac{1}{2}\ln\frac{UV}{s^2}\left[2n\pi - \frac{1}{2}\mathrm{tg}^{-1}\frac{uv\left(s^2-1\right)+us^2+v}{s\left(2uv+u-v-1\right)}\right]^{-1}. \tag{C.20}$$

Equation (C.20), where u is replaced by its expression (4.24), is the relation between s and v which should be satisfied to ensure complete absorption within the considered approximation. More explicitly, we rewrite the left-hand side of (C.20) by using (A.10, A.14, A.15), then replacing X, Y, Z by their expressions (4.22), and simplifying the ratio by means of (4.29); this yields:

$$\frac{\sqrt{U-u+1}-\sqrt{V+v+1}}{\sqrt{U+u-1}-\sqrt{V-v-1}}$$

$$= \frac{\sqrt{2}sX-\sqrt{V+v+1}}{\sqrt{2}\,(X-Y+YZ)-\sqrt{V-v-1}}$$

$$= \frac{s\sqrt{V+v+1+2v^2s^{-2}}-V\sqrt{V+v+1}}{\sqrt{V+v+1+2v^2s^{-2}}+s\,(V-v-vs^{-2})\sqrt{V+v+1}}$$

$$= \frac{s\sqrt{2V-2v-1}-V}{\sqrt{2V-2v-1}+s\,(V-v-vs^{-2})}.$$

Multiplying then the numerator and denominator by $s\sqrt{2V-2v-1}+V$, we obtain the relation (C.20) between s and v in the form

$$\frac{2s^2V}{1+s^2}-\left(2v+1+\frac{v^2}{s^2}\right) = \frac{\left[\dfrac{sV}{1+s^2}+\dfrac{V-v}{2}\left(\sqrt{2V-2v-1}-\dfrac{v}{s}\right)\right]\ln\dfrac{UV}{s^2}}{2n\pi-\dfrac{1}{2}\mathrm{tg}^{-1}\dfrac{uv\left(s^2-1\right)+us^2+v}{s\,(2uv+u-v-1)}}, \tag{C.21}$$

where u and U are functions of s and v given by (4.22, 4.24) and (A.19).

Finally the thickness $l = w/\kappa_x$ is expressed in the considered approximation $\left|\mathrm{e}^{2\mathrm{i}k_z l}\right| \ll 1, \left|\mathrm{e}^{-2\beta_z l}\right| \ll 1$ by (C.19), which reads

$$w = \frac{2n\pi-\frac{1}{2}\mathrm{tg}^{-1}\frac{uv\left(s^2-1\right)+us^2+v}{s(2uv+u-v-1)}}{X+Y\,(Z-1-V)} \tag{C.22}$$

in terms of the functions V, X, Y, Z of v and s defined by (4.22). Altogether, for given s, the parameters u and v for which the wave is completely absorbed are given by (4.22) and (C.21), and the parameters t and w by (4.23) and (C.22).

Let us work out these equations for $s \gg 1$. We first check that for $s \to \infty$, they are satisfied for the solution (6.48, 6.49). Indeed, for $s \to \infty$, with u and v/s finite, we have $U \sim us, V \approx v+1+\frac{1}{2}vs^{-2}, X \sim v^{-1/2}, Y \sim \frac{1}{2}v^{-1/2}s^{-1}, Z \sim 2s^2$, and hence from (4.24) $uv \sim 2s$; the argument of tg^{-1} in (C.21) and (C.22) is large as $us/\left(2u-1\right)$, and the bracket on the right-hand side of (C.21) is $\frac{1}{2}\left(1+vs^{-1}\right)$ while the left-hand side is $1-v^2s^{-2}$, so that we recover from (C.21) the expressions (6.48) for u and v, with η given by (6.49); the resulting values (4.23) and (C.22) for t and w are also seen to be given by (6.48, 6.49). We can now find the corrections of relative order s^{-1} and s^{-2} for u and v by expanding (4.22, 4.24) and iterating (C.21). Since η is small, at most equal to 0.063, we systematically regard it as being of order s^{-1}. Noting that s and v have the same order, we thus find

$$X \approx \frac{1}{\sqrt{v+1}}\left(1+\frac{v}{2s^2}-\frac{1}{s^2}\right),$$

$$YZ \approx \frac{s}{\sqrt{v+1}}\left(1-\frac{3}{8s^2}\right),$$

and hence

$$u \approx \frac{2s}{v}\left(1-\frac{1}{v}+\frac{1}{s}+\frac{v}{2s^2}-\frac{11}{8s^2}\right), \tag{C.23}$$

which after insertion into (C.21) yields:

$$1-\frac{v^2}{s^2}-\frac{v}{s^2}-\frac{1}{s^2} \approx \frac{\left(1+\dfrac{v}{s}+\dfrac{2}{s}+\dfrac{v}{s^2}-\dfrac{v^2}{2s^3}-\dfrac{3}{8s^2}\right)\ln\left[2\left(1+\dfrac{1}{s}+\dfrac{v}{2s^2}-\dfrac{1}{4s^2}\right)\right]}{4n\pi-\dfrac{\pi}{2}+\mathrm{tg}^{-1}\dfrac{2-\dfrac{v}{2s}-\dfrac{1}{v}+\dfrac{3}{2s}+\dfrac{v}{s^2}}{s+1+\dfrac{v}{2s}}}.$$

Iteration, starting from $v \simeq s$, yields for each branch $n = 1, n = 2, ...$ the asymptotic expansion for the solution of $R = T = 0$:

$$v_n(s) \approx s(1-\eta) - \left(\frac{1}{2}+\frac{3}{4\nu}+\eta-\frac{\eta}{\nu}\right) - \frac{1}{s}\left(\frac{3}{8}-\frac{1}{16\nu}-\frac{3}{4\nu^2}\right), \tag{C.24}$$

where we introduced the notations

$$\nu = 2n\pi-\frac{\pi}{4}, \quad \eta = \frac{1}{2\nu}\ln 2. \tag{C.25}$$

Numerically, for $n = 1$ and $n = 2$, (C.24) provides:

$$v_1(s) \approx 0.94s-0.69-\frac{0.34}{s},$$
$$v_2(s) \approx 0.97s-0.59-\frac{0.36}{s}. \tag{C.26}$$

From (C.23) we obtain the asymptotic expansion of $u_n(s)$:

$$u_n(s) \approx 2\left[\frac{1}{1-\eta}+\frac{1}{s}\left(1+\frac{3}{4\nu}+\eta+\frac{\eta}{2\nu}\right) -\frac{1}{s^2}\left(\frac{5}{4}+\frac{1}{16\nu}+\frac{3}{16\nu^2}\right)\right], \tag{C.27}$$

that is, numerically,

$$u_1(s) \approx 2.13+\frac{2.41}{s}-\frac{2.54}{s^2},$$
$$u_2(s) \approx 2.06+\frac{2.19}{s}-\frac{2.51}{s^2}. \tag{C.28}$$

The expansions of $t_n(s)$ and $w_n(s)$, drawn from (4.23) and (C.22), are up to first order in s^{-1}:

$$t_n(s) \approx \frac{1}{\sqrt{s}}\left[1-\frac{\eta}{2}-\frac{1}{s}\left(\frac{5}{4}+\frac{3}{8\nu}\right)\right], \quad \text{(C.29)}$$

$$t_1(s) \approx \frac{1}{\sqrt{s}}\left(0.97-\frac{1.32}{s}\right),$$

$$t_2(s) \approx \frac{1}{\sqrt{s}}\left(0.99-\frac{1.28}{s}\right), \quad \text{(C.30)}$$

$$w_n(s) \approx \frac{\nu}{\sqrt{s}}\left[1-\frac{\eta}{2}-\frac{1}{s}\left(\frac{1}{4}-\frac{3}{8\nu}\right)\right], \quad \text{(C.31)}$$

$$w_1(s) \approx \frac{1}{\sqrt{s}}\left(5.32-\frac{1.0}{s}\right),$$

$$w_2(s) \approx \frac{1}{\sqrt{s}}\left(11.61-\frac{2.57}{s}\right). \quad \text{(C.32)}$$

We obtain therefrom the deviations to the simple expressions (6.51) for the wavevectors, where $\chi \equiv \kappa_x\sqrt{s}$:

$$k_z \approx \chi\left[(1+\mathrm{i})\left(1+\frac{\eta}{2}+\frac{3}{16s\nu}\right)+\frac{1}{2s}\right]$$
$$\approx \frac{\nu}{l}(1+\mathrm{i})\left(1+\frac{9}{16s\nu}-\frac{\mathrm{i}}{4s}\right), \quad \text{(C.33)}$$

$$\beta_z \approx \chi\left[1-\frac{\eta}{2}+\frac{3}{4s\nu}+\frac{1-2\mathrm{i}}{4s}\right]$$
$$\approx \frac{\nu}{l}\left(1-\eta-\frac{3}{8s\nu}-\frac{\mathrm{i}}{2s}\right). \quad \text{(C.34)}$$

The extrapolation of these expansions towards smaller values of s suggests that the curves $t_n(s)$, $u_n(s), v_n(s), w_n(s)$ can be continued until $v_n(s)$ vanishes. Indeed, the allowed domain for the parameters s,t,u,v,w is the region where they are positive and $t \leqslant 1$; when s decreases, v also decreases while t,u and w increase, but these quantities t,u,v are not expected to reach the border of their allowed domain before v vanishes. Actually, the curves $v_n(s)$ given by (C.24) lie *below the line* $v = s - \frac{1}{2}$, and the maps of Figures 1 and 2 show that in this region t remains smaller than $\frac{1}{2}$ and u smaller than 4.

Let us therefore explore the region $v \simeq 0$. We still make the approximations $\left|\mathrm{e}^{2\mathrm{i}k_z l}\right| \ll 1, \left|\mathrm{e}^{-2\beta_z l}\right| \ll 1$, to be checked later. Up to first order in v, we have $V \approx 1+v$, and equations (4.22) provide $X \approx 1-\frac{1}{2}v, Y \sim \frac{v}{2s}, YZ \approx s\left(1-\frac{1}{2}v\right)$. Hence, the expansions of (4.23, 4.24) and (A.19) read:

$$t \approx (s+1)^{-1}+\frac{1}{2}vs(s+1)^{-2},$$
$$u \approx 2(s+1)-v\left(2s+2+s^{-1}\right),$$
$$U \approx 2s^2+2s+1-v\left(2s^2+2s+2+s^{-1}\right). \quad \text{(C.35)}$$

The value s_n of s such that $v_n(s)$ vanishes is then given by (C.21) where v is replaced by $0, u$ by $2(s_n+1)$ and U by $2s_n^2+2s_n+1$, that is:

$$s_n - 1 = \frac{s_n+1}{2}\,\frac{\ln\left[s_n^{-2}\left(2s_n^2+2s_n+1\right)\right]}{2n\pi-\mathrm{tg}^{-1}\frac{s_n}{s_n+1}}. \quad \text{(C.36)}$$

This provides:

$$s_1 \simeq 1.28 \quad , \quad s_2 \simeq 1.13. \quad \text{(C.37)}$$

Each curve $v_n(s)$, which ends up as (C.24) for large s, thus starts from the point $s_n, 0$. Its initial slope is obtained by inserting the expansions (C.35) into (C.21), which yields

$$s-1-\frac{2v}{s+1} \approx \frac{s+1+v\left(1-s^{-1}\right)}{2}$$
$$\times\frac{\ln s^{-2}\left[\left(2s^2+2s+1\right)-v\left(1+s^{-1}\right)\right]}{2n\pi-\frac{1}{2}\mathrm{tg}^{-1}\frac{2s^2(s+1)-v(3s+1)}{s(2s+1)+v\left(2s^2+s-1\right)}},$$

where the denominator can be replaced by:

$$2n\pi-\mathrm{tg}^{-1}\left[\frac{s}{s+1}-\frac{v\left(2s^2+s+1\right)}{2s(s+1)^2}\right].$$

Chasing now this denominator, expanding up to first order in $s-s_n$ and in v, and using (C.36), we obtain the slope through

$$\left(s_n^2+1\right)\frac{v_n(s)}{s-s_n} \to 2s_n + \quad \text{(C.38)}$$
$$\frac{(s_n+1)^2(2s_n+1)}{\left[s_n^2+(s_n+1)^2\right]\left(2n\pi-\mathrm{tg}^{-1}\frac{s_n}{s_n+1}\right)-s_n(s_n+1)}.$$

Numerically, (C.37) and (C.38) provide

$$v_1(s) \sim 1.16(s-s_1), \quad v_2(s) \sim 1.09(s-s_2), \quad \text{(C.39)}$$

and hence, using (C.35),

$$u_1(s) \approx 4.56-4.21(s-s_1),$$
$$u_2(s) \approx 4.27-3.60(s-s_2), \quad \text{(C.40)}$$

$$t_1(s) \approx 0.44-0.05(s-s_1),$$
$$t_2(s) \approx 0.47-0.08(s-s_2). \quad \text{(C.41)}$$

The expansion of (C.22) reads

$$w \approx \frac{2n\pi - \mathrm{tg}^{-1}\dfrac{s_n}{s_n+1} + \dfrac{1}{s_n^2+(s_n+1)^2}\left[\dfrac{v\left(2s_n^2+s_n+1\right)}{2s_n} - (s-s_n)\right]}{1+s_n+(s-s_n)-\dfrac{1}{2}v\left(s+1+2s^{-1}\right)}, \tag{C.42}$$

or numerically, from (C.39)

$$\begin{aligned} w_1(s) &\approx 2.53 + 1.46\,(s-s_1)\,, \\ w_2(s) &\approx 5.66 + 3.07\,(s-s_2)\,. \end{aligned} \tag{C.43}$$

Finally, the expansions around $v=0$ of the wavevectors corresponding to $R=T=0$ are given either by (6.33) and (C.35), or by (4.10) and (A.10), as

$$\begin{aligned} k_z l &\approx w\left[(s+1+\mathrm{i}s)\left(1-\frac{1}{2}v\right) - \frac{1}{2}vs^{-1}\right], \\ \beta_z l &\approx w\left[1+\frac{1}{2}v\left(1-\mathrm{i}s^{-1}\right)\right], \end{aligned} \tag{C.44}$$

which yields numerically, using (C.39) and (C.43),

$$\begin{aligned} (\mathrm{Re}\ k_z l)_1 &\approx 5.77 + 1.37\,(s-s_1)\,, \\ (\mathrm{Re}\ k_z l)_2 &\approx 12.08 + 2.93\,(s-s_2)\,, \end{aligned} \tag{C.45}$$

$$\begin{aligned} (\mathrm{Im}\ k_z l)_1 &\approx 3.24 + 2.52\,(s-s_1)\,, \\ (\mathrm{Im}\ k_z l)_2 &\approx 6.42 + 5.65\,(s-s_2)\,, \end{aligned} \tag{C.46}$$

$$\begin{aligned} (\mathrm{Re}\ \beta_z l)_1 &\approx 2.53 + 2.93\,(s-s_1)\,, \\ (\mathrm{Re}\ \beta_z l)_2 &\approx 5.66 + 6.15\,(s-s_2)\,, \end{aligned} \tag{C.47}$$

$$\begin{aligned} (\mathrm{Im}\ \beta_z l)_1 &\approx -1.15\,(s-s_1)\,, \\ (\mathrm{Im}\ \beta_z l)_2 &\approx -2.72\,(s-s_2)\,. \end{aligned} \tag{C.48}$$

Together with the asymptotic expressions (C.24–C.34) for large s, equations (C.39–C.48) indicate that when s varies from s_n to ∞, $v_n(s)$ increases nearly linearly, $u_n(s)$ decreases from $2(1+s_n)$ to 2, $t_n(s)$ decreases from $(s_n+1)^{-1}$ to 0, as $s^{-1/2}$, while $w_n(s)$ first increases before it reaches a maximum then decreases proportionally to $s^{-1/2}$. The values of Re $k_z l$, Im $k_z l$ and Re $\beta_z l$, which all lie for large s close to ν, that is, to 5.49 for $n=1$ and 11.75 for $n=2$ are according to (C.44–C.46) significantly different from one another for finite s. Moreover for $n=1$ and $s=s_1=1.28$, the exponentials

$$\left|\mathrm{e}^{2\mathrm{i}k_z l}\right| \simeq 1.5\times 10^{-3}, \quad \left|\mathrm{e}^{-2\beta_z l}\right| \simeq 6.3\times 10^{-3} \tag{C.49}$$

are no longer as small as for large s. However our present approximation which relies on equations (C.16, C.17) instead of (6.35, 6.42) remains justified, except maybe for the last figure in the above numerical results. This is confirmed by the direct numerical solution of (6.35, 6.42) represented by Figures 5 and 6.

We have not been able to prove that the branches studied above are the only solutions of equations (6.35, 6.42) which express that $R=T=0$, but this seems likely. In particular, we have seen in Section 6.4 that small values of s are precluded, even for the cancellation of T alone.

References

1. See, for instance, S.R. de Groot, P. Mazur, *Non-equilibrium thermodynamics* (Dover, New York, 1984), chap XIII, § 5; N.W. Ashcroft, N.D. Mermin, *Solid state physics* (Saunders College Publ., Philadelphia, 1976), chap. 29; R. Balian, *From microphysics to macrophysics*, Vol. II (Springer–Verlag, 1992), Sections 11.3.3, 14.4.2 and 15.2.1.
2. A review is given by the article of R. Fuchs and P. Halevi in *Spatial dispersion in solids and plasmas*, edited by P. Halevi (North-Holland, 1992) p. 1–107.
3. M.F. Bishop, A.A. Maradudin, Phys. Rev. B **14**, 3384 (1976).
4. J.T. Foley, D.N. Pattanayak, Opt. Com. **12**, 113 (1974).
5. R. Ruppin, J. Opt. Soc. Am. **71**, 755 (1981).
6. R. Ruppin, Phys. Rev. B **11**, 2871 (1975).
7. M. Barthélémy, H. Orland, G. Zerah, Phys. Rev. E **52**, 1123 (1995).
8. R. Balian, J.-J. Niez, J. Phys. I France **5**, 7 (1995).
9. E.M. Lifshitz, L.P. Pitaevskii, *Landau and Lifshitz course of theoretical physics*, vol. 10, *Physical kinetics* (Pergamon, 1981); J. Sheffields, *Plasma scattering of electromagnetic radiation* (Academic Press, 1975).
10. I.S. Gradshteyn, I.M. Ryzhik, *Table of integrals, series, and products* (Academic Press, 1980).